C 51.17/12:986/10

Tech Notes

OCTOBER 1986

PB86-925910

NTIS

U.S. DEPARTMENT OF COMMERCE
National Technical Information Service
Center for the Utilization of Federal Technology

Comments

I hope you like the new format of *Tech Notes*. By seeing all of the monthly fact sheets in one publication, you will find it easier to locate specific items of interest as well as to browse for technologies and know-how not directly applied to your area of work. The ten original subject sections also have been expanded to better fit the input received from Federal agencies and their laboratories.

The concept behind *Tech Notes* always has been to facilitate the transfer of U.S. Government technologies and know-how to U.S. businesses. Therefore, *Tech Notes* offers its readers not only access to new developments in their specific areas of interest, but also the encouragement to look for "spin-off" applications of R&D and engineering results with which they normally may not come in contact.

Two other improvements with this issue are the special listings within each subject section for *software* and *testing and instrumentation*. Items in these areas often offer some of the best "spin-off" potential for use outside of their original application.

Edward Lehmann
Editor

U.S. DEPARTMENT OF COMMERCE
Malcolm Baldrige, Secretary of Commerce

National Technical Information Service
Joseph F. Caponio, Director

ISSN 0889-8464

COPYRIGHT WARNING
International Copyright © National Technical Information Service, 1986. All portions of this publication are protected against copying or other reproduction outside of the United States under the provisions of Article II of the Universal Copyright Convention. United States copyright is not asserted under the United States Copyright Law, Title 17, United States Code.

The Secretary of Commerce has determined that the publication of this periodical is necessary in the transaction of the public business required by law of this department. Use of funds for printing this periodical has been approved by the Director of the Office of Management and Budget through 1986.

Tech Notes

Highlighting Selected U.S. Government Technology & Resources

OCTOBER 1986

PENNSYLVANIA STATE UNIVERSITY
OCT 11 1986
DOCUMENTS COLLECTION

Contents

Agriculture & Food 1043
Computers 1046
Electrotechnology 1050
Energy 1064
Engineering 1073
Environmental Science & Technology 1089
Manufacturing, Machinery, & Tools 1093
Materials 1109
Medicine & Biology 1124
Natural Resources Technology & Engineering 1131
Physical Sciences 1134
Transportation 1142

Published monthly by the National Technical Information Service (NTIS), Tech Notes bring togeather individual one to two page fact sheets prepared by Federal agencies, their laboratories, or contractors. These fact sheets highlight current Federal technology determined to have commercial or practical application. Topics cover new processes, materials, techniques, software, instrumentation, and resources.

Some of the current sources are the Department of the Navy, Department of the Army, NASA, Department of Energy , Environmental Protection Agency, Department of the Interior, and the Department of Agriculture.

Special assistance is provided by the Federal Laboratory Consortium.

Change of address or questions concerning subscriptions should be sent to:
Subscriptions Department
National Technical Information Service
Springfield, VA 22161
(703) 487-4630

Suggestions, comments, or questions concerning Tech Notes should be directed to:
Tech Notes Editor
Room 11R
National Technical Information Service
Springfield, VA 22161
(703) 487-4838

U.S. Depository Copy

How to Use Tech Notes

Every Tech Notes fact sheet lists a source for additional information. The source of this information may be a special support package from the originating agency, a personal contact, a licensing opportunity, or a backup report available from NTIS.

Each fact sheet also is perforated to allow for easy removal for those subscribers who may wish to keep a special fact sheet file or route to others in their organization

Sources of Further Backup Information

Below are two representative examples of how each Tech Note fact sheet provides you with a source of further information. In most cases, this information is provided directly by the agency or its laboratory. However, there are cases where NTIS is the source for backup documentation. In these cases, use the order form at the end.

Examples:

significant distance from the endwalls. Therefore, a radial variation in efficiency should be used when designing small stators.
Project Officer Jeffrey E. Haas
(216) 433-4000.

FOR ADDITIONAL INFORMATION

You can learn more about this technology by ordering the NTIS report(s):
Cold-Air Performance of Compressor Drive Turbine
Order number: AD-A101066/NAA
Price code: A02
Order from:
National Technical Information Service
5285 Port Royal Road
Springfield, VA 22161
(703) 487-4650

158

- Agency contact who can supplement the information contained in the backup report.
- NTIS Order Number*
- NTIS Price Code*

* See the order form and price code table at the end of the issue.

Suggested applications include other kinds of refrigerators, heat engines, thermal instrumentation, and heat switches.
This work was done by Emanuel Tward of Caltech for NASA's Jet Propulsion Laboratory.
NPO-15479/TN

FOR ADDITIONAL INFORMATION
Contact: Director, Technology Transfer Division, P.O. Box 8587, BWI Airport, MD 21240: (301) 621-0100 Ext.241.
REFER TO THE NUMBER LISTED AT THE END OF THE ARTICLE

178

- Agency reference number
- Source of more information about the technology described in the fact sheet
- Page number

Agriculture & Food

1043 Yellowjacket Pheromone

1044 Method Identifies Irradiated Foods

1045 Small-Portion Water Dispenser—Pressure is regulated and flow is timed to control the amount dispensed.

1073 Wind Tunnel Checks Spray Drift

1089 Disposal of the Pesticide, Coumaphos, Using Microbial and UV-Ozonation Reactions

1110 Leather Production from Pigskins

United States
Department of
Agriculture

Research Technology
Agricultural Research Service

Yellowjacket Pheromone

Keeping yellowjackets with their threatening stingers from swarming around backyard picnic tables may someday be easier to do. An Agricultural Research Service scientist has developed a chemically baited trap to catch them.

Entomologist Jeffrey R. Aldrich lures the most menacing types of yellowjackets in the eastern United States into traps using a blend of artificial, nontoxic chemicals similar to a natural insect pheromone, or attractant. It is most effective in spring and early summer, when the sweet-smelling chemicals attract yellowjacket queens before they establish nests.

"If queens can be captured before they make nests, then they can either be killed or moved so they establish colonies in woods, fields, and other areas away from people," says Aldrich, who works at the ARS research center in Beltsville, MD. "The traps can also be used in late summer and fall to catch yellowjacket workers after a colony has started."

Some species of yellowjackets are a nuisance to people, but they also play a valuable role as predators, feeding on flies, caterpillars, and other insects.

"It's hard to convince people who have been stung by yellowjackets that they are beneficial insects, but they are," says Aldrich. "Yellowjackets prey on other insects and do a small amount of pollinating."

Aldrich says his chemicals and trap work particularly well against the eastern and German yellowjackets, among the most menacing types in the eastern United States. Other attractants have worked against the western yellowjacket but have been ineffective against yellowjacket species in eastern North America.

Eastern yellowjacket queen.
(0684W751-4)

In field tests, Aldrich used several types of traps hung at shoulder height on tree branches along borders of woods and pasture areas. The chemicals inside are either a sticky liquid or part of a small plastic pellet.

Aldrich caught queens from two of the most pesky species—the eastern and German yellowjackets. He says the chemicals are better than current attractants, which include cat and dog food. His baited traps will be most effective in urban and suburban areas, he says, where there are fewer queens.

Aldrich's chemical blend has the same major ingredients that are in a pheromone from a predatory insect called the spined soldier bug. While testing artificial attractants for this member of the stink bug family, Aldrich found that certain types of yellowjackets were also attracted to the bug's pheromone. He is not sure exactly why, but he has two theories.

One is that the yellowjacket responds to the pheromone because it wants to steal the stink bug's prey. The other is that yellowjackets are drawn to the pheromone because it smells like chewed tree leaves, where yellowjackets often find insects on which to feed.

The eastern and German yellowjackets eat other insects but also scavenge in garbage and at picnic tables for food and, if disturbed, can sting humans. They are particularly threatening because they can nest in buildings as well as underground and because their colonies are large—up to 4,000 or 5,000 to a colony. Also, yellowjackets, unlike honey bees, can sting repeatedly and stay alive.

"The one or two yellowjackets that may sting you during a barbecue or in your backyard, for example, will not seriously hurt you, unless you are allergic to their venom," Aldrich says.

"But if a child stepped on an underground nest, or if you ran over a nest with the lawnmower, that could be a life-threatening situation. Having a few hundred yellowjackets coming after you is dangerous."

One advantage of his method, Aldrich says, is that the chemical pheromone only attracts yellowjackets that are about 3 feet away from the trap. That means once yellowjackets in the immediate area are caught, others from farther away won't be drawn to it.

Aldrich has been field-testing the chemicals at Beltsville over the last several years, seeking a chemical blend that not only catches yellowjackets but that does not harm honey bees. He says honey bees are generally not strongly attracted to the chemicals.

Jeffrey R. Aldrich is at the USDA-ARS Insect and Nematode Hormone Laboratory, Bldg. 467, BARC-East, Beltsville, MD 20705. ■

Above: To lure yellowjackets, entomologist Jeffrey Aldrich loads insect trap with a chemical attractant. (0386X427-27)

NBS technology update

National Bureau of Standards
U.S. Department of Commerce
Gaithersburg, MD 20899

Method Identifies Irradiated Foods

NBS scientists have developed an extremely sensitive procedure to detect whether or not a sample of meat has received radiation processing to sterilize it or to inhibit decay. Until now, no reliable test method has been available for determining whether or not a foodstuff, other than dried spices, has been treated with ionizing radiation. The technique should work with vegetable matter and seafood as well as with meats. In addition, it should be possible to develop a scale to determine how much radiation has been administered. Although the food itself does not become radioactive, the total dose of radiation given to foods must be carefully controlled to produce the desired effect while not damaging the food. The Food and Drug Administration sets maximum exposure limits for lifetime of the food product. These limits present a problem for regulators and food importers, who may need to determine whether a shipment has ever been irradiated, and if so, to what extent. While further experiments are needed, the NBS researchers are optimistic that their procedure will provide a useful, accurate test. NBS is continuing to study the process, with funding from the Department of Agriculture and the FDA.

FOR ADDITIONAL INFORMATION: Contact: Dr. Michael Simic, Room C216, Radiation Physics Bldg., National Bureau of Standards, Gaithersburg, MD 20899; (301) 921-2374.

NASA Tech Brief
National Aeronautics and Space Administration
Lyndon B. Johnson Space Center, Houston, Texas

Small-Portion Water Dispenser

Pressure is regulated and flow is timed to control the amount dispensed.

A dispenser provides a measured amount of water for reconstituting dehydrated foods and beverages. The dispenser holds the food or beverage package while it is being filled with either cold or room-temperature water (see figure). Other uses might include the dispensing of fluids or medicine.

A pressure regulator in the dispenser reduces the varying pressure of the water supply to a constant pressure. An electronic timer stops the flow after a predetermined length of time. The timed flow at regulated pressure ensures that a controlled volume of water is dispensed.

The user inserts a package to be filled in a nest in the dispenser and adjusts the dispensing needle to pierce the septum of the package. The "power" button is then depressed and a selector valve is turned to the cold ("CHD" in the figure) or room-temperature ("AMB" in the figure) position. After choosing the amount of water — 2, 3, 4, or 8 ounces (59, 89, 118, or 237 milliliters) — the user depresses the "fill" button. When the dispenser has filled the package, the user disengages the needle and removes the package.

This work was done by Jack C. Joerns of Technology Inc., for **Johnson Space Center.** *MSC-20534 /TN*

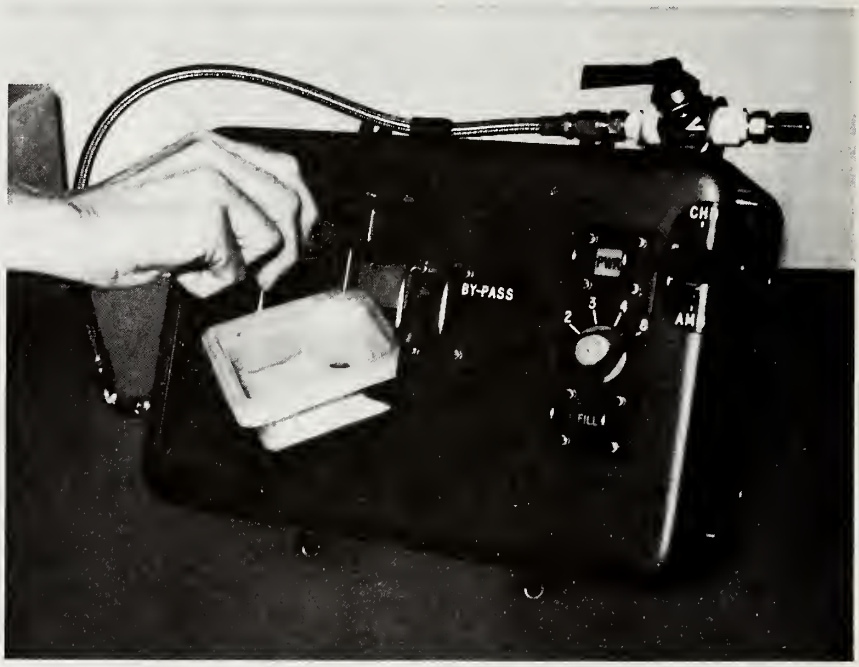

The **Dispensing Unit** is shown here in operation with the dispensing needle about to penetrate a plastic food package.

FOR ADDITIONAL INFORMATION: *Contact: Director, Technology Transfer Division, P.O. Box 8757, BWI Airport, MD 21240; (301) 621-0100 Ext. 241*
REFER TO THE NUMBER LISTED AT THE END OF THIS ARTICLE

Computers

1046 Artificial Vision Device Performs High-Speed Processing of Images

1047 General Purpose Bit-Slice Minicomputer Interface—The bit-slice-interface (BSI) concept saves engineering time in custom designing.

1048 Fast Initialization of Bubble-Memory Systems—The improved scheme is several orders of magnitude faster than the normal initialization scheme.

1049 Radiation Hardening of Computers—Single-event upsets are reduced by use of oversize transistors.

Other items of interest

1072 Lithium-Counterdoped Solar Cells—Resistance to damage by energetic electrons is increased.

NBS technology update

National Bureau of Standards
U.S. Department of Commerce
Gaithersburg, MD 20899

Artificial Vision Device Performs High-Speed Processing of Images

Researchers at NBS are testing a prototype of a new computing device for machine vision systems that continually processes images from a television camera at previously unheard-of levels of performance.

The device, called a Pipelined Image Processing Engine (PIPE), is expected to have applications in a wide variety of advanced image-sensing equipment where continuous, "real-time" processing is necessary. Examples range from artificial "eyes" for robots and robotic vehicles to improved medical diagnostic tools.

PIPE, according to its inventor, Dr. Ernest Kent, is a comparatively low-cost computing "engine" that handles the vast number of calculations necessary to pre-process a television image so that it can be understood by a computer. "PIPE does not actually 'recognize' the image it is working with. Rather, it handles all the analysis needed to recognize specific features of the image—for example, texture, shade, the presence or absence of an edge, and motion—at each point in the picture. It is modeled after the processes in the human visual cortex," says Kent.

A standard black-and-white digital video camera sends numbers corresponding to the levels of gray in a 256 x 256 point "frame" 60 times a second—65,536 points every 1/60 of a second.

PIPE . . . is a comparatively low-cost computing "engine" that handles the vast number of calculations necessary to pre-process a television image so that it can be understood by a computer.

For each point in each frame, PIPE can be programmed to do mathematical computations on not only the point itself, but also on its relationship to surrounding points in "neighborhoods" of varying sizes.

PIPE maintains several frames—up to 10 in the current prototype—simultaneously as they move through the computational "pipeline." As a result, it can also compare a point or its neighborhood with the equivalent points and neighborhoods both backwards and forwards in time, noting, for example, whether anything changes.

The current prototype PIPE performs approximately 450 million 8-bit operations per second, outpacing even supercomputers at its particular task.

PIPE was created for the NBS Automated Manufacturing Research Facility (AMRF) project to meet the need for a powerful, flexible vision processor that could handle data at

a.

b.

Inventor Dr. Ernest Kent demonstrates some of the capabilities of the Pipelined Image Processing Engine. Every point on the screen has a "gray scale" value ranging from −128 (black) to 127 (white). PIPE can perform calculations on each individual point, including its relationship to other points around it, or before or after it in time. First (a), the image is rescaled to expand the values near 0 to cover the full range, resulting in a high-contrast image. In the next image (b), only changes in intensity along the horizontal axis are displayed.

the speeds needed for practical applications on the factory floor. General-purpose computers cannot begin to do the calculations fast enough, and even though highly specialized image-analysis machines exist that can perform more calculations than PIPE, none is capable of the continuous, frame-after-frame calculations necessary to analyze a constant video signal in a rapidly changing situation.

A typical problem might be to detect moving objects from a robot arm or some sort of robot vehicle while the robot's camera "eye" is itself moving.

One way of solving this with PIPE is to compare an older neighborhood of points in the pipeline with its equivalent in a more recent image to detect horizontal motion, do the same thing to detect vertical motion, and combine the two calculations using trigonometric functions to get a number that represents the magnitude and direction of the motion. The processed image at this point, instead of showing the original view, shows the direction and amount of motion of each point in that scene. Further calculations ther are done to detect "edges" in the scene. Anything which is moving on its own in the robot's field of vision shows up as a moving object against a dull gray background.

The entire set of calculations is repeated 65,536 times every 1/60 of a second.

PIPE features include a "multiple instruction-stream, multiple data-stream" (MIMD) facility that allows it to perform different types of analyses on the same frame, depending on the nature of each point, and the ability to do a wide variety of motion-analysis, and stereo operations. Other features include a sophisticated, graphics-oriented programming capability and a high-speed interface system that organizes the results of PIPE analyses in a convenient form in the memory of another computer.

PIPE is designed as a series of processing modules that can be assembled to provide the desired number of processing stages. The current prototype is a three-stage PIPE.

. Prototype versions of PIPE were developed and built for NBS by Digital/Analog Design Associates, Inc., of New York City; PIPE is a registered trademark of Digital/Analog Design Associates, Inc. NBS is applying for a patent on the device.

c.

d.

Vertical lines are sharply defined, but horizontal lines are invisible. Here (c) logical operations are used to display only those points at which the gray scale value changes between negative and positive. These points are displayed in black. PIPE can "pyramid" images as well (d). In a process repeated three times, each 2 x 2 area of points on the screen is averaged, and the resulting value becomes a single point in an image half the size of the original. The final image is then magnified. PIPE is the only full-scale machine capable of doing this pyramiding in real time.

For Additional Information

Dr. Martin Herman
Room A 127-Metrology Bldg.
National Bureau of Standards
Gaithersberg, MD 20899
(301) 921-2156

MANUFACTURING TECHNOLOGY NOTE

U.S. ARMY MATERIEL COMMAND

Deputy Chief of Staff for Manufacturing Technology, Alexandria, VA

Project Number: MMT0XX5071-57 Filing Code : 49H031

General Purpose Bit-Slice Minicomputer Interface

The bit-slice-interface (BSI) concept saves engineering time in custom designing.

The U.S. Army Test and Evaluation Command completed a study of its future bit-slice minicomputer interface requirements to determine the features essential to a general purpose computer interface. Such a general purpose interface could increase instrumentation reliability and enable more projects to be supported with existing instrumentation. Substantial cost savings could result because it costs roughly $10,000 of engineering effort to produce a specialized bit-slice interface for each project.

The study established that the proposed BSI must handle parallel data, make high speed decisions, and be versatile enough to permit field changes. It would allow users to decide on the amount of required processing and control, and would give them the flexibility to create their own customized instruction set with no redesign other than a simple firmware update and a one-to-one replacement of control store memory. As the complexity of operations and the number of control signals increase, bit-slice devices become increasingly efficient compared to conventional-hardware units (see figure).

Use of the BSI provides the designer the following additional advantages:

- Quick instrumentation response,
- Economical operation,

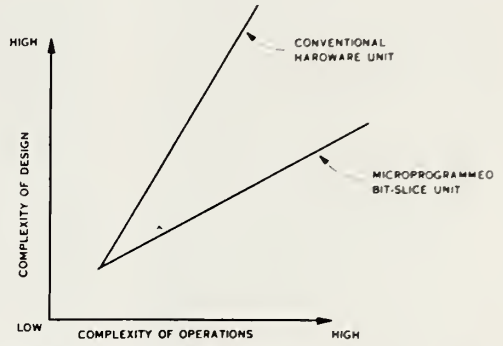

Bit-Slice-Design Benefits increase as complexity of operations increases; compared to conventional-hardware units, BSI units require smaller increases in design complexity to perform increasingly complex operations.

- Reduction in procurement lead time,
- Reduced technical expertise requirements,
- Decreased design time,
- Higher system reliability and maintainability,
- Self-test features, and
- Simple field changes.

FOR ADDITIONAL INFORMATION

You can learn more details about this technology by contacting

Commander
U.S. Army White Sands Missile Range
Attn. STEWS-TE-AG (S. Parra)
U.S. Army White Sands Missile Range, NM 88002
Telephone No. (505) 678-4808 or AV 258-4808

This document was prepared under the sponsorship of the U.S. Government. Neither the United States Government nor any person acting on behalf of the United States Government assumes any liability resulting from the use of the information contained in this document, or warrants that such use will be free from privately owned rights.

NASA Tech Brief
National Aeronautics and Space Administration
Langley Research Center, Hampton, Virginia

Fast Initialization of Bubble-Memory Systems

The improved scheme is several orders of magnitude faster than the normal initialization scheme.

Bubble-memory systems are quickly becoming preferred in environments where nonvolatile storage mediums are required. The implementation of large bubble-memory systems in spacecraft applications requires that the memory modules be power-strobed for the conservation of the available energy resources. Each time a module is turned on for use, it must be initialized to code the redundant loop information of the selected bubble devices into the bubble controller. Present structures of bubble systems dictate that a faster initialization procedure is needed to capitalize on the advantages offered by a bubble-memory system.

EPROM (electrically-programable read-only memory) was chosen as the simplest method to demonstrate the viability of this fast initialization technique. A state-of-the-art commercial bubble-memory device was used. A hardware interface was designed to connect the controlling microprocessor to the bubble-memory circuitry. System software was written to exercise the various functions of the bubble-memory system. A comparison was made between the normal and fast techniques. Future implementations of this approach will utilize the E^2PROM (electrically-erasable programable read-only memory) to provide greater system flexibility.

The figure shows the flow charts for the normal and fast initialization procedures. Both initialization procedures require a system reset (ABORT) before the command is sent to the controller. When the system is initialized normally, the bubble-memory controller (BMC) reads the entire bootloop, decodes it, transfers it to the bootloop register in the format/sense amplifier (FSA), and places the bubble at page zero. This process could take up to 160 ms since there could be two rotations of the minor loops to find and read the bootloop code.

Alternatively, the fast initialization procedure uses system software to load the bootloop information from an external memory into the bootloop register of the FSA. The first different step in the fast initialization process is to issue the PURGE command to clear the controller registers. Next, the parametric register data must be loaded with the same data as those required for the normal initialization. Upon the completion of this, the bootloop register must be loaded from the external memory to the bootloop register in the FSA, accomplished by using the WRITE BOOTLOOP REGISTER MASKED command.

A calculation of the normal initialization time was made from the time the command was issued to the BMC to the time that an "operation complete" status was received in the status register. This time was 117.84 ms. A calculation of the fast initialization time began with the issuance of the PURGE command and ended with the receipt of an "operation complete" in the BMC status register after the completion of the WRITE BOOTLOOP REGISTER MASKED command. This time was only 641 μs. The results of this experiment show that the fast-initialization concept provides several-orders-of-magnitude improvement over the normal initialization scheme. The fast-initialization technique is conceptually applicable to all bubble-memory devices and to systems having higher densities than that of the one used in this investigation.

This work was done by Karen T Looney, Charles D. Nichols, and Paul J. Hayes of **Langley Research Center.** *Further information may be found in NASA TM-85832 [N84-27977/NSP], "Investigation of Fast Initialization of Spacecraft Bubble Memory Systems" [A05] A copy may be purchased [prepayment required] from the National Technical Information Service, Springfield, Virginia 22161.*
LAR-13357 / TN

FOR ADDITIONAL INFORMATION: *Contact: Director, Technology Transfer Division, P.O. Box 8757, BWI Airport, MD. 21240; (301) 621-0100 Ext. 241*
REFER TO THE NUMBER LISTED AT THE END OF THE ARTICLE

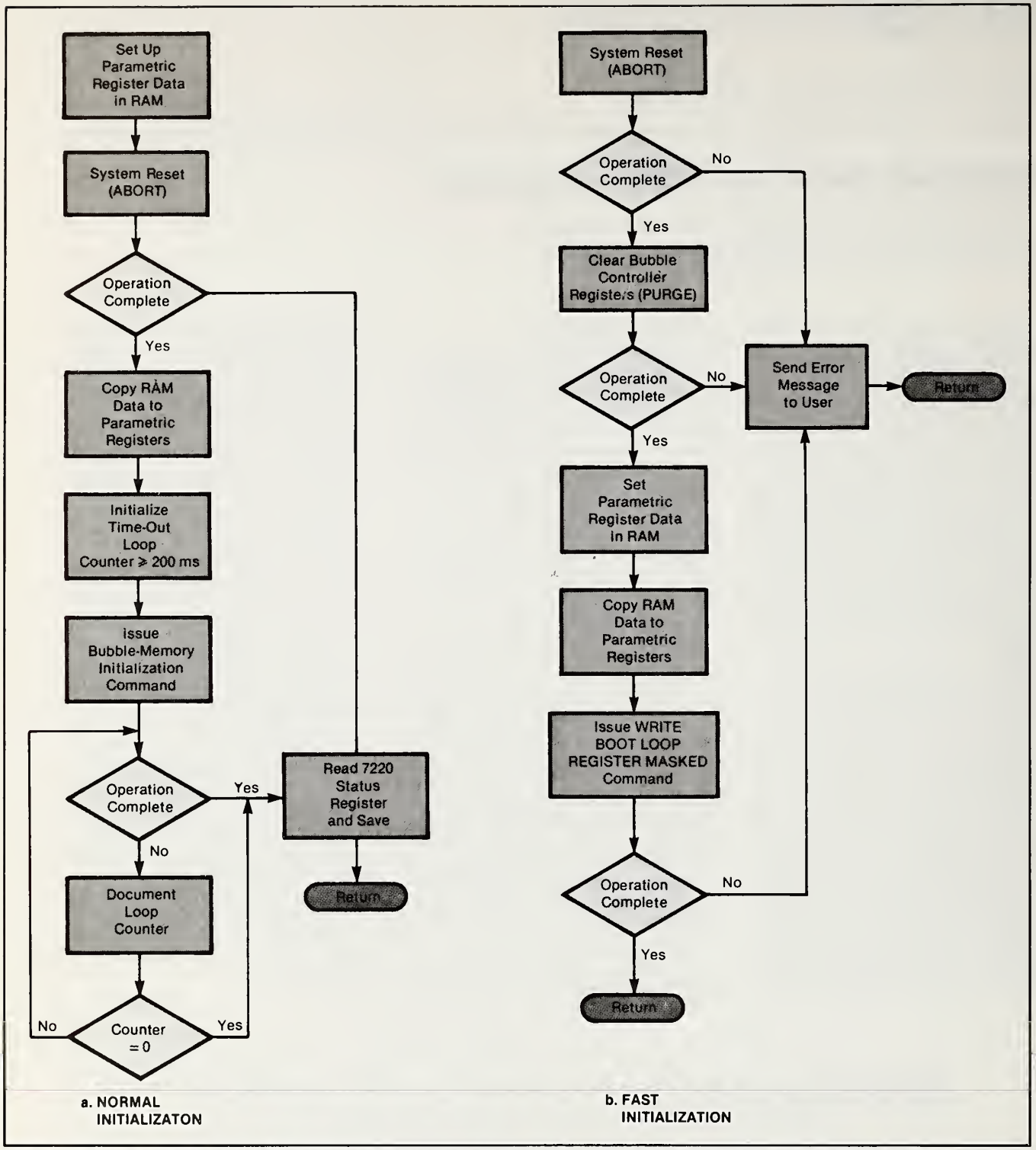

The **Normal and Fast Initialization Techniques** are represented by these flow charts. The fast technique uses a small amount of external storage to load the controller registers at high speed.

NASA Tech Brief
National Aeronautics and Space Administration

Radiation Hardening of Computers

Single-event upsets are reduced by use of oversize transistors.

Computers can be made less susceptible to ionizing radiation by replacing bipolar integrated circuits with properly-designed, complementary metal-oxide-semiconductor (CMOS) circuits, according to a report. CMOS circuit chips can be made highly resistant to single-event upset (SEU), especially when certain feedback resistors are incorporated. The redesigned chips also consume less power than do the original chips.

CMOS replacements for nine types of bipolar logic circuits were constructed. Two techniques were used to increase the resistance to radiation. One is the use of oversize transistors. Feedback resistors are also inserted in the regeneration path of most latches to increase the time of responses to particle hits to well beyond the durations of the disturbances.

The use of larger-than-minimum transistors helps in two ways: The increased current drive causes a struck node to be restored more quickly, and the higher gate capacitance permits a corresponding decrease in the size of the feedback resistor required to achieve a given regeneration time. The increase in size beyond the minimum required for sufficient speed, reduces the dependence on resistors to the point where they are not critical to adequate immunity to SEU. Moreover, because the CMOS chips are small relative to area constraints imposed by processing yield, it is feasible to use oversize transistors without making the replacement chips unduly large.

When resistors are used to enhance the resistance to SEU, they are incorporated into the chips by one additional processing mask step; it is thus possible to fabricate in parts with and without the extra resistors in one wafer lot. The resistors are positioned in circuits so that the read-access times of memories and the propagation delays of latches are not significantly degraded. The resistors degrade the computer speed somewhat. For example, the write time for memories and the setup time for latches are increased by about 12 ns and 2 ns, respectively, for a 2901 4-bit microprocessor slice when 80-kΩ resistors are added.

Tests were conducted to determine the linear-energy-transfer (LET) thresholds for the CMOS replacement parts by subjecting them to 165-MeV krypton ions at a minimum fluence of 2×10^7 particles/cm^2 in a cyclotron. All data were taken with a power supply operating at 4.5 V, making the devices more susceptible to SEU than at their normal 5.0 V operation. The LET thresholds of all the tested CMOS circuits, both with and without resistors, were above the desired LET value of 37 MeV/mg/cm^2.

This work was done by Donald K. Nichols, Lawrence S. Smith, and John A. Zoutendyk of **NASA's Jet Propulsion Laboratory** *and Alfred E. Giddings, Frank W. Hewlett, and R. Keith Treece of Sandia National Laboratories.*

"SEU Immune ICs for Project Galileo," NPO-16767 /TN

FOR ADDITIONAL INFORMATION: *Contact: Director, Technology Transfer Division, P.O. Box 8757, BWI Airport, MD 21240; (301) 621-0100 Ext. 241*

REFER TO THE NUMBER LISTED AT THE END OF THIS ARTICLE

1050 Phased Array Antenna Interelement Interactions

1051 Improved Power Transistors for Radars

1052 Video Processor for Transponder Pulses—A circuit helps determine whether pulses are from the main lobe of a radar beam.

1053 Positive-Index Guiding in CDH-LOC Lasers—A nonabsorbing passive region has beam-guiding capability.

1054 Bidirectional dc-to-dc Power Converter—A solid-state, series-resonant converter would use high-voltage thyristors.

1055 Cross-Array Antenna With Switched Steering—Selected phase shifting of the feeds to antenna elements aims the antenna beam.

1056 A 25-kW Series-Resonant Power Converter—A prototype exhibited an efficiency of 93.9 percent.

1057 Correcting for Nonlinearity in a Photodetector—A simple positive-feedback circuit would vary the bias voltage as necessary

1058 Broadband Ultrasonic Transducers—A new geometry spreads out the resonance region of a piezoelectric crystal.

1059 Ejection Mechanism for Circuit Boards—Damage to connectors is reduced and special tools are not needed.

Software

1060 Economic-Analysis Program for a Communication System—Prices and profits of alternative designs can be compared.

Testing and Instrumentation

1061 Laser-Induced Optical Degradation—The performance of irradiated optical systems is modeled.

1062 Determining Microwave Power Delivered to an Antenna

1063 Electro-optical Tuning of Fabry-Perot Interferometers—A compact unit can operate much faster than conventional piezoelectric scanners.

NBS technology update

National Bureau of Standards
U.S. Department of Commerce
Gaithersburg, MD 20899

Phased Array Antenna Interelement Interactions

Large phased array antennas can be more efficiently and effectively designed, and their performance more accurately predicted, if we understand the effects of mutual impedances on array element excitations, and the role played by multiple reflections and mutual impedances in producing elementary patterns that combine to form the radiated field. The first results of a study of these issues are presented in Interelement Interactions in Phased Arrays: Theory, Methods of Data Analysis, and Theoretical Simulations (TN 1091). A principal objective of the study is to determine if it will be possible to predict the far-field pattern of a large phased array from measurements of some of its subarrays in the near field. Since many large arrays are too big or immobile to be economically measured using present techniques, the study is intended to solve a major measurement problem.

FOR ADDITIONAL INFORMATION: Copies may be purchased for $2 prepaid from the Superintendent of Documents, U.S. Government Printing Office, Washington, D.C. 20402; order by stock no. 003-003-02715-4.

Improved Power Transistors for Radars

The AN/SPS-40 transmitter contains 128 power amplifier modules, each of which utilizes 10 RF transistors to achieve 2500 watts of output power at 425 MHz. These 10 transistors represent the single most significant cost factor in the module. Thus, the cost of the transmitter can be greatly reduced by lowering the cost of the 1280 transistors it requires. This can be achieved through improved manufacturing processes.

The goal of the present Navy MT project number X0311 for "Improved MT for AN/SPS-40 rf Power Transistors" is to achieve a reduction in cost of AN/SPS-40 rf power transistors through application of improved transistor design, yield, die bonding, assembly and packaging techniques. Also, improved passivation techniques and automated testing and inspection techniques are being applied to manufacturing.

Highlights of the improvements are shown in the table below. The power from each die has been increased by 11%, but more importantly from the point of view of cost, the yield was increased from 30% to 60%. Other cost savings were made by automated die attaching, die bonding, and testing. The savings to the Navy over a five year period will be considerable as a result of this program. Each SPS-40 radar uses 1280 transistors. For a five year projected production of 100 systems, a total of 128,000 transistors will be required. As a result of this program, a cost reduction from $100.00 to $60.00 is expected to be achieved, for a five year savings of $5.12M.

End of program MT Demonstrations are scheduled for May 14 at Thomson-CSF and May 28 at M/A-COM PHI.

For further information contact:
Dr. W. T. Anderson, Code 6815
Naval Research Laboratory
Washington, D.C. 20375
(202) 767-2523

SPS-40 MT CONTRACT HIGHLIGHTS

	PRE-MT	PRESENT MT PROGRAM
Output Power at 425 GHz	400 W	483 W
Die Yield to Spec:	30%	60%
Die Type:	R1D	R1DA
Emitter Periphery:	441 mm	524 mm
Material:	Uncertain	Optimized
Process:	Standard	Simplified & Improved
Packaging:	Gain Function	Flatter Gain Across Band
Assembly:	Manual	Collet-Automated
Bonding:	Manual	Semi-Automatic
Testing:	Manual	ATE (Computer Driven, Automated)

NASA Tech Brief
National Aeronautics and Space Administration
John F. Kennedy Space Center, Florida

Licensing Opportunity

Video Processor for Transponder Pulses

A circuit helps determine whether pulses are from the main lobe of a radar beam.

A circuit detects interrogation signals from an air-traffic-control station and helps to determine whether the transponder of an airplane should respond. The circuit examines the relative magnitudes of the first two pulses in the three-pulse sequence of an interrogation signal. On the basis of the relative magnitudes, the circuit decides whether the main lobe of the interrogating radar beam has been received (and a response should be generated) or whether only a side lobe has been received (and the interrogation should therefore be ignored). The circuit differs from previous circuits for distinguishing the main lobe from the side lobe in that it is simple and inexpensive.

The new circuit is used in conjunction with a scheme for reducing clutter on the radar screens viewed by air-traffic controllers. The ground radar transmits a special side-lobe suppression pulse with other pulses during interrogation. An interrogation pulse train consists of a sequence of three pulses: P_1, P_2, and P_3. Pulses P_1 and P_3 are transmitted by a directional antenna, and the side-lobe suppression pulse P_2 is transmitted by an omnidirectional antenna.

If P_2 is greater than or about equal to P_1, the transponder should not reply, since it has received only a side lobe of the interrogating beam. When pulse P_1 is at least 9 decibels greater than P_2, however, the transponder has been directly addressed by the beam and should reply.

An intermediate-frequency transformer converts the received signals to levels suitable for driving a diode in a detector (see figure). The detector generates positive pulses for all pulses received from the ground station. The detected pulses are fed to the base of a transistor Q_1.

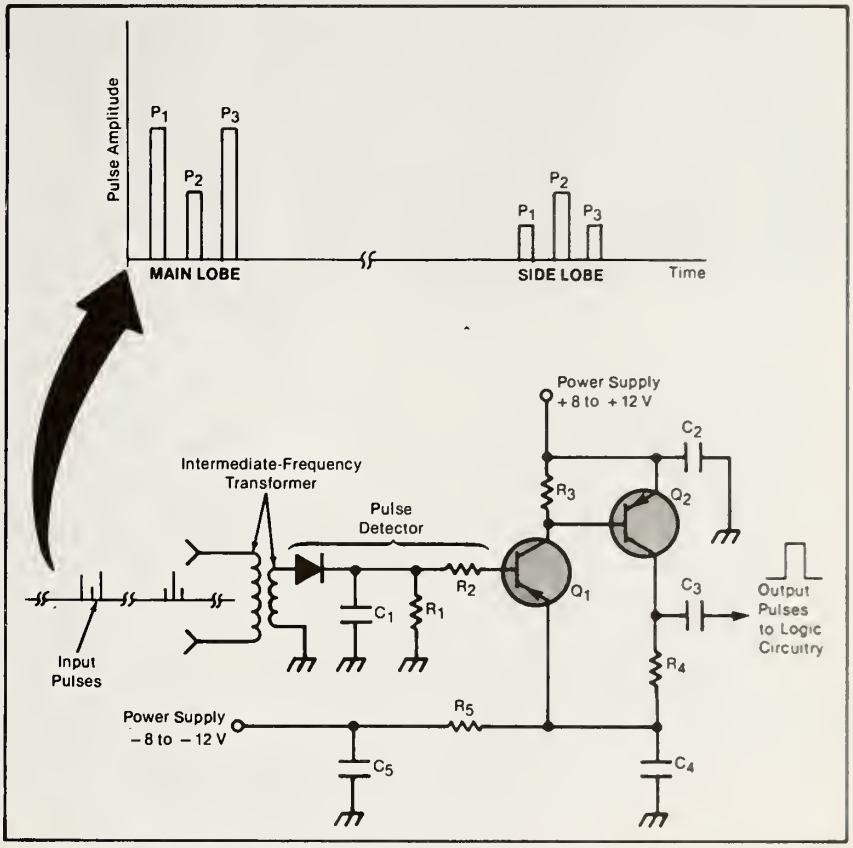

The Pulse-Processing Circuit determines whether the amplitude of pulse P_2 exceeds that of pulse P_1. If so, the circuit puts out a double pulse that a logic circuit interprets to mean that a valid interrogation signal has not been received.

Pulse P_1 turns on this transistor, thereby turning on transistor Q_2, which is connected by its base to the collector of Q_1. When Q_2 turns on, it applies a dc voltage to resistor R_4, thereby charging capacitor C_4 to about the voltage of P_1 and sending an output pulse to the logic circuitry through capacitor C_3.

At the end of P_1, the transistors return to their off state, while C_4 slowly discharges through resistor R_5, with a time constant considerably greater than the interval between the pulses in one sequence. Pulse P_2 arrives shortly but does

not activate Q_1 unless the pulse amplitude exceeds the voltage remaining on the capacitor from P_1. Thus, if P_2 is less than P_1 (indicating the main lobe), the transistors remain off, and a second pulse is not sent to the logic circuitry. The logic circuitry interprets the lack of a second pulse as an instruction to transmit the response code.

If, however, P_2 is greater than the capacitor voltage remaining from P_1 (indicating a side lobe), it turns on Q_1, which then produces a second output pulse. The logic circuitry interprets the two-pulse sequence as an instruction not to transmit the response code.

This work was done by Frank Byrne of **Kennedy Space Center.**

This invention has been patented by NASA (U.S. Patent No. 4,540,986). Inquiries concerning nonexclusive or exclusive license for its commercial development should be addressed to the Patent Counsel, Kennedy Space Center Refer to KSC-11155/TN

James O. Harrell
John F. Kennedy Space Center
Mail Code: PT-PAT
Kennedy Space Center, FL 32899
(305) 867-2544

FOR ADDITIONAL INFORMATION: *Contact: Director, Technology Transfer Division, P.O. Box 8757, BWI Airport, MD. 21240; (301) 621-0100 Ext. 241*
REFER TO THE NUMBER LISTED AT THE END OF THE ARTICLE

NASA Tech Brief
National Aeronautics and Space Administration
Langley Research Center, Hampton, Virginia

Positive-Index Guiding in CDH-LOC Lasers

A nonabsorbing passive region has beam-guiding capability.

A previous approach to a nonabsorbing-mirror (NAM) constricted-double-heterojunction, large-optical-cavity (CDH-LOC) laser involved passive regions formed by etching and regrowth. Lateral mode control was to be provided in the passive region by lateral thickness variations of the guide layer. However, if the guide layer has the same shape in the passive region as in the active region (i.e., minimum thickness in its middle tapering laterally to larger thicknesses), light will be quickly dispersed in the passive region since the result is essentially an antiguiding structure without gain.

A new technique for providing positive-index guiding in the passive sections of NAM-CDH-LOC lasers consists of having two layers regrown: (1) a convex-shaped layer of an index of refraction close to that of the guide layer and of material that does not absorb the light generated in the active portion of the CDH-LOC structure and (2) the ν-type $Al_{0.3}Ga_{0.7}As$ burying material (see figure). The convex-lens-shaped $Al_{0.2}Ga_{0.8}As$ layer (see figure) provides positive-index guiding in the passive region. That occurs while the guide layer keeps the same shape in both the active and passive regions. By varying the Al concentration and thickness of the regrown convex-lens-shaped layer, beam shaping can be achieved. The convex-lens-shaped layer could be of any material (for example, AlGaAs or InGaAsP) as long as its index of refraction is close to that of the guide layer so as to allow light spreading from the guide layer into the convex layer and as long as it does not absorb the light generated in the active section.

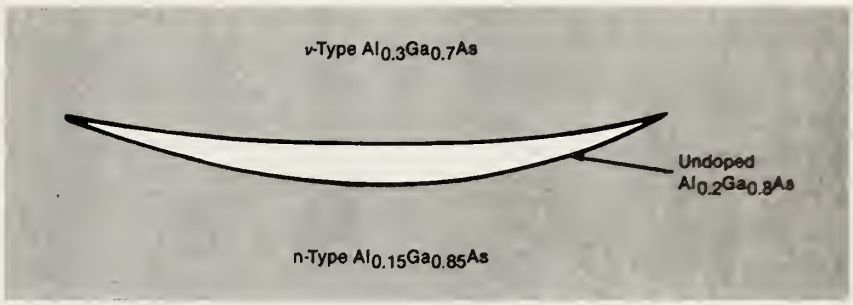

The **Convex-Lens-Shaped Layer** has a refractive index higher than that of the surrounding material so that it serves as an optical waveguide.

A semiconductor laser incorporating these principles was fabricated by sequential liquid-phase epitaxy deposition onto the surface of an n^+-GaAs substrate wafer. After chemical etching and regrowth of the appropriate layers to obtain the convex-lens-shaped configuration shown, individual laser chips were formed from the substrate wafer by cleaving through the burying region. A maximum output power of about 1.5 W was obtained with 100-ns pulses at a 1-kHz rate. This is about four times more power than is achieved for devices of this type not incorporating the passive region.

This work was done by Dan Botez of RCA Corp. for **Langley Research Center.**

Title to this invention has been waived under the provisions of the National Aeronautics and Space Act [42 U.S.C. 2457(f)], to the RCA Corp., Princeton, NJ 08540.
LAR-13312/TN

FOR ADDITIONAL INFORMATION: *Contact: Director, Technology Transfer Division, P.O. Box 8757, BWI Airport, MD. 21240; (301) 621-0100 Ext. 241*
REFER TO THE NUMBER LISTED AT THE END OF THE ARTICLE

NASA Tech Brief
National Aeronautics and Space Administration
Marshall Space Flight Center, Alabama

Bidirectional dc-to-dc Power Converter

A solid-state, series-resonant converter would use high-voltage thyristors.

A conceptual solid-state, series-resonant dc-to-dc power converter would be used either to convert high-voltage, low-current dc power to low-voltage, high-current power or the reverse. It takes advantage of newly-available high-voltage thyristors to provide better reliability and efficiency than do traditional converters that use vacuum tubes as power switches: Vacuum tubes have short lifetimes, and the power required to heat their filaments reduces conversion efficiency.

The new circuit uses no rotating machinery, such as the motor/generator sets used in some converters. Having neither moving parts nor vacuum tubes, the new converter should be essentially maintenance free and should provide greatly increased mean time between failures. Converters of the new type should be attractive in industrial applications whether or not bidirectional capability is required.

The converter would be built of ten modules in parallel, each carrying a tenth of the total power. Except for the need to use pairs of thyristors in series on the high-voltage side, the high- and low-voltage sides of the circuit are topologically equivalent (see figure). The only other things that distinguish the two sides of the circuit are the asymmetry in the turns ratios of the two transformers and, of course, the voltage and current ratings of the components.

In one mode, the converter would transmit power from the high-voltage side (4,000 to 5,240 V) to the low-voltage side (140 V). The converter could deliver as much as 120 kW to the low-voltage side in

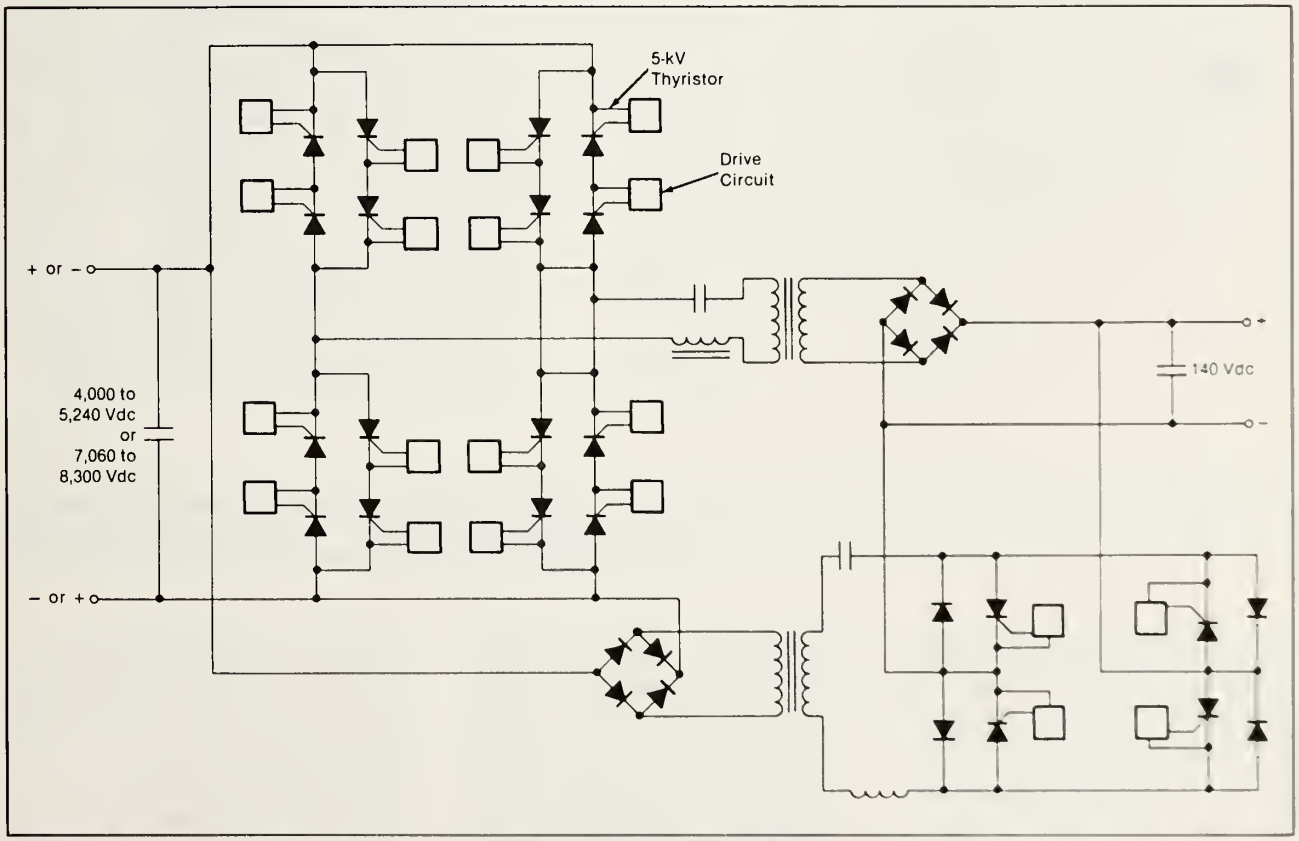

A **Bidirectional dc-to-dc Power Converter** with no moving parts or vacuum tubes can be constructed using newly available high-voltage thyristors.

cent. The transition between the two modes would be gradual; that is, the amount of power transferred in either direction would be continuous from one extreme to the other.

this mode. In the opposite mode, the converter would transfer power from the low- to the high-voltage side, delivering as much as 331 kW at 7,060 to 8,300 V. The anticipated conversion efficiency is 94 per-

This work was done by Carl R. Griesbach of Martin Marietta Corp. for **Marshall Space Flight Center.**
MFS-28095 /TN

FOR ADDITIONAL INFORMATION: *Contact: Director, Technology Transfer Division, P.O. Box 8757, BWI Airport, MD. 21240; (301) 621-0100 Ext. 241*
REFER TO THE NUMBER LISTED AT THE END OF THE ARTICLE

NASA Tech Brief
National Aeronautics and Space Administration
Lyndon B. Johnson Space Center, Houston, Texas

Cross-Array Antenna With Switched Steering

Selected phase shifting of the feeds to antenna elements aims the antenna beam.

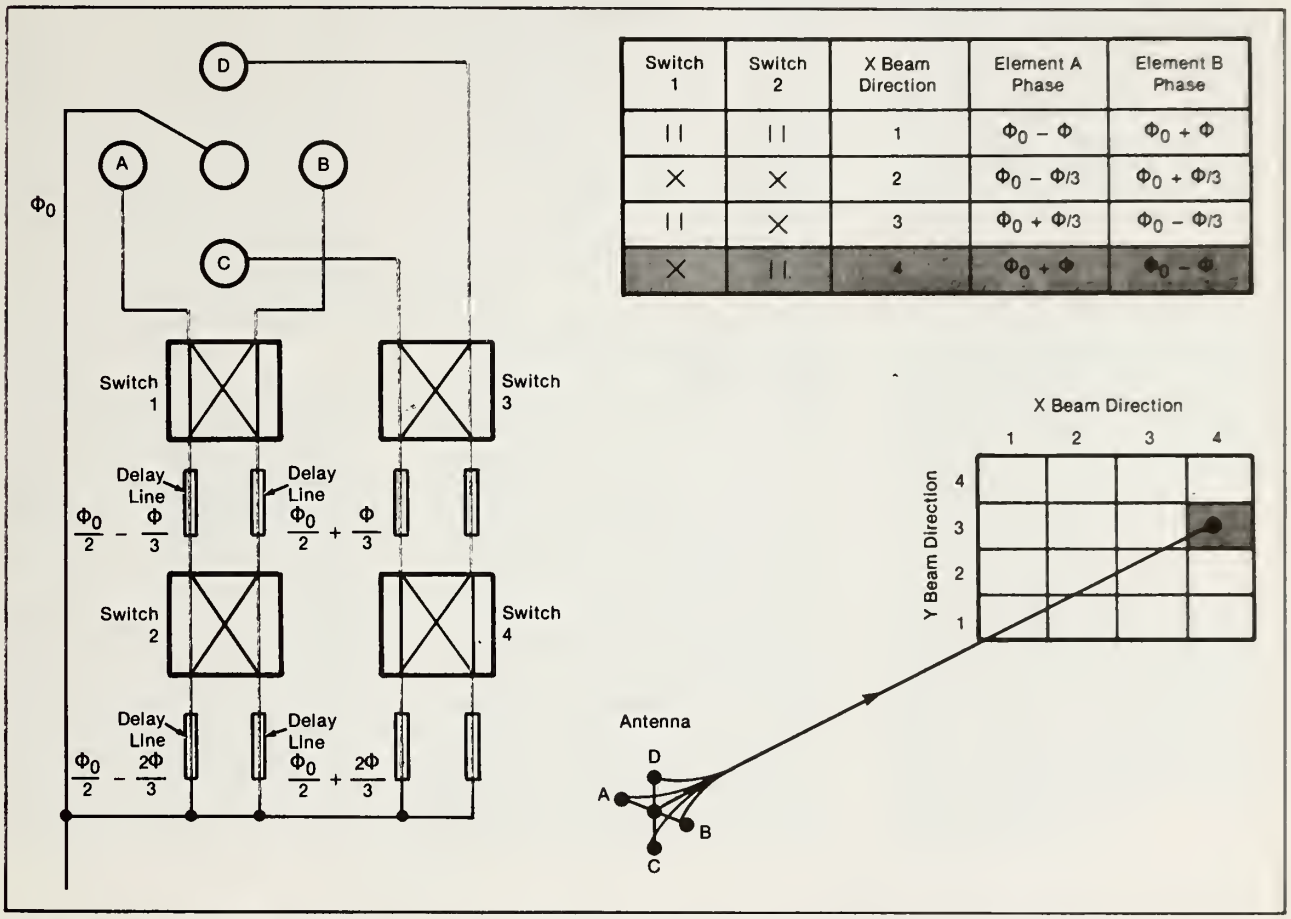

Switch 1	Switch 2	X Beam Direction	Element A Phase	Element B Phase
| |	| |	1	$\Phi_0 - \Phi$	$\Phi_0 + \Phi$
×	×	2	$\Phi_0 - \Phi/3$	$\Phi_0 + \Phi/3$
| |	×	3	$\Phi_0 + \Phi/3$	$\Phi_0 - \Phi/3$
×	| |	4	$\Phi_0 + \Phi$	$\Phi_0 - \Phi$

The **Five-Element Cross-Array Antenna** is shown in a 4-switch configuration. The table shows the phases (ϕ's) obtained at elements A and B by setting switches 1 and 2. A similar tabie applies to switches in the feeds to elements C and D. For the switch settings shown in color, the antenna aims toward the shaded region in the perspective drawing.

The aiming direction of a S-band cross-array antenna proposed for Space Shuttle use would be controlled in two dimensions by double-pole, double-throw switches in the antenna feeds. The switches would control the phasing of the antenna elements by transpo ing transmission-line delay elements between the feeds to pairs of elements located on opposite sides of the antenna.

The figure shows a 5-element antenna with 4 switches, capable of 16 different beam directions. The two switches in the feeds to antenna elements A and B control the horizontal component of the beam direction; the switches in the feeds to C and D, the vertical.

The angular separation between aim directions is determined by the spacing between the antenna elements and the amount of phase shift from element to element at the operating frequency. Except for a small correction due to the directionality of the radiation pattern of the individual elements, the maximum gain of the antenna would occur in the direction in which all the elements contribute in phase. By turning off either or both of the outer pairs of elements, the beam pattern can be broadened along one or both axes.

Each of the phase-changing switches has

a 0.2-dB insertion loss. Since only the phase differences between the elements (but not the absolute phases) are significant, one element may be fed directly. Therefore, the total power loss is minimized by feeding the center element directly, since this element receives the feed of highest amplitude.

The number of switches and delay lines determines the number of different aim directions that will be available. For n switches, there can be up to 2^n aim directions, provided that appropriate delays are selected. While the example of the figure uses two switches in each feed axis, more or fewer than two can be used. Similarly, the same principles can be applied to antennas with additional elements along each axis.

For a configuration with n switches, an n-bit binary number suffices to specify the aim direction: Each bit represents the setting of one switch. A microprocessor could be used to control the switches.

This work was done by Richard S. Iwasaki of Axiomatix for **Johnson Space Center.** *MSC-20889 /TN*

FOR ADDITIONAL INFORMATION: *Contact: Director, Technology Transfer Division, P.O. Box 8757, BWI Airport, MD. 21240; (301) 621-0100 Ext. 241*

REFER TO THE NUMBER LISTED AT THE END OF THE ARTICLE

NASA Tech Brief
National Aeronautics and Space Administration
Lewis Research Center, Cleveland, Ohio

A 25-kW Series-Resonant Power Converter

A prototype exhibited an efficiency of 93.9 percent.

The feasibility of processing 25 kW of power with a single, transistorized, series-resonant converter stage has been demonstrated by the successful design, development, fabrication, and testing of such a device. This technology was built on the strong technical base of multikilowatt series-resonant converters that have been developed in recent years. This technical base includes advanced switching components, magnetic components, filter components, mathematical circuit models, control philosophies, and switch-drive strategies.

Much of the recent effort had been centered around the application of high-power transistors in resonant converters. Transistor switches display marked advantages over the more commonly applied thyristors. Among these advantages are higher frequency operation, lower switch losses, positive commutation, lower-peak tank currents, and inherent current limiting in the switch. It is anticipated that the eventual application of this technology base to multikilowatt space-power systems will result in both reduced specific mass due to the higher conversion frequencies and in reduced thermal control due to more efficient operation.

To date, the highest-known power level of a resonant power converted designed for space operation was 2.5 kW. However, studies had shown that a module size of 25 kW was appropriate for a multihundred-kilowatt space-power system. As a first step, a 10-kW transistorized dc/dc resonant power converter was designed and tested. As a result of this program, the development of series-resonant converters to the 25-kW power level for spaceborne and airborne applications was successfully accomplished.

A 25-kW resonant dc/dc power converter was designed, developed, fabricated, and tested, using Westinghouse D7ST transistors as the high-power switches. The D7ST transistor was characterized for use as a switch in series-resonant converters, and a refined base-drive circuit was developed.

The converter developed employs four D7ST transistors in a full bridge configuration, operates from a 250- to 350-Vdc input bus, and provides an output power of 25 kW (1,000 V or ± 500 V at 25 Adc). It has a resonant frequency of 20.6 kHz, an output ripple of 3 percent peak-to-peak, regulation of better than 0.1 percent, a response time of less than 2 ms, and its output can be either constant voltage or constant current with automatic crossover. The full-power, 250-V-input electrical efficiency measured was 94.8 percent for the power stage alone, 94.4 percent with housekeeping power included, and 93.9 percent with the losses of the solid-state input circuit breaker and output transient-current limiters included. There are no inherent problems that would prevent this 25-kW design from being upgraded to a space-qualified status.

The developed converter technology provides an efficient, lightweight, high-power converter that can be used by itself or as a module for a higher power (multi-100-kW) system. This technology can also be used as the basis for a high-power, high-frequency (20-kHz), ac power distribution system. In either case, power-system benefits such as lower losses when used for high-voltage distribution, and reduced magnetics and filter mass will be realized.

This work was done by Robert J. Frye of **Lewis Research Center** *and Ronald R. Robson of Hughes Research Laboratories. Further information may be found in NASA CR-168273 [N84-17481/NSP], "25 kW Resonant dc/dc Power Converter" [A09]. A copy may be purchased [prepayment required] from the National Technical Information Service, Springfield, Virginia 22161.*
LEW-14197 / TN

FOR ADDITIONAL INFORMATION: *Contact: Director, Technology Transfer Division, P.O. Box 8757, BWI Airport, MD. 21240; (301) 621-0100 Ext. 241*
REFER TO THE NUMBER LISTED AT THE END OF THE ARTICLE

NASA Tech Brief
National Aeronautics and Space Administration
NASA's Jet Propulsion Laboratory, Pasadena, California

Correcting for Nonlinearity in a Photodetector

A simple positive-feedback circuit would vary the bias voltage as necessary.

Positive feedback is proposed for compensating for the internal series resistance of a photoconductive detector. The feedback would ensure that the detector-circuit output current varies linearly with the photon flux. The principle can be applied to linearizing mercury cadmium telluride infrared detectors in Fourier-transform spectrometers and other spectral and imaging instruments.

In an ideal photoconductive detector with no internal series resistance, the conductivity is proportional to the incident photon flux. If this ideal detector is biased with a constant voltage, the detector current is proportional to the photon flux plus a constant offset. Such a detector could be connected between an inverting input and ground (see top of figure), and feedback from an operational amplifier through feedback resistor R_f would make the voltage at the inverting input equal to that at the noninverting input. The bias voltage would thus be held constant.

A real photoconductive detector, however, contains an internal series resistance R_s so that the detector conductance no longer varies linearly with the photon flux. Adding a resistor R_3 to the circuit, as shown in the lower half of the figure, allows positive feedback to biasing resistors R_1 and R_2. This feedback increases the detector bias voltage as the flux increases and opposes the effect of R_s. The value of R_3 can be selected so that the positive feedback is just enough to balance out the nonlinear effect of R_s, thereby making the output voltage E_0 vary linearly with the photon flux. This value is given by

$$R_3 = \frac{R_f R_1 R_2}{R_s R_b} \left(\frac{R_s + R_b}{R_1 + R_2} \right)$$

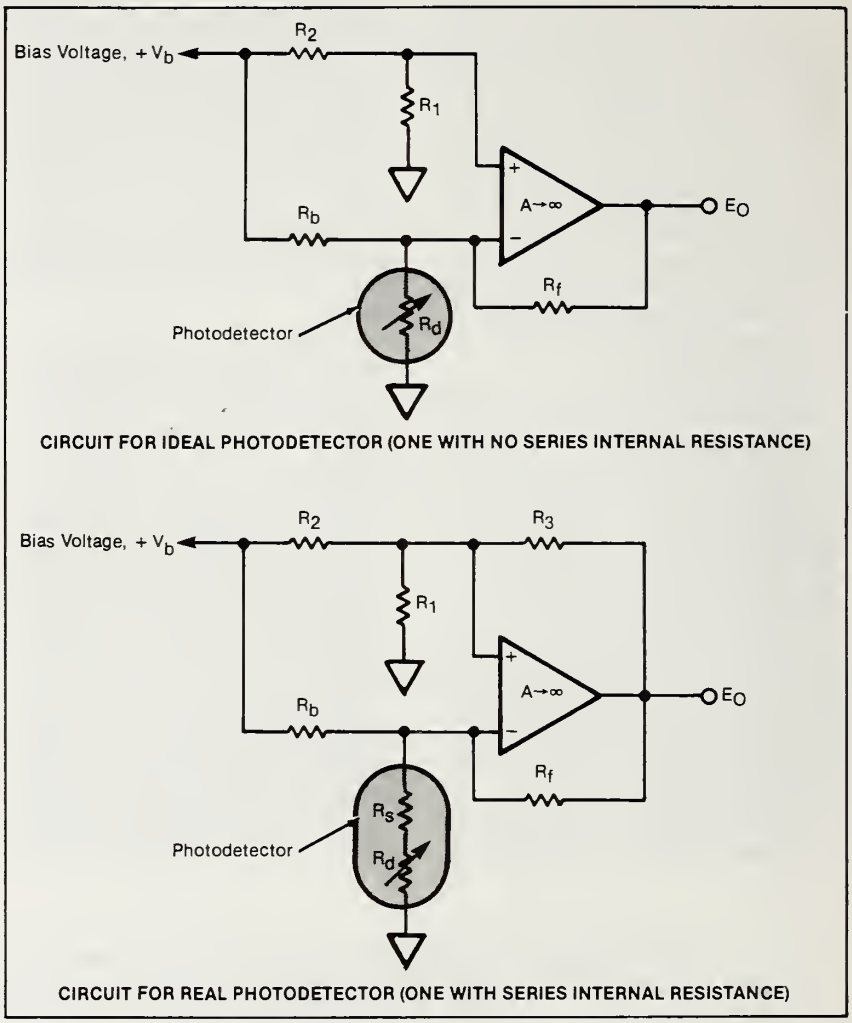

For an **Ideal Photoconductor,** a simple negative-feedback resistor R_f provides a nearly constant bias voltage on the device. For a **Real Photoconductor,** an additional resistor R_3 provides positive feedback for linearity.

This work was done by Rudolf A. Schindler of Caltech for **NASA's Jet Propulsion Laboratory.** *NPO-16055 / TN*

FOR ADDITIONAL INFORMATION: *Contact: Director, Technology Transfer Division, P.O. Box 8757, BWI Airport, MD. 21240; (301) 621-0100 Ext. 241*
REFER TO THE NUMBER LISTED AT THE END OF THE ARTICLE

NASA Tech Brief
National Aeronautics and Space Administration
NASA's Jet Propulsion Laboratory, Pasadena, California

Broadband Ultrasonic Transducers

A new geometry spreads out the resonance region of a piezoelectric crystal.

The bandwidth of a piezoelectric transducer can be greatly increased by fabricating the transducer with a nonuniform thickness. The greater bandwidth improves the accuracy of sonar and ultrasonic imaging equipment.

A conventional piezoelectric transducer consists of a crystal disk with metal films on its two flat, parallel surfaces. Applying an alternating electrical potential to the films expands and contracts the crystal rapidly so that it launches compressional elastic waves into the material around it. With its parallel faces, the crystal resonates at a narrow range of frequencies, and the ultrasonic waves it sets up in the surrounding medium have essentially the same narrow range.

In the new transducer, the crystal surfaces are made nonparallel. One surface may be planar; and the other, concave, for example. The geometry can be designed to produce a nearly uniform response over a predetermined band of frequencies and to attenuate strongly the frequencies outside the band (see figure).

The new transducer may make it unnecessary to use signal-processing circuits to compensate for the transducer frequency response or to use auxiliary circuits to modify the frequency spectrum of the voltage applied to the crystal. Such circuits would add to the cost of the transducer system.

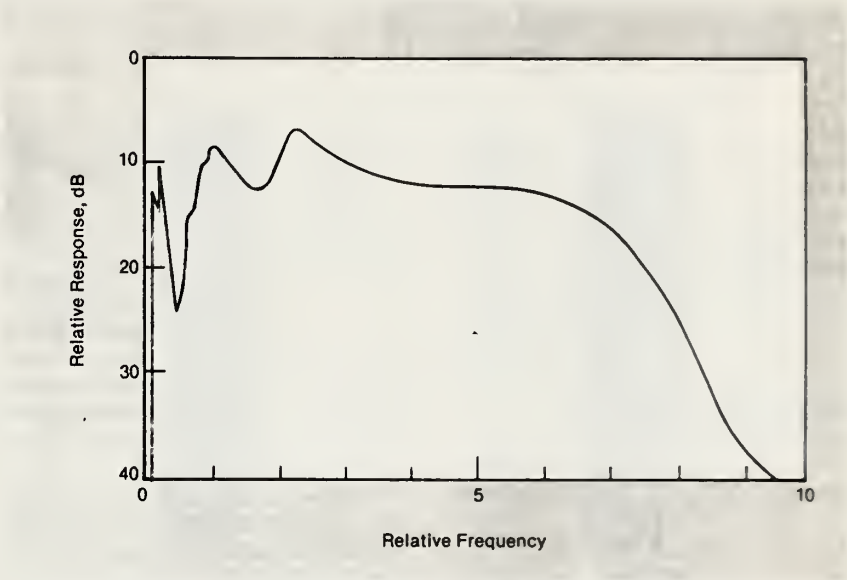

The **Frequency Response of a Plano-Concave Transducer** covers a broad range. The steep sides of the response curve show that the transducer cuts off extraneous frequencies cleanly.

This work was done by Richard C. Heyser of Caltech for **NASA's Jet Propulsion Laboratory.** *NPO-16590/TN*

FOR ADDITIONAL INFORMATION: *Contact: Director, Technology Transfer Division, P.O. Box 8757, BWI Airport, MD. 21240; (301) 621-0100 Ext. 241*
REFER TO THE NUMBER LISTED AT THE END OF THE ARTICLE

NASA Tech Brief
National Aeronautics and Space Administration
Lyndon B. Johnson Space Center, Houston, Texas

Ejection Mechanism for Circuit Boards

Damage to connectors is reduced and special tools are not needed.

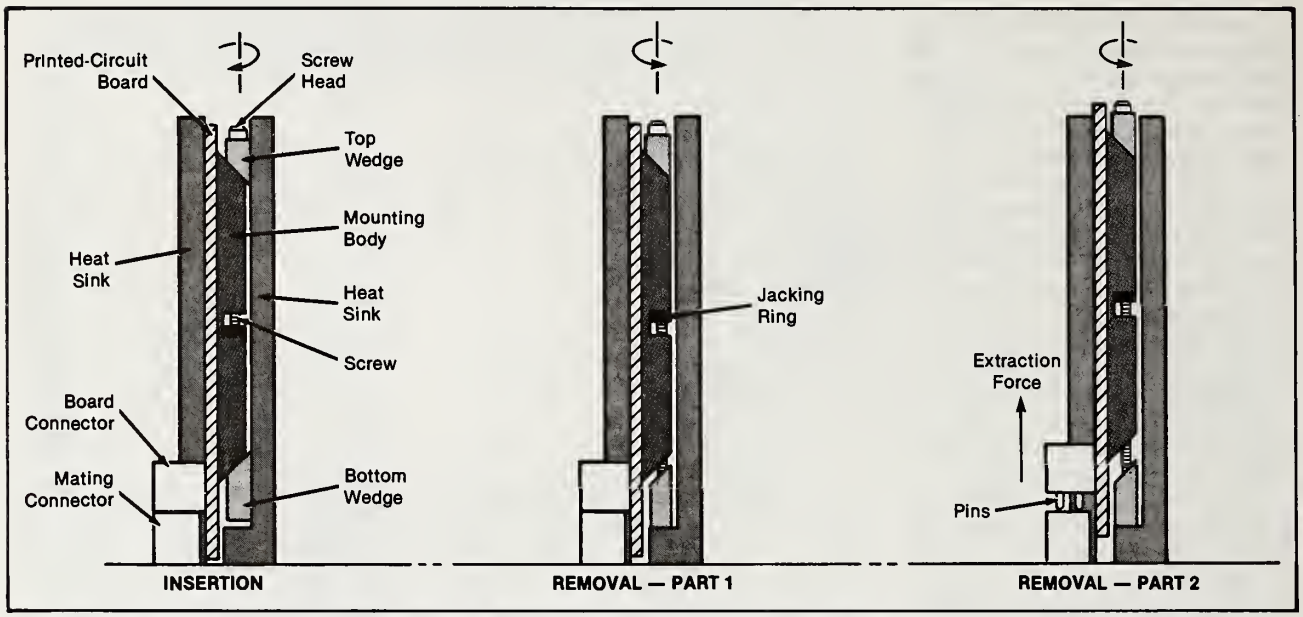

Clockwise Rotation of the Screw Tightens the Wedges against the mounting body and the right heat sink. Counterclockwise rotation of the screw drives the bottom wedge downward and the jacking ring upward, pulling the pins away from the mating connector.

A mechanism attached to a printed-circuit board partially ejects the board from an electronics assembly so that an operator can remove it for repair or replacement. A pulling tool, which could damage circuit patterns and components, is unnecessary.

A screw in the mechanism is turned to produce a jacking force that disengages the board from its mating connector. The force is parallel to the connector pins so that they do not become bent or broken. When disengaged, the board protrudes from the assembly and can readily be grasped by the operator.

The retainer/extractor screw, along with top and bottom wedges, is inserted in a mounting body, which is crimped onto the circuit board (see figure). To fasten the circuit board in a board frame, the operator inserts the board in the frame between two heat sinks, then turns the screw clockwise. The screw motion forces the wedges toward each other and against the wedging surfaces on the mounting body: This pushes the board against the left heat sink, and the wedges against the right heat sink, thereby locking the board in place and assuring thermal contact between the board and the heat sinks.

To remove the board from the frame, the operator turns the screw counterclockwise. This action drives the wedges away from the mounting body. Continued turning of the screw thrusts the bottom wedge against the frame and pushes the jacking ring upward against the mounting body. The ring thus raises the circuit board away from the frame and disengages it from the connector.

This work was done by Takeshi L. Houff and Douglas Shinno of Hughes Aircraft Co. for **Johnson Space Center.**
MSC-20763/TN

FOR ADDITIONAL INFORMATION: *Contact: Director, Technology Transfer Division, P.O. Box 8757, BWI Airport, MD. 21240; (301) 621-0100 Ext. 241*
REFER TO THE NUMBER LISTED AT THE END OF THE ARTICLE

NASA Tech Brief
National Aeronautics and Space Administration

Economic-Analysis Program for a Communication System

Prices and profits of alternative designs can be compared.

The objective of the Land Mobile Satellite Service Finance Report (LMSS) program is to provide a means for comparing alternative designs of LMSS systems. This program is actually a Multiplan worksheet program. The labels used in the worksheet were chosen for a satellite-based cellular communication service, but the analysis is not restricted to such cases.

A comprehensive financial model is used to calculate a figure of merit, which can be used to compare effects of equipment and operating costs, pricing strategy, and customer demand for different systems.The program also calculates the price that a company would have to charge customers to meet all its expenses and make a specified profit. A price estimate can be obtained for almost any service that is heavily dependent on capital investment and which has operating costs that depend on the amount of service sold.

The economic analysis has two main components: supplier finances and customer finances. Supplier finances include amortization, interest, insurance, taxes, and operating and maintenance expenses. Customer finances include usage rate, subscription fees, equipment costs, and estimated traffic. Prices can be defined as real or nominal to account for the effects of escalation and inflation, and the profits can be regulated or unrestricted.

LMSS is written for interactive execution with Multiplan (version 1.2) and has been implemented on an IBM PC series computer operating under DOS (version 2.11). The LMSS worksheet program has a space requirement of approximately 38K of 8-bit bytes. This worksheet program was developed in 1984.

This program was written by R. G. Chamberlain of **NASA's Jet Propulsion Laboratory.** *NPO-16606 /TN*

FOR ADDITIONAL INFORMATION *CONTACT:*

COSMIC®
112 Barrow Hall
University of Georgia
Athens, GA 30602
(404) 542-3265

MANUFACTURING TECHNOLOGY NOTE

U.S. ARMY MATERIEL COMMAND

Deputy Chief of Staff for Manufacturing Technology, Alexandria, VA

Project Number: 15263749D462 Filing Code : 466077

Laser-Induced Optical Degradation

The performance of irradiated optical systems is modeled.

Models developed by the U.S. Army Ballistic Research Laboratory predict (a) laser-irradiation-caused physical damage to an optical system, (b) the optical aberrations corresponding to the physical damage, and (c) the point-spread function (or optical-transfer function) for the optical system with laser-induced aberrations. The general methodology used to evaluate glass damage by laser irradiation, is shown in the figure.

The optical aberrations caused by physical damage are represented as a local change in amplitude and phase of the light. Surface cracks effectively reduce the local transmission to zero. Exfoliation reduces the transmission slightly, but its main effect is to introduce a random phase-difference between different flakes. Vaporization does not affect transmission, but it introduces potentially large phase differences over distances associated with variations in the vaporization dynamics.

The point-spread function has been calculated for a simple optical system that has optical aberrations produced by laser irradiation. The main features of the point-spread function are (a) a central spike with width determined by the overall aperture dimensions and height proportional to the square of the undamaged area, and (b) a damage halo with width determined by the characteristic size of the individual damage elements and total height proportional to the incoherent sum of the square of the area of each damaged element.

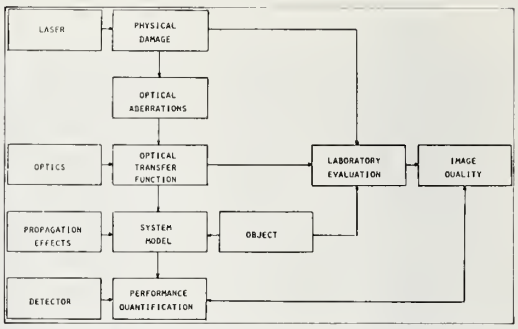

This **General Methodology** was used to evaluate glass damage by laser irradiation.

Project officer Paul H. Dietz
(301) 671-3447 or AV 283-3447.

FOR ADDITIONAL INFORMATION:

You can learn more details about this technology by ordering the NTIS report(s):
Theoretical Modeling of Laser Induced Optical Degradation.
Order number: AD-A155302/NAA
Price code: A06
Order from:
National Technical Information Service
5285 Port Royal Road
Springfield, VA 22161

This document was prepared under the sponsorship of the U.S. Government. Neither the United States Government nor any person acting on behalf of the United States Government assumes any liability resulting from the use of the information contained in this document, or warrants that such use will be free from privately owned rights.

NBS technology update

National Bureau of Standards
U.S. Department of Commerce
Gaithersburg, MD 20899

Determining Microwave Power Delivered to an Antenna

In laboratory settings as well as in the field, it is often desirable, even essential, to know the net power delivered to a microwave horn or other antenna. For example, standard-gain horns are used to establish known electromagnetic fields in anechoic chambers, and uncertainties in knowing the net delivered power cause uncertainties in knowledge of the fields. NBS has developed a procedure for measuring the net delivered power and evaluating its uncertainty. This measurement and computation procedure also can be used to self-calibrate the system by placing terminations of known characteristics, such as shorts or matched loads, on certain ports.

FOR ADDITIONAL INFORMATION:

You can learn more details about this technology by ordering the NTIS report(s):

A Radio-Frequency Power Delivery System: Procedures for Error Analysis and self-Calibration. (TN 1083)
Order number: PB86-115680
Price code: A03

Order from:
National Technical Information Service
5285 Port Royal Rd.
Springfield, VA 22161

NASA Tech Brief
National Aeronautics and Space Administration
Goddard Space Flight Center, Greenbelt, Maryland

Electro-optical Tuning of Fabry-Perot Interferometers

A compact unit can operate much faster than conventional piezoelectric scanners.

A proposed electro-optical method of tuning or scanning the passband of a Fabry-Perot interferometer can be much faster than previous methods and employ more compact equipment. In a Fabry-Perot interferometer, two parallel glass plates, separated by a few centimeters, are partly silvered on their inner surfaces so that an incoming light beam is repeatedly reflected between them before it is transmitted to instrumentation. Until now, this type of interferometer has been tuned by the adjustment of separation between the plates. This separation could be changed either by a voltage applied to a piezoelectric transducer on one of the mirrors or by a change in pressure of a gas between the mirrors.

Piezoelectric scanners, however, are limited in their tuning speeds. For visible light, a piezoelectric scanner takes about 10 milliseconds per interferometer order, and scanning time is longer for light of longer wavelengths. Moreover, piezoelectric scanners add to the interferometer size and become bulkier when greater scanning range is needed. Pressure scanners are even slower than the piezoelectric models and require gas-handling equipment.

In one version of the proposed scanner, a Pockels cell crystal is placed between the mirrors of the Fabry-Perot interferometer (see figure). Such a cell, usually made of a birefringent material like potassium dihydrogen phosphate, changes its refractive index under an applied electric field. The Pockels crystal is oriented so that one of its electrically induced axes is parallel to the plane of polarization of the incident light beam. A voltage applied across the crystal surfaces changes the optical path length between the mirrors without changing the gap between them. The interferometer therefore can be scanned by changes in voltage on the Pockels cell.

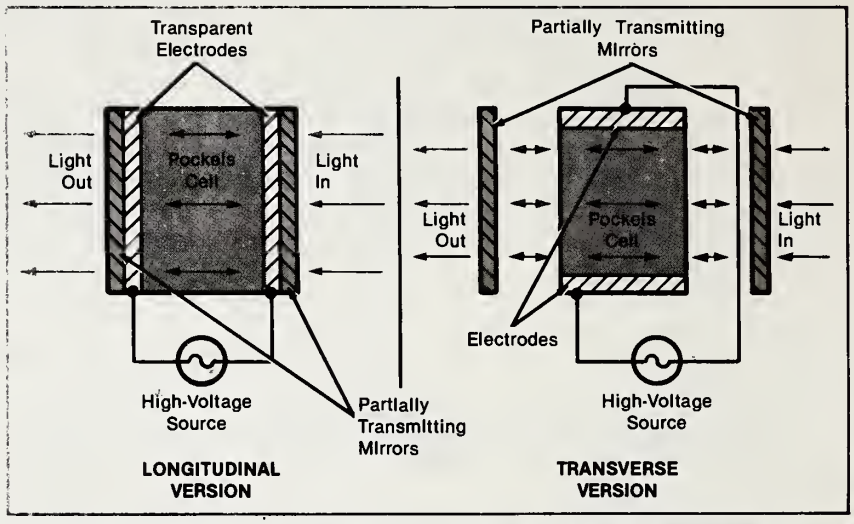

A High Voltage creates an electric field in a Pockels cell, changing its refractive properties. The cell therefore changes the optical path length between the mirrors without mechanically moving anything in the gap. The high voltage can be varied rapidly to scan the interferometer. The voltage is applied longitudinally or transversely, depending on the type of Pockels cell.

The voltage is applied through electrodes on opposite faces of the cell. The mirrors may be affixed directly to the cell faces. If a longitudinal electric field is used and the electrodes are not only conductive but also transparent to the incident light, these electrodes can be deposited as films over the entire end faces of the crystal. (Indium tin oxide, for example, is conductive and is transparent at visible wavelengths.) The electrodes would then create a highly-uniform electric field within the crystal, and the Pockels cell could be made very thin. Reflective film could be deposited directly on the electrodes, and the entire interferometer would be compact.

The new electro-optic scanner would scan a given range in one-millionth the time of a piezoelectric scanner — tens to hundreds of nanoseconds per interferometer order. At the same time, its small size would reduce the size of an interferometer.

This work was done by Geary K. Schwemmer of **Goddard Space Flight Center.** *GSC-12971/TN*

FOR ADDITIONAL INFORMATION: *Contact: Director, Technology Transfer Division, P.O. Box 8757, BWI Airport, MD. 21240; (301) 621-0100 Ext. 241*
REFER TO THE NUMBER LISTED AT THE END OF THE ARTICLE

1064 Photovoltaic Powered Lights Cut Energy System Costs
1065 Molten Carbonate Fuel Cells
1066 Life of Fluorescent Lamps Operated at High Frequencies with Solid-State Ballasts
1067 Electrodeless High-Intensity-Discharge Lamp Study
1068 Phosphoric Acid Fuel Cells
1069 Fuel Gas Cleanup for Molten Carbonate Fuel Cells
1070 Heat-Pipe Array for Large-Area Cooling—High rates of heat transfer are anticipated.
1071 Improved High/Low Junction Silicon Solar Cell—The air-mass-zero open-circuit voltage is increased to 650 mV.
1072 Lithium-Counterdoped Solar Cells—Resistance to damage by energetic electrons is increased.

Other items of interest

1077 A Simplified Model of Thermal Comfort in Buildings

NECL
Techdata Sheet
Naval Civil Engineering Laboratory, Port Hueneme, CA 93043

Photovoltaic Powered Lights Cut Energy System Costs

Harnessing sunshine to generate electricity for security lights on AA&E bunkers at U.S. DOD facilities can reduce system costs by 50%. In 1985, 30 photovoltaic-powered security light systems were installed at Navy facilities in California, New Mexico, and Maine.

In 1982 the Department of Defense issued regulations that all arms, ammunition and explosive (AA&E) bunkers should be lighted. Since the bunkers are located in remote areas, the cost of installing utility grids to the bunker site was prohibitive in most cases. Research in the use of photovoltaic (solar) cells to provide the necessary power was undertaken by the Naval Civil Engineering Laboratory (NCEL). The capital cost savings for using reliable photovoltaic (PV) power can be a factor of 2 over using more conventional power sources.

Each lighting system consists of three subsystems: (1) the photovoltaic array power source, (2) battery storage with regulator, and (3) lamp. The PV array generates DC electricity during daylight hours (some power is generated even in cloudy weather). This power is provided to the battery storage subsystem any time the battery is less than fully charged. The regulator adjusts the power flow from the PV array and to the lamp after the sun goes down. The lamp used for the 30 systems installed during 1985 was a 13-watt fluorescent lamp with a 12-VDC ballast. The systems were installed in widely diverse areas of the United States (NWS Fallbrook, Calif.; NAS Brunswick, Maine; and NOMTC White Sands, N.M.) to gain operational experience under varying climate and environmental conditions. Availability of sunshine varies widely from region to region. However, there are no regions, including Antarctica, where PV is not now being used to provide reliable electric power.

Figure 1. PV powered security light installed at NWS Fallbrook, California.

Designing a PV power system requires consideration of the solar resource, the electrical demand, and the likelihood of

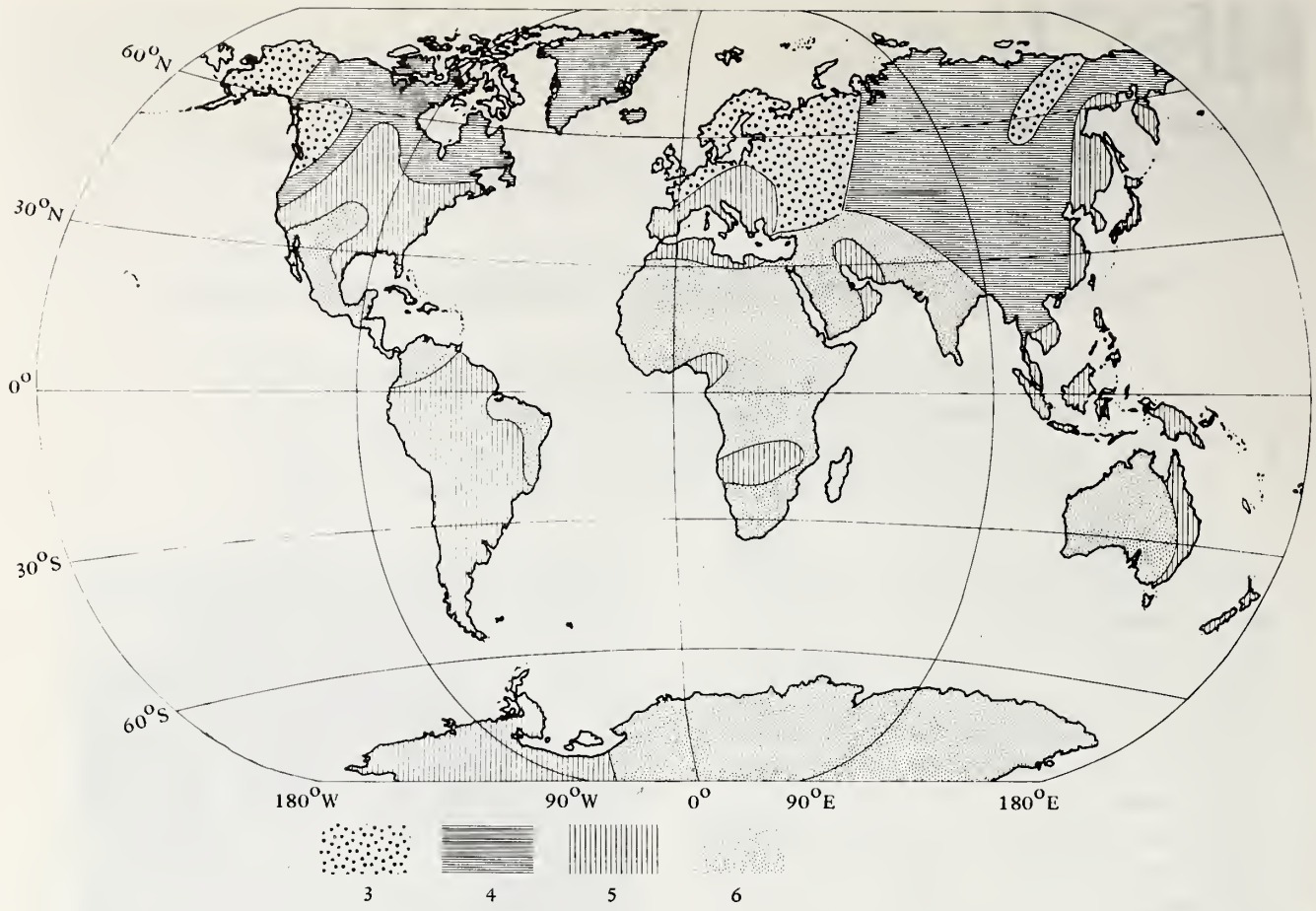

Figure 2. Photovoltaic power available - kilowatt-hours per day.

successive cloudy days. Optimum designs require specific information for each of these parameters. However, many successful and cost-effective designs can be developed using general guidelines. Figure 2 gives the projected daily energy output, in kilowatt-hours, of a 1-kW "rated" PV array located anywhere in the world. Specific long-term weather data from over 1,100 sites were used to generate the map. If the electrical demand is known, the amount of PV power necessary can be easily calculated. Add battery storage and a lamp and the result is a reliable security light system that can be installed anywhere.

To date, operational experience with photovoltaic lighting systems has been good. The 30 systems installed during 1985 have performed flawlessly for several months. System development tests on prototype systems at NCEL have shown that the concept is sound for a number of illumination schemes with the fluorescent lamp being most adaptable in terms of durability and tolerance of ambient conditions.

O&M concerns for photovoltaic lighting systems address maintaining electrolyte levels and assuring that the voltage regulator is working. System failures can be easily resolved through standard circuit check out procedures.

For Additional Information, Contact

Mr. G. H. Watson, Code L73,
Naval Civil Engineering Laboratory,
Port Hueneme, CA 93043; (805) 982-4207
Refer to Techdata Sheet 86-03/TN

energygram®

Molten Carbonate Fuel Cells

DOE/TIC/EG-86/055
OFFICE OF SCIENTIFIC AND TECHNICAL INFORMATION

This technical note was based on an Application Assessment Record from the Morgantown Energy Technology Center, Office of Fossil Energy, for the U.S. Department of Energy.

METC
Morgantown Energy Technology Center

Technology Description. The incentive for the U.S. Department of Energy fuel cell program is a need for modular, low-cost, electricity generating capacity. A molten carbonate fuel cell (MCFC) system has a projected operating efficiency of 45 to 60 percent from fuel to AC power. The MCFC is fueled by natural gas or synthetic gas at 1,200°F and can be a direct fueled (internal reforming) system. This system avoids the use of noble metal catalyst and can use carbon monoxide, which poisons lower temperature fuel cells. This capability coupled with the higher operating temperature makes the MCFC an attractive fossil fuel option.

A. General Electric: The contract was completed.

B. United Technologies Corporation: The subscale stack was operated for over 5,000 hours. Results of this test allow life projection of full-size stacks to at least 20,000 hours.

C. Energy Research Corporation: Demonstrated internal methane reforming capability with single cells.

D. Institute of Gas Technology: Completed model of effects of sulfur on MCFC.

Why Is This Better Than Existing Technology? More efficient method of converting fossil fuels to electric power; nonpolluting conversion of fuel to electric power; more efficient and less complex than phosphoric acid fuel cell.

Stage of Development. Commercialization projected in late 1990's or early 2000's.

Potential Uses and Spinoffs. Electricity utilities, on-site electricity generation.

FOR ADDITIONAL INFORMATION

DOE report(s):
Morgantown Energy Technology Center
Fuel Cells Topical Report.
Report number: DOE/METC/SP-203/NAB
Order number: DE84003076/NAB
Price: $11.95
Morgantown Energy Technology Center
Fuel Cells Technology Status Report.
Report number: DOE/METC-85/0223/NAB
Order number: DE85008591/NAB
Price: $11.95

Order from:
National Technical Information Service
5285 Port Royal Road
Springfield, VA 22161

For additional information, contact:
Frank D. Gmeindl
Morgantown Energy Technology Center
P.O. Box 880
Morgantown, WV 26507-0880
Telephone No.: (304) 291-4751

energygram®

Life of Fluorescent Lamps Operated at High Frequencies with Solid-State Ballasts

DOE/TIC/EG-86/003
OFFICE OF SCIENTIFIC AND TECHNICAL INFORMATION

This technical note was based on research conducted by Lawrence Berkeley Laboratory for the U.S. Department of Energy.

Lawrence Berkeley Laboratory

When solid-state fluorescent ballasts were developed, there was concern that high-frequency operation of the lamps might adversely affect their service life. This problem was studied by measuring the life of 40-watt, F-40, T-12, rapid-start fluorescent lamps operated by two-lamp solid-state ballasts.

The lamp had a rated life (the period after which 50% of a group of lamps fails) of 20,000 hours when operated with a certified ballast on a cycle of 3 hours on/20 minutes off or more than 30,000 hours for continuous operation.

The recommended procedures were used to measure the lamp life. The key operating factors included the open-circuit peak voltage, lamp current, filament voltages, and current crest factor. Results of testing later ballast models showed a progressive improvement in the life of the lamps with improved design; however, the early models did not approach the lamp manufacturer's life rating.

It was found that the lamps can achieve the rated life if they are operated at a high frequency at full light output or dimmed to 20% of the full output. Full rated life occurs only if the solid-state ballast is designed to operate the lamp properly.

When operated at high frequency instead of at 60 Hz, the anode fall is reduced from 17 to 6 V. The present American National Standards Institute specified ranges may have to be amended with respect to filament power and arc current to maintain the rated life. High-frequency operation of the lamps does not influence the rate of lumen depreciation; this value depends on the lamp loading and not on the operational frequency.

The results also show that fluorescent lamps can be suitably operated in a dimmed mode, but full filament power must be supplied to maintain the rated lamp life. Lamps operated with the new solid-state ballast maintained their normal life.

FOR ADDITIONAL INFORMATION

DOE report(s):
Life of Fluorescent Lamps Operated at High Frequencies with Solid-State Ballasts.
Report number: LBL-19778/NAB
Order number: DE85017647/NAB
Price: $9.95

Order from:
National Technical Information Service
5285 Port Royal Road
Springfield, VA 22161

For additional information, contact:
R. R. Verderber
Lighting Systems Research Group
Lawrence Berkeley Laboratory
University of California
Berkeley, CA 94720

energygram®

Electrodeless High-Intensity-Discharge Lamp Study

DOE/TIC/EG-86/001
OFFICE OF SCIENTIFIC AND TECHNICAL INFORMATION

This technical note was based on research conducted by Lawrence Berkeley Laboratory for the U.S. Department of Energy.

Lawrence Berkeley Laboratory

The purpose of the study was to demonstrate the operation of high-intensity-discharge (HID) lamps excited with solenoidal electric fields (SEF). The SEF/HID lamps have no electrodes; their arc current is continuous and closes upon itself within the arc containing the envelope. The electric field is created by a changing magnetic field; therefore it is solenoidal or divergence-free.

Current commercial HID lamps use electrodes that are responsible for many design and performance limitations, such as a significant consumption of lamp power. Loss of activator material, dissolution of tungsten in the molten silicon condensate, etc., limit the service life of the lamps. Problems arise also because of the incompatibility between the fill materials and the electrodes.

There is a need to develop an electrodeless lamp design that would avoid the electrode-related difficulties. However, such a lamp presents other shortcomings: heat loss from the discharge to the inner wall of the quartz toroid which results in excessive heating of the wall at high power loading. In the current work, the discharge envelope was redesigned to be in the shape of a pill box, having no inner wall, locating the primary excitation coil somewhat removed from the plasma, with the magnetic coupling path consisting partly of air.

In the course of this study, HID lamps were successfully excited by solenoidal electric fields in the range from about 400 to 1000 W with an operational frequency of 13.56 MHz in the IMS (Industrial, Medical, Scientific) band. Power loss was high and thus reduced the overall system efficacy considerably. Difficulty was encountered getting into the solenoidal mode of operation. The calculated efficiencies were found to agree with the positive column efficiencies of conventional HID lamps containing only mercury and with additives of sodium, thallium, and scandium iodide.

Even though good efficacies with stable operation are indicated, there is need to design a practical ballast/matching network/coil/lamp assembly with emphasis on mechanical ruggedness and good light release and control.

FOR ADDITIONAL INFORMATION

DOE report(s):
Electrodeless HID Lamp Study: Final Report.
Report number: LBL-19035/NAB
Order number: DE85010626/NAB
Price: $11.95

Order from:
National Technical Information Service
5285 Port Royal Road
Springfield, VA 22161

For additional information, contact:
J. M. Anderson
Lighting Systems Research Group
Lawrence Berkeley Laboratory
University of California
Berkeley, CA 94720

energygram®

Phosphoric Acid Fuel Cells

DOE/TIC/EG-86/053
OFFICE OF SCIENTIFIC AND TECHNICAL INFORMATION

This technical note was based on an Application Assessment Record from the Morgantown Energy Technology Center, Office of Fossil Energy, for the U.S. Department of Energy.

METC
Morgantown Energy Technology Center

Technology Description. The incentive for the U.S. Department of Energy fuel cell program is a need for modular, low-cost, electricity generating capacity. The phosphoric acid fuel cell (PAFC) has a projected efficiency of 40 percent from fuel to AC power. The PAFC converts a hydrocarbon fuel (hydrogen from natural gas or naphtha) and an oxidant (air) at reaction sites (electrodes) into DC electricity. The PAFC operates around 400°C with a phosphoric acid electrolyte. Recovery of reaction heat for cogeneration of power will also markedly increase overall fuel use efficiencies.

A. On-Site Programs: One METC on-site program is a 40 kW On-Site Fuel Cell Field Test Project. A modified Interagency Agreement has been signed with the Department of Defense to test three power plants on three military sites. A fourth power plant will be tested in Alaska under a separate agreement. Forty-six power plants were acceptance tested, installed in utility/users sites, and operated in excess of 230,000 load hours.

The second on-site program is the IFC Components Development Project. A new configuration PAFC with enhanced electrolyte-retention capabilities was successfully developed through the 3.7-ft^2 stage and was operated for 4,000 hours with initial performance at the on-site program goal. An improved on-site PAFC water coolant system design has been successfully demonstrated at the 3.7-ft^2 stack-stage with no evidence of deterioration, corrosion, or plugging. A development reformer has been fabricated and has been operated under various burner and tube configurations to arrive at the most efficient on-site design for a 200-kW power plant.

The third on-site program is being conducted by Englehard Industries. The first full-area, full-height, 25-kW, dielectric-cooled stack has been fabricated and operated on pure hydrogen and reformed methanol at below goal performance levels.

B. Electric Utility Programs: At Con-Ed, power plant was dismantled, the equipment was sent back to the manufacturer (IFC), the Con-Ed site was restored, and the final report is being prepared by Con-Ed.

At Westinghouse, a total of 32 developmental 9- and 10-cell stacks have been built during the program. Testing is complete with 27 of the stacks, and 5 are presently being tested. The beginning of the life performance goal (690 mV) was demonstrated with 3 stacks. The degradation rate goal (8 mV/1,000 hours) was demonstrated in short-term (~ 1,000 hours) tests on 3 stacks. Operating time in excess of 2,900 hours has been attained by a 10-cell stack under test. Six additional stacks have demonstrated more than 1,300 hours each.

As part of the IFC Electric Utility Project, the second 10-ft^2 stack, having 28 cells, exceeded its test goal of 1,500 hours and has shown excellent performance. A 30-cell, 3.7-ft^2 endurance stack exceeded its operating goal of 15,000 hours with stable operation. A third 10-ft^2 stack, having 28 cells, was built and has begun testing. Cell seal development is complete. Tolerance to pressure imbalance was increased from $^1/_6$ psi to approximately 4 psi. A new contract was awarded to IFC to develop new technologies in the areas of the fuel reformer, the inverter, cells at the subscale level, and liquid coolant treatment. The government has approved a novation agreement with United Technologies. This results in recognition of a new company, International Fuel Cells (IFC), formed by a venture agreement between United Technologies and Toshiba.

Why Is This Better Than Existing Technology? More efficient method of converting fossil fuels to electric power, nonpolluting conversion of fuel to electric power.

Stage of Development. Operation and sale of prototype plants are projected in 1988. Commercialization is projected in early 1990's.

Potential Uses and Spinoffs. Electricity utilities, on-site electricity generation.

FOR ADDITIONAL INFORMATION

DOE report(s):

Morgantown Energy Technology Center
Fuel Cells Topical Report.
Report number: DOE/METC/SP-203/NAB
Order number: DE84003076/NAB
Price: $11.95
Morgantown Energy Technology Center
Fuel Cells Technology Status Report.
Report number: DOE/METC-85/0223/NAB
Order number: DE85008591/NAB
Price: $11.95

Order from:

National Technical Information Service
5285 Port Royal Road
Springfield, VA 22161

For additional information, contact:

Edmund F. Beyma
Morgantown Energy Technology Center
P.O. Box 880
Morgantown, WV 26507-0880
Telephone No.: (304) 291-4064

energygram®

Fuel Gas Cleanup for Molten Carbonate Fuel Cells

DOE/TIC/EG-86/056
OFFICE OF SCIENTIFIC AND TECHNICAL INFORMATION

This technical note was based on an Application Assessment Record from the Morgantown Energy Technology Center, Office of Fossil Energy, for the U.S. Department of Energy.

METC
Morgantown Energy Technology Center

Technology Description. Molten carbonate fuel cells require fuel sources with low levels of sulfur and other trace contaminants. Current research is aimed at reducing the levels of these substances in hot, low-Btu coal-derived gases. There are several processes that are being developed to remove these contaminants through the use of various sorbents: zinc ferrite, mixed metal oxides of cobalt titanate, and other novel sorbents that may achieve high desulfurization efficiency at high temperatures and pressure.

Zinc ferrite is a zinc oxide-based regenerable sorbent that is capable of removing sulfur compounds (H_2S and COS) to the 1 to 10 ppm range. It has proved to be efficiently regenerated with mixtures of air and steam or nitrogen diluent.

A solid supported molten salt (SSMS) hot gas cleanup process has been developed to reduce 200 parts per million by volume (ppmv) HCl and 6,000 ppmv sulfur compounds to less than 1 ppmv. It would operate at or above the MCFC temperature (1,200°F) (60 to 200 psig) and in the presence of sufficient steam and/or carbon dioxide to prevent carbon deposition from carbon monoxide. A regeneration gas would be produced, from which elemental sulfur could be economically recovered.

In the laboratory-scale study, cobalt titanate has been identified as a potentially suitable sorbent for use with coal-derived fuel gases in the mixed metal oxide high-temperature desulfurization process. The ceramic-supported molten, alkali carbonate sorbent has been shown to be able to reduce the HCl content of a high-temperature fuel gas to less than 1 ppmv and to have an exceptional capacity for HCl.

The experimental study has established the feasibility of using nickel sorbents for hot trace contaminant removal from coal gas to sub-ppm level. Chemisorption and desorption characteristics of hydrogen sulfide and arsine on different nickel catalysts have been measured between 930 and 1,300°F.

These nickel catalysts can maintain the desired cleanup levels for sulfur and arsenic with a sorption capacity of 2,000 to 15,000 ppmv sulfur and in excess of 100,000 ppmv arsenic, respectively. Thermogravimetric analyzer tests at 1,200°F have shown that carbon soot formation does not occur on fuel cell nickel electrodes in the presence of steam.

The screening of 10 catalysts to test their effectiveness in destroying coal tars in low-Btu gas has been completed. Tests were conducted at pressures of 10 and 18 atmospheres and temperatures from 850 to 1,200°F. The average tar conversion with no catalyst was 31 percent. Several catalysts of about equal activity for tar destruction have been identified: Pt/LZ-Y82, LZ-Y82, Pd/Y-zeolite on alumina, CoMo/LZ-Y82, Y-zeolite on SiO_2-Al_2O_3, CoMo on Al_2O_3, Fe_2O_3, Bauxite, NiW on SiO_2-Al_2O_3, and NiCuMo on SiO_2-Al_2O_3. Tar conversion with active catalysts has been determined at increased pressure and temperature. Conversion increased significantly at the higher pressure and improved only slightly with increased temperature.

Why Is This Better Than Existing Technology? Conventional cleanup has high capital and operating costs. It also creates wastewater streams that require treatment to remove pollutants. Hot gas cleanup avoids the wastewater problem. High-temperature cleanup of coal gas for molten-carbonate fuel-cell power-plant application would yield considerable thermal efficiency gains over conventional water quench and cold gas cleanup.

Stage of Development: Basic science.

Potential Uses and Spinoffs: Coal gas cleanup for gas turbine firing.

FOR ADDITIONAL INFORMATION

DOE report(s):

Morgantown Energy Technology Center
Advanced Environmental Control Technology Topical Report.
Report number: DOE/METC/SP-194/NAB
Order number: DE83009222/NAB
Price: $11.95

Mortangown Energy Technology Center
Proceedings of the Fifth Annual Contractors Meeting on Contaminant Control in Coal-Derived Gas Streams.
Report number: DOE/METC-85/6025/NAB
Order number: DE85013703/NAB
Price: $40.95

Order from:

National Technical Information Service
5285 Port Royal Road
Springfield, VA 22161

For additional information, contact:

Suresh Jain
Morgantown Energy Technology Center
P.O. Box 880
Morgantown, WV 26507-0880
Telephone No.: (304) 291-4446

NASA Tech Brief
National Aeronautics and Space Administration
Lyndon B. Johnson Space Center, Houston, Texas

Licensing Opportunity

Heat-Pipe Array for Large-Area Cooling

High rates of heat transfer are anticipated.

A prototype evaporative cold plate would gather waste heat from equipment mounted on it. The plate is made by welding together the flanges of several sections of heat pipe (see figure). The heat pipe is a slightly modified version of a type used in heat-rejecting radiator elements.

The heat pipe contains a vapor channel, a liquid channel, and a porous nickel felt wick connecting the channels. The walls of the vapor channel contain 160 circumferential grooves per inch (63 grooves per centimeter). As the heat-transfer liquid evaporates from the grooves, more liquid is drawn up from the liquid channel through the wick.

As the liquid depletes, an ultrasonic sensor detects its absence. The sensor signals a solenoid valve to open to fill the liquid channel from a pressurized supply. When the liquid channel is replenished, the sensor signals the valve to close.

Evaporation occurs continuously while the valve cycles on and off. Vapor from the vapor channels in the separate heat pipes is combined into a single outlet header, which directs it to a condenser. The vapor header contains a liquid trap to catch any liquid that is carried into the vapor space. Two liquid headers on each end of the plate assure proper filling and liquid flow to the more-heavily-loaded plate sections.

The plate is expected to transfer heat at high rates by surface evaporation from the many sites in the grooved channels. Heat fluxes in zero gravitation are expected to be 2 W/cm^2 for refrigerant 11 (CCl_3F) and substantially higher for ammonia. Since the plate separates the liquid and vapor phases at the inlet and outlet ports, it eliminates the complexities and uncertainties of two-phase flow in zero gravity. On Earth, the inlet valve enables the plate to operate at relatively-large height differences with other plates in the same system.

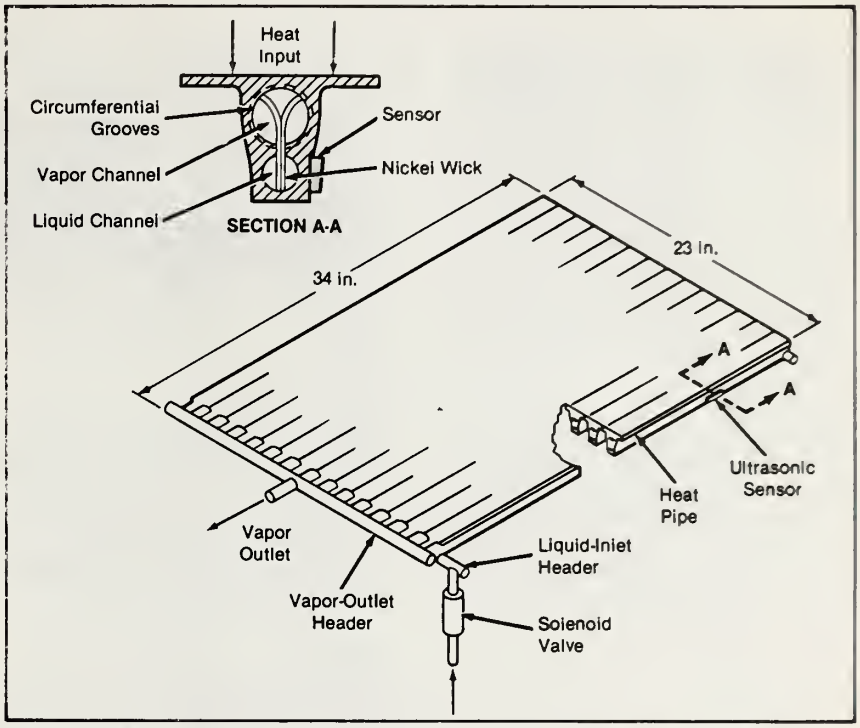

The Cold Plate consists of sections of heat pipe welded together side-by-side at the flanges.

This work was done by Fred Edelstein and Richard F. Brown of Grumman Aerospace Corp. for **Johnson Space Center.**

Inquiries concerning rights for the commercial use of this invention should be addressed to the Patent Counsel, Johnson Space Center Refer to MSC-20946/TN

William Chmylak
Lyndon B. Johnson Space Center
Mail Code AL32
Houston, TX 77058
(713) 483-3809

FOR ADDITIONAL INFORMATION: *Contact: Director, Technology Transfer Division, P.O. Box 8757, BWI Airport, MD. 21240; (301) 621-0100 Ext. 241*
REFER TO THE NUMBER LISTED AT THE END OF THE ARTICLE

NASA Tech Brief
National Aeronautics and Space Administration
Lewis Research Center, Cleveland, Ohio

Licensing Opportunity

Improved High/Low Junction Silicon Solar Cell

The air-mass-zero open-circuit voltage is increased to 650 mV.

A method has been developed to raise the value of the open-circuit voltage in silicon solar cells by incorporating a high/low junction in the cell emitter.

The power-conversion efficiency of the low-resistivity silicon solar cell is considerably less than the maximum theoretical value mainly because the open-circuit voltage is smaller than simple p/n junction theory predicts. With this method, the air-mass-zero open-circuit voltage has been increased from the 600 mV level to approximately 650 mV.

The figure gives a cross-sectional schematic view of the proposed cell. Shown is the p-type substrate and the n-type emitter comprising a low region and a high-electron-accumulation region. An oxide layer on the illuminated surface contains a high positive charge. Shallow n^+ contact diffusion regions underlie each of the one or more aluminum emitter contacts, and an ohmic contact underlies the p region.

A p/n junction exists between the emitter region and the substrate. A high/low junction has been formed between the high-electron-accumulation region and the low emitter region. An aluminum metal contact is in ohmic contact with the emitter, and a shallow n^+ diffusion contact is made under this metalized portion of the top surface area. The aluminum emitter contact covers no more than 5 to 10 percent of the surface area.

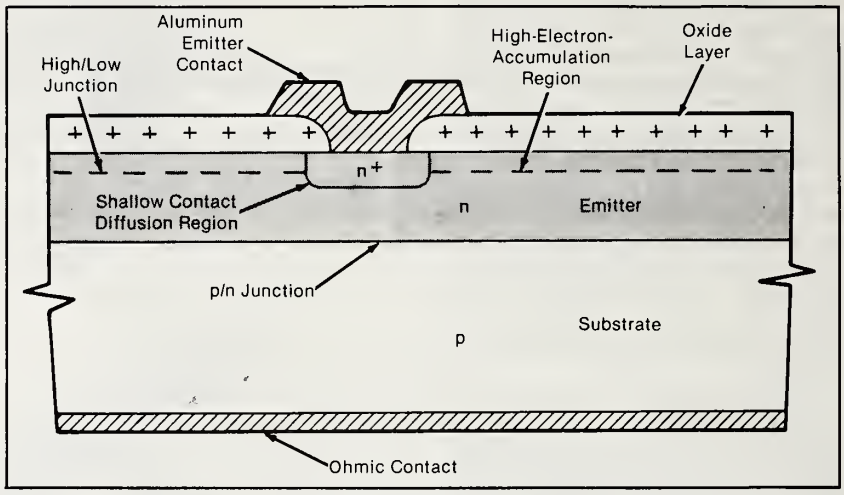

In an **Oxide-Charge-Induced High/Low Emitter Solar Cell**, electron accumulation layer is induced by a positive charge.

Provided in the proposed solar cell is a suppression of dark emitter current and an increase of short-circuit current. The emitter is less heavily doped — preferably in the $\sim 10^{18}$ to 10^{19} cm^{-3} range — compared to emitters of conventional cells, which are typically doped to about 10^{20} cm^{-3}. A heavily doped emitter region has the disadvantage that the dark emitter recombination is so large that it limits the maximum open-circuit voltage to about 600 mV. The high/low emitter suppresses the dark emitter recombination current, resulting in power-conversion efficiencies significantly higher than were previously achieved.

This work was done by Arnost Neugroschel, Shing-Chong Pao, Fred A. Lindholm, and Jerry G. Fossum of the University of Florida for **Lewis Research Center.**

Inquiries concerning rights for the commercial use of this invention should be addressed to the Patent Counsel, Lewis Research Center
Refer to LEW-13618/TN

Gene E. Shook
Lewis Research Center
Mail Code: 60-2
21000 Brookpark Road
Cleveland, OH 44135
(216) 433-5753

FOR ADDITIONAL INFORMATION: *Contact: Director, Technology Transfer Division, P.O. Box 8757, BWI Airport, MD. 21240; (301) 621-0100 Ext. 241*
REFER TO THE NUMBER LISTED AT THE END OF THE ARTICLE

NASA Tech Brief
National Aeronautics and Space Administration
Lewis Research Center, Cleveland, Ohio

Licensing Opportunity

Lithium-Counterdoped Solar Cells

Resistance to damage by energetic electrons is increased.

Future space missions will require increased end-of-life output power from solar-cell arrays. To achieve this goal, researchers have been seeking ways to minimize the degrading effects of space radiation on solar cells. A new technique has been demonstrated using an n^+p silicon solar cell with a boron-doped p-type base counterdoped with lithium. Lithium is an n dopant in silicon. However, in the present case, the lithium is introduced in small enough quantities so that the cell base remains p-type. The purpose is to increase the radiation resistance of the silicon cells currently used to supply electrical power to spacecraft. Since cell performance can be partially restored after radiation damage, by annealing, a second purpose is to reduce the annealing temperature substantially lower than that currently required to restore performance in conventional n^+p silicon solar cells.

The prior-art lithium-doped p^+n silicon solar cells have shown no improvement in radiation resistance, over conventional n^+p silicon cells, when exposed to 1-MeV electron irradiations. Such irradiations are the industry laboratory standard utilized to test solar cells for use in space. Also, the prior-art conventional n^+p boron-doped silicon solar cells have the disadvantage of requiring annealing temperatures of 400° C or higher. At this temperature, irreversible damage to solar-cell-array components occurs. This precludes the possibility of in situ annealing in space, which, if it were possible, would extend the useful space lifetime of solar-cell arrays in space.

It has long been recognized, by workers in space photovoltaics, that p-type silicon is innately more radiation-resistant than n-type silicon. Since most of the radiation damage occurs in the cell base region, the present n^+p lithium-counterdoped silicon solar cell retains the increased-radiation-resistance feature of the p-type base with the added advantage offered by lithium, which tends to increase further the radiation resistance of the cell. Hence, the present invention is more radiation-resistant than the conventional n^+p boron-doped silicon cell currently used in space. This is demonstrated in the figure, where the lithium-counterdoped cells can be seen to produce more output power than the presently-used, conventional n^+p silicon cells, after irradiation by MeV electrons.

In addition to possessing increased radiation resistance, the lithium-counterdoped silicon solar cells show significant performance restoration when

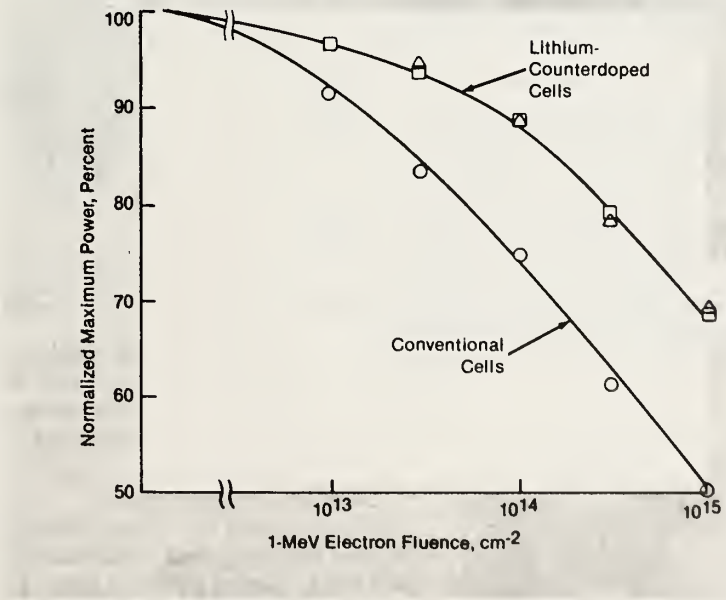

The **Performances of Lithium-Counterdoped and Conventional** cells are compared after irradiation with 1-MeV electrons.

annealed at a temperature of 100° C. The conventional silicon cells now used in space require annealing temperatures of 400° C, or higher, to remove the radiation-induced degradation. Components of solar-cell arrays now used in space, such as adhesives, degrade irreversibly at this high temperature and will not degrade at 100° C. Thus, the present lithium counterdoped solar cell offers the potential for in situ annealing in space, a process that would increase the electrical power available from the solar-cell array during its use in space missions subject to the degrading particulate environment of space.

This work was done by Irving Weinberg and Henry Brandhorst of **Lewis Research Center.** *Further information may be found in "Increased Radiation Resistance in Lithium Counterdoped Silicon Solar Cells."*

Inquiries concerning rights for the commercial use of this invention should be addressed to the Patent Counsel, Lewis Research Center LEW-14177/TN

Daniel G. Soltis
Lewis Research Center
Mail Stop 7-3
21000 Brookpark Road
Cleveland, OH 44135
(216) 433-4000, Ext. 422

FOR ADDITIONAL INFORMATION: *Contact: Director, Technology Transfer Division, P.O. Box 8757, BWI Airport, MD. 21240; (301) 621-0100 Ext. 241*

REFER TO THE NUMBER LISTED AT THE END OF THE ARTICLE

1073 Wind Tunnel Checks Spray Drift

1074 Safe Temporary Storage of Explosives—Safe separation distances were determined for sand-covered corrugated steel pipes containing explosives

1075 Analytical Simulation of Field Service Performance—Different approaches for field support of an operation system in a specific area are modeled.

1076 Automatic Cryogenic Liquid Filling System

1077 A Simplified Model of Thermal Comfort in Buildings

1078 Detoxification of Halon Fire-Extinguishant Products—Ammonia compounds absorb toxic hydrogen halides as they are produced.

1080 Equations for Annular-Heat-Transfer Coefficients Tables of coefficients have been converted to algebraic expressions.

1081 Acoustic-Liner Admittance in a Duct—The method calculates the admittance from easily obtainable values.

Software

1082 Shadowed Space Heating of Sparse Structures—Complete heat-flux and temperature maps can be computed.

1083 Analyzing Static Loading of Complex Structures—Critical loading conditions are determined from the analysis of each structural element.

1084 Variable-Conductance Heat Pipes—It calculate the length of the gas-blocked region and the vapor temperature in the active portion.

1085 Programing Structural Synthesis System

1086 Vibration-Response Analysis—The dynamic behaviors of structures are analyzed interactively.

Testing & Instrumentation

1079 Acoustic/Magnetic Stress Sensor—This high-resolution sensor is fast, portable, and does not require permanent bonding to the structure.

1087 Three-Axis Load-Cell Assembly—A force-measuring device is both sensitive and rugged.

1088 Matching Vibration Testing to "Real-World" Conditions—Vibration spectrum of test machine is adjusted to that observed in operation.

United States Department of Agriculture

Research Technology
Agricultural Research Service

Wind Tunnel Checks Spray Drift

How far can a pesticide be sprayed—sprayed accurately, that is—on a windy day?

Farmers need to know to make sure that pesticide sprays from commonly used airblast systems reach the crops they are aimed at. Sometimes a mere breeze can force the jet-propelled pesticides into near right-angle turns that make them miss their target completely.

"A lot of pesticide chemicals are wasted during spraying operations because of wind," says Robert D. Fox, an Agricultural Research Service engineer in Wooster, OH, who has been studying computer simulations of windblown pesticide sprays as well as watching the real thing in wind tunnel experiments.

"By learning exactly how pesticides get diverted by the wind," he says, "we should be able to develop wind-resistant spraying mechanisms and procedures that could reduce pesticide costs by 30 percent."

Can't farmers simply skip spraying operations on a windy day?

"It doesn't take a strong wind to wreak havoc with a pesticide spray," says Fox.

"Even a mild breeze, at certain angles, can radically alter the direction of conventional airblast sprays," he says.

Fox is particularly concerned about pesticides sprayed from airblast sprayers mounted on tractors or other machines that move through orchards. To reach the tops of the trees, the pesticide has to be sprayed in a high arc that is easily disrupted by the wind.

"We've found that a 15-mi/h crosswind can bend a 120-mi/h spray from that type of equipment as much as 80 degrees," he says. "In fact, with winds from certain directions, the spray can be forced backwards before it gets 6 feet from the nozzle."

Fox and coworkers at the Ohio Agricultural Research and Development Center in Wooster built a 1/12th-size model of a sprayer used in nearby orchards and placed it inside a wind tunnel to measure how various crosswinds and forward travel speeds affect sprays once they leave the nozzle.

"We have to remember that significant wind problems can arise from movement of the spraying machinery," Fox says as he points to test data which show that an orchard sprayer driven at more than 10 mi/h could lose most of its pesticide to air currents created by the travel of the sprayer itself.

"One solution is to have a sprayer system with nozzles attached to lifting mechanisms that can rise to treetop levels," he says, adding that a prototype of such a system has already been built by ARS engineers.

The wind tunnel tests conducted by Fox enabled him to check and refine a computer program previously developed to simulate how wind affects pesticide sprays.

"For the most part, the computer simulations and our wind tunnel measurements matched up pretty well," says Fox. "At the higher wind velocities, however, the computer tended to underestimate how far the pesticide spray would actually shift. We've now modified the program accordingly."

Fox also used wind tunnel measurements to refine numerical values in the computer program that were based on the flow of air over certain airplane wing designs.

"The arc formed by a high-angle pesticide spray is a lot like a swept-back airplane wing," Fox explains, "and it has some of the same aerodynamic characteristics. Before the wind tunnel tests, aeronautical engineering figures were all we had—but they weren't that far off."

But the wind tunnel data did make the computer program more accurate, says Fox, and that makes it a more reliable engineering tool in the future.

"We can use it with greater confidence," he says, "when designing new pesticide equipment to meet the challenge of a windy day."

Robert D. Fox is in USDA-ARS Applied Technology Research at the Ohio Agricultural Research and Development Center, Wooster, OH 44691. ■

MANUFACTURING TECHNOLOGY NOTE

U.S. ARMY MATERIEL COMMAND

Deputy Chief of Staff for Manufacturing Technology, Alexandria, VA

Project Number: NONE

Filing Code : 79A057

Safe Temporary Storage of Explosives

Safe separation distances were determined for sand-covered corrugated steel pipes containing explosives.

To determine safety design parameters for safe, temporary storage sites for explosive charges and ammunition, the U.S. Army Ballistic Research Laboratory conducted a series of donor/acceptor tests employing sand-covered corrugated steel pipes. The results of a regression and discriminant analysis of the test results can help in the design of new storage facilities or in the evaluation of the safety of existing ones. Limited test data are also provided on the influence of venting, explosive charge position, top cover depth, and the effectiveness of sand/air/sand barriers.

Conducted to determine what separation distance between pipes would localize damage in the event that the explosives in one pipe detonate en masse, the donor/acceptor tests involved steel pipes with diameters ranging from 0.5 to 2.0 ft (15 to 61 cm), with length twice the diameter, and containing explosive charges weighing up to 47.5 lb (21.5 kg). A comparison of the observed and the predicted safe separation distances is presented in the figure; the predicted values were generated using both regression and discriminant equations. Additional testing will be required to identify debris and overpressure hazards.

Project officer Harry Reeves
(301) 278-3677 or AV 283-3677

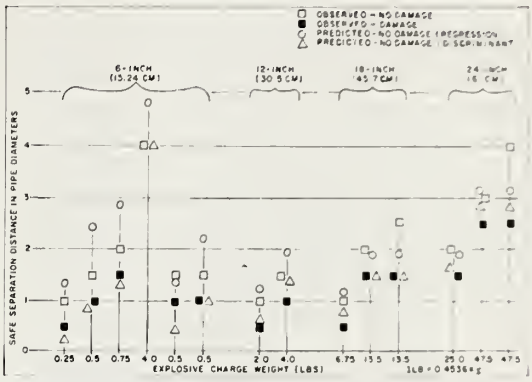

Safe Separation Distances Versus Explosive Charge Weight were both determined experimentally and predicted using regression and discriminant equations.

FOR ADDITIONAL INFORMATION

You can learn more details about this technology by ordering the NTIS report(s)
Safe Separation-Distances Between Sand Covered Corrugated Steel Pipes Containing Explosive Charges
Order number AD-A157000/NAA
Price Code. A03
Order from:
National Technical Information Service
5285 Port Royal Road
Springfield, VA 22161

This document was prepared under the sponsorship of the U.S. Government. Neither the United States Government nor any person acting on behalf of the United States Government assumes any liability resulting from the use of the information contained in this document, or warrants that such use will be free from privately owned rights.

MANUFACTURING TECHNOLOGY NOTE

U.S. ARMY MATERIEL COMMAND

Deputy Chief of Staff for Manufacturing Technology, Alexandria, VA

Project Number: NONE

Filing Code : 94C004

Analytical Simulation of Field Service Performance

Different approaches for field support of an operational system in a specific area are modeled.

The U.S. Army Armament, Munitions, and Chemical Command has developed an analytical model to describe the peformance of mobile maintenance contact teams (C-teams) that support an operational system within a specific service area; the teams are dispatched to a failed unit, diagnose and repair the fault, and move to the next customer without leaving the service area. This model may contribute to the establishment of improved systems for customer service in the field.

The model describes the stochastic steady-state in terms of Markov process theory. The solutions of the linear, steady-state equations are provided by an efficient numerical procedure. The implementing computer-program source code is included in the report.

A parametric analysis was performed using values characteristic of an air defense system. Parameters examined include: (a) intercustomer speed and variation in speed, (b) density of the C-teams, (c) dedicated versus nondedicated teams, (d) mean time between failures (service requests), (e) mean diagnostic and repair time, and (f) form of the probability distribution for total service time. The figure shows curves calculated for the average number of nonfunctional customer units as a function of the mean time between failures, with the mean diagnostic and repair time as a parameter.

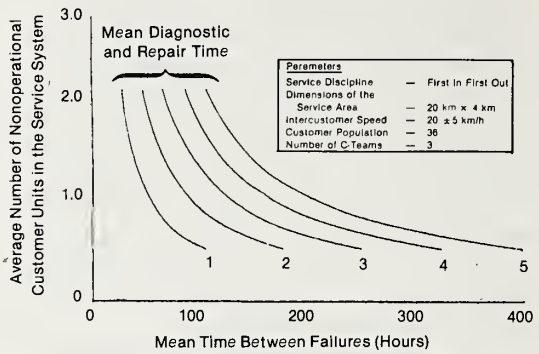

Average Number of Nonoperational Customer Units is shown as a function of the mean time between failures, with the mean diagnostic and repair time as a parameter. The curves are generated from equations that describe the performances of mobile maintenance contact teams.

Project officer George J. Schlenker
(309) 794-5075 or AV 793-5075

FOR ADDITIONAL INFORMATION:

You can learn more details about this technology by ordering the NTIS report(s):

Analytic Simulation of the Performance of Mobile Maintenance Contact Teams.
Order number: AD-A156317/NAA
Price code: A04

Order from:

National Technical Information Service
5285 Port Royal Road
Springfield, VA 22161

This document was prepared under the sponsorship of the U.S. Government. Neither the United States Government nor any person acting on behalf of the United States Government assumes any liability resulting from the use of the information contained in this document, or warrants that such use will be free from privately owned rights.

energygram®

Automatic Cryogenic Liquid Filling System

DOE/TIC/EG-86/081
OFFICE OF SCIENTIFIC AND TECHNICAL INFORMATION

This technical note was based on research conducted by Lawrence Berkeley Laboratory for the U.S. Department of Energy.

Lawrence Berkeley Laboratory

Technology Description. This is a system for automatically maintaining the height of the coolant liquid (liquid nitrogen in this case) in a cryostat at a predetermined level. The system includes a monitor that provides a continuous analog reading of the liquid level in the cryostat vessel or container. Level sensing depends on the difference in dielectric constant in a liquid and a gas (about 50% higher in the liquid) in a coaxial probe suspended vertically within the vessel. The capacitance between the center conductor and the outer conductor of the probe is measured to determine liquid level.

A fill controller responds to the reading and activates a refill system if needed. Since valve operation is unreliable at cryogenic temperatures, valves are eliminated in the supply line between the cryostat and the supply dewar. Liquid in the supply dewar is heated to raise the pressure and cause liquid to flow through the supply line to the cryostat.

Why Is This Better Than Existing Technology? The overall system conserves coolant and is relatively troublefree.

Stage of Development. Two units have been operated at a remote unattended location for over a year without failure.

Potential Uses and Spinoffs. The monitoring system could be used with any nonconducting liquid.

FOR ADDITIONAL INFORMATION

DOE report(s):
Reliable Automatic Liquid Nitrogen Filling System.
Report number: LBL-19674/NAB
Order number: DE86003990/NAB
Price: $9.95

Order from:
National Technical Information Service
5285 Port Royal Road
Springfield, VA 22161

For additional information, contact
Donald Landis and Norman Madden
Lawrence Berkeley Laboratory
MS 29-100
Berkeley, CA 94720
Telephone No. (415) 486-5130

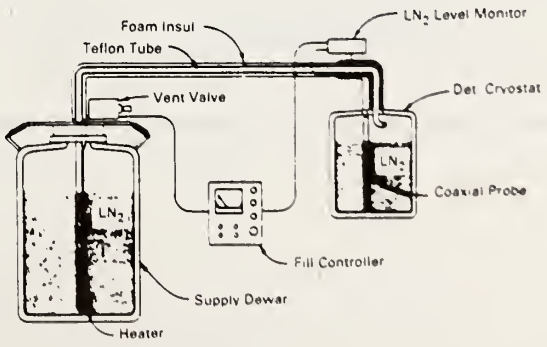

Drawing of automatic liquid nitrogen filling system

energygram®

A Simplified Model of Thermal Comfort in Buildings

DOE/TIC/EG-86/007
OFFICE OF SCIENTIFIC AND TECHNICAL INFORMATION

This technical note was based on research conducted by Lawrence Berkeley Laboratory for the U.S. Department of Energy.

Lawrence Berkeley Laboratory

Significant efficiency improvements could be achieved if heating, ventilating and air-conditioning systems responded to comfort levels rather than to air-temperature levels.

The purpose of this work was to derive simplified expressions for thermal comfort that can be used in engineering calculations and devise a simplified model of thermal human comfort, that is, the interaction of variables, including air temperature, mean radiant temperature, humidity, and air speed, with a persons's metabolic rate and clothing.

A report from Lawrence Berkeley Laboratory describes simplified solutions that allow the calculation of predicted mean vote and effective temperature which (in the comfort zone) are linear in the air temperature and mean radiant temperature and quadratic in the dew point and which can be calculated without any iteration.

The simplified comfort equation presented should have many applications. For example, it could be used as a control algorithm in a large heating, ventilating and air-conditioning system where a competent controller could adjust the environmental conditions to maintain acceptable comfort levels at a minimum cost.

It could involve estimating the efficacy of radiant heating and the suitability of humidity control for comfort.

Natural ventilation through windows, which may eliminate the need for cooling plants or reduce cooling loads, may be one of the most important applications of the model, the researcher says. Natural ventilation has two separable effects: the increased ventilation causes an increase in interior air speed, which allows comfort at higher air temperatures through increased evaporation and convective cooling (technically this may not be true for air temperatures that are higher than skin temperatures; such a situation, however, is very unlikely in the comfort range), and greater ventilation removes internally generated heat and humidity and thus lowers the effective temperature. The effect of increased air speed on the comfort zone can be calculated directly from the comfort equations given in the paper.

Sample plots of the comfort zones for different air speeds and conditions are included to allow designers to estimate the air speed necessary to keep a particular space comfortable under specific conditions. The amount of natural ventilation required for a prototypical house for arbitrary outdoor conditions can be estimated from such plots.

FOR ADDITIONAL INFORMATION

Reference(s):
A Simplified Model of Thermal Comfort, Energ. Build., *8: 37-50 (1985).*

For additional information, contact:
Max Sherman
Building 90, Room 3076
Lawrence Berkeley Laboratory
Berkeley, CA 94720

NASA Tech Brief
National Aeronautics and Space Administration
Lyndon B. Johnson Space Center, Houston, Texas

Licensing Opportunity

Detoxification of Halon Fire-Extinguishant Products

Ammonia compounds absorb toxic hydrogen halides as they are produced.

Toxic acid vapors resulting from the use of Halon (or equivalent) fire extinguishers are immediately changed into nontoxic ammonium compounds when the extinguishers contain some ammonia or ammonium carbonate. If ammonium carbonate is used, the particle size of the resulting neutral compounds can be controlled to eliminate virtually any absorption into the lungs.

When used to extinguish a fire, a Halon (halogenated hydrocarbon) is partially decomposed to form hydrogen fluoride, chloride, or bromide, which are toxic, irritating, and corrosive vapors. In some instances lethal concentrations of these gases are formed.

However, when the Halon fire extinguishers contain powdered ammonium carbonate, aqueous ammonia, or ammonia gas, the ammonia compound is discharged with the Halon and reacts with the toxic vapors to produce solid, nontoxic, nonirritating, and much less corrosive ammonium halides: These are stable at all pressures and temperatures up to 300° C. (When ammonium carbonate is used, water and carbon dioxide are also produced as byproducts.)

The quantities of ammonia or ammonium carbonate placed in the extinguishers are about three times the stoichiometric amounts required to neutralize the quantities of acid gases formed by the extinguishing process, as determined in previous tests. Ammonium carbonate is a dry powder and aqueous ammonia is a liquid; neither is significantly soluble in any Halon extinguishing agent. Theoretical considerations and actual test results have demonstrated that the presence of ammonium carbonate or aqueous ammonia in the extinguishing agent impairs neither its capacity nor its rapidity of extinguishment.

In a White Sands Test Facility application, in which a diesel fuel fire within a 600-ft^3 (17-m^3) armored personnel carrier was extinguished, 250 g of ammonium carbonate, or 250 ml of aqueous ammonia were added to the Halon extinguishing compound. The estimated amount of Halon 1301 required to extinguish a fire in this volume is 4.4 kg. Therefore, the weight of the ammonium carbonate (250 g) added to the extinguisher is only 5.6 percent of the weight of the Halon 1301 — amounting to a negligible increase in extinguisher weight.

This work was done by Eric L. Miller of Lockheed Engineering & Management Services, Inc., for **Johnson Space Center.**

Inquires concerning rights for the commercial use of this invention should be addressed to the Patent Counsel Johnson Space Center. Refer to MSC-20962/TN

Marvin F. Matthews
Lyndon B. Johnson Space Center
Mail Code AL3
Houston, TX 77058
(713) 483-4871

FOR ADDITIONAL INFORMATION: *Contact: Director, Technology Transfer Division, P.O. Box 8757, BWI Airport, MD. 21240; (301) 621-0100 Ext. 241*
REFER TO THE NUMBER LISTED AT THE END OF THE ARTICLE

NASA Tech Brief
National Aeronautics and Space Administration
Langley Research Center, Hampton, Virginia

Acoustic/Magnetic Stress Sensor

This high-resolution sensor is fast, portable, and does not require permanent bonding to the structure.

A high-resolution acoustic/magnetic stress sensor measures nondestructively the type (compressive or tensile) and magnitude of stresses and the stress gradients present in a class of materials. The sensor (see figure) includes a precise high-resolution acoustic interferometer, a sending acoustic transducer, a receiving acoustic transducer, an electromagnet coil and core, a power supply, and a magnetic-field-measuring device such as a Hall probe.

The device is portable, fast, nondestructive, and does not require permanent bonding to a structure. The technique requires small magnetic fields and thus fits many applications where magnetization is difficult. Because the sensor functions very well with magnetic steel solids, it promises to be very useful for alloys.

The sensor uses low magnetic field effects that alter magnetic domains in a way that interrogates local stress fields. The measurement depends on the shift in acoustic velocity that accompanies the change in magnetization. Since stress also changes the magnetic-domain structure, the acoustic measurement senses the presence of stress through the cycling of the magnetic field. Only low magnetic fields can sense the effect on magnetization without compromising effects from the domain-wall rotation that occurs at high fields.

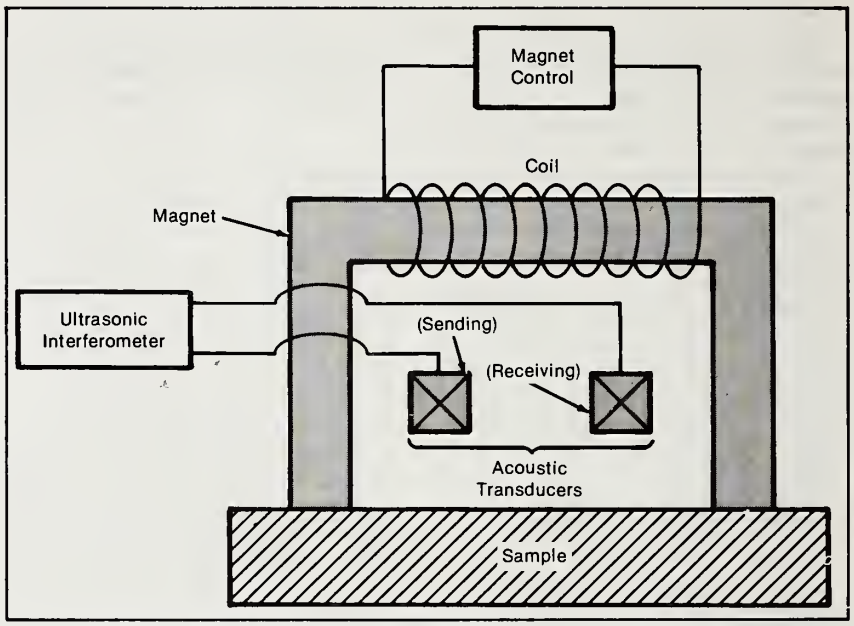

The **Acoustic/Magnetic Stress Sensor** measures stress in the sample via the interactions among the magnetic and stress fields and the speed of sound.

This type of measurement is especially important for construction and applications where steel is widely used. The sensor may be useful especially for the nondestructive evaluation of stress in steel members because of its portability, rapid testing, and nonpermanent installation.

This work was done by Joseph S. Heyman of **Langley Research Center** *and Min Namkung of the College of William and Mary. LAR-13320 / TN*

FOR ADDITIONAL INFORMATION: *Contact: Director, Technology Transfer Division, P.O. Box 8757, BWI Airport, MD. 21240; (301) 621-0100 Ext. 241*
REFER TO THE NUMBER LISTED AT THE END OF THE ARTICLE

NASA Tech Brief
National Aeronautics and Space Administration
Marshall Space Flight Center, Alabama

Equations for Annular-Heat-Transfer Coefficients

Tables of coefficients have been converted to algebraic expressions.

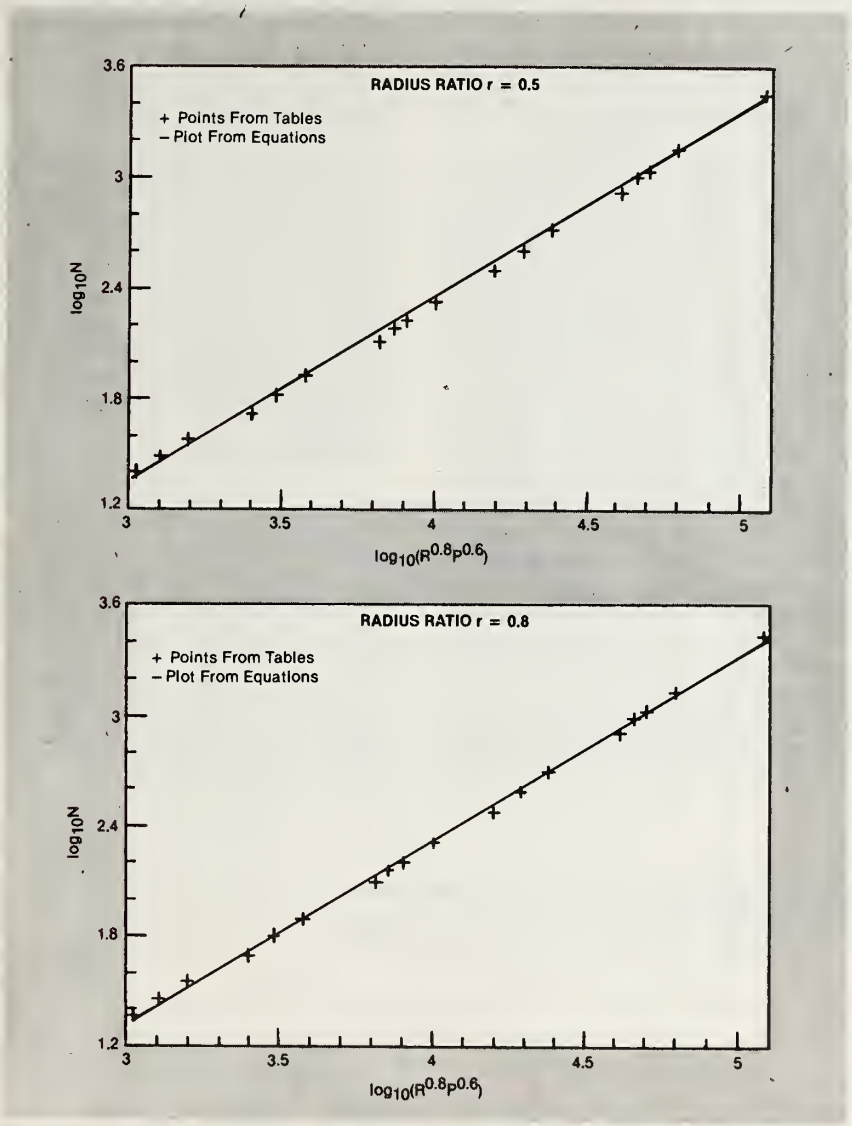

A **Plot of the Equation for the Nusselt Number** agrees closely with points from tabulated data. The equation for the Nusselt number and those for coefficients A and B were obtained by a regression analysis of the data. Other plots (not shown) also show close agreement for radius ratios of 0.1 and 0.2.

A set of equations has been developed for heat-transfer coefficients for the annulus between the inner and outer tubes of a concentric-tube heat exchanger. Previously, the coefficients were available only in tabular form. In equation form, the coefficients can be incorporated into mathematical models more readily than as tabular data. The equations simplify the design and analysis of heat exchangers.

The equations were obtained by a regression analysis of the tabular data of W. M. Kays and E. Y. Leung, published in the *International Journal of Heat Mass Transfer* in 1963. The Nusselt number on the inner surface of an annulus with a constant rate of heat transfer and an insulated outer surface can be calculated as a function of the Prandtl number, the Reynolds number, and the annulus radius ratio, as follows:

$$\log_{10}N = A \log_{10}(R^{0.8}P^{0.6}) + B$$

$$A = -0.123r^2 + 0.172r + 0.937$$

$$B = 0.958r^2 - 1.336r - 1.217$$

where r = the ratio of the outside diameter of the inner tube to the inside diameter of the outer tube, R = the Reynolds number, and P = the Prandtl number.

These equations are correlated with the tabular data for $10^4 \leq R \leq 10^6$, $0.5 \leq P \leq 3$, and $0.1 \leq r \leq 0.8$. The coefficient of determination of the correlation is 0.987. The curves plotted from the equations agree well with the data points in the Kays and Leung tables (see figure).

This work was done by Barry Yao of Rockwell International Corp. for **Marshall Space Flight Center.**

MFS-29074 /TN

FOR ADDITIONAL INFORMATION: *Contact: Director, Technology Transfer Division, P.O. Box 8757, BWI Airport, MD 21240; (301) 621-0100 Ext. 241*

REFER TO THE NUMBER LISTED AT THE END OF THIS ARTICLE

NASA Tech Brief
National Aeronautics and Space Administration
Langley Research Center, Hampton, Virginia

Acoustic-Liner Admittance in a Duct

The method calculates the admittance from easily obtainable values.

The acoustic admittance of practical acoustic liners may be a function of the aeroacoustic environment in which they are located. The properties of these liners in such an environment are evaluated in the laboratory with a grazing-flow impedance tube. In such a tube, the acoustic material is alined so that the sound and mean flow graze over the surface of the material in a controlled manner to simulate the environment typical of that found in a real jet engine.

Since acoustic admittance is defined as the ratio of normal particle velocity to pressure at the wall surface, the admittance could be determined experimentally by direct measurements of normal particle velocity and pressure.

In practice, measurements of particle velocity in the presence of grazing flow are currently not reliable. Instead, an indirect approach must be taken, which depends only on the measurement of acoustic pressure at selected locations in the test configuration. These measurements are then used as input to an analytical program that determines the admittance based on these measured data.

Previous methods for determining acoustic admittance in grazing flow, from measured values of the axial propagation constant and cross modes, are based on the solution to an ordinary differential equation and are restricted to mean flows with transverse gradients in one direction only. However, grazing-flow duct facilities commonly employ ducts with relatively small rectangular cross sections in which the grazing flow possesses gradients in both transverse directions of the impedance tubes. Such is the case in the flow-impedance test laboratory at Langley Research Center; therefore, the present effort was motivated by the need to account for the more realistic flow environment in laboratory flow-impedance tubes such as those in the Langley facility.

The new method for calculating acoustic-liner admittance in a rectangular duct with grazing flow is based on a finite-element discretization of the acoustic field and a reposing of the unknown admittance value as a linear eigenvalue problem on the admittance value. This eigenvalue problem is solved by Gaussian elimination. Unlike existing methods that are based on the integration of an ordinary differential equation and are thus limited to mean flows with one-dimensional boundary layers, the present method is extendable to mean flows with two-dimensional boundary layers as well.

Admittance values determined from the method compared excellently with the exact solutions obtained for a constant mean flow profile. In the presence of shear, the results of the method compared well with the results of a Runge-Kutta integration technique.

This work was done by Willie R. Watson of **Langley Research Center.** *Further information may be found in NASA TP-2310 [N84-27543/NSP], "A New Method for Determining Acoustic-Liner Admittance in a Rectangular Duct With Grazing Flow From Experimental Data" [A02] A copy may be purchased [prepayment required] from the National Technical Information Service, Springfield, Virginia 22161.*
LAR-13399 /TN

FOR ADDITIONAL INFORMATION: *Contact: Director, Technology Transfer Division, P.O. Box 8757, BWI Airport, MD 21240; (301) 621-0100 Ext. 241*
REFER TO THE NUMBER LISTED AT THE END OF THIS ARTICLE

NASA Tech Brief
National Aeronautics and Space Administration

Shadowed Space Heating of Sparse Structures

Complete heat-flux and temperature maps can be computed.

A computer program SSQ has been developed to address and quantify the complex, solar-shadowing conditions inherent in sparse, lattice-type space structures. The analysis procedure is one of assessing partial shadowing of structural elements by multiple, similar slender members. The program yields schedules of incident-solar, Earth-thermal, and Earth-albedo radiation throughout a complete orbit for elemental locations on selected structural members. Thermal response can be computed in an optional routine. Complete heat-flux and temperature mapping can be obtained by repeated computations for selected elements of interest.

Thermal analysis of relatively sparse structures in the space environment has customarily omitted the consideration of shadowing by up-Sun structural members. This convention has been frequently questioned in the case of lattice-type structures supporting very large, near-planar, Earth-facing surfaces (e.g., antennas). For these, significant shadowing can occur whenever the solar vector is nearly tangent to the orbital path. It thus becomes advisable to quantify the shadowing effect, but sparse structures present an exceptional element of complexity.

Space-heating analysis procedures usually assume either total shadowing or total solar irradiation of individual elemental areas of mapped surfaces. While the latter convention is reasonably sound for structural assemblies of which most or all geometric dimensions are of the same order of magnitude, it is less realistic for sparse structures composed of slender members having extremely-high length-to-diameter (L/d) ratios. In such cases, multiple up-Sun (i.e., shadowing) members may yield only partial shadowing of an elemental area of interest, with the degree and duration of shadowing being a strong function of the size and density of the structural assembly. No prior analysis procedure addressing this problem is known to have been developed.

The SSQ program permits the definition of numbered structural-node locations in the spacecraft coordinate system, followed by the definition of line segments (structural members) in terms of bounding-node numbers. Slender structural members are assumed to be cylindrical and are assigned values of diameter, thermal mass per unit of length, solar absorptance, emittance, and view factor to space. Partially or totally opaque bodies are also defined in terms of bounding-line segments, and the latter surfaces are assigned transmissivities that may vary as functions of solar angle of incidence.

The SSQ program heat-flux output can easily be formatted as required for input to other thermal-analysis programs. Temperature output can also be formatted to accommodate the input requirements of structural-analysis programs.

This program was written by R. F O'Neill and J. L. Zich of General Dynamics Corp. for **Lewis Research Center.**

LEW-13977 / TN

FOR ADDITIONAL INFORMATION

CONTACT:

COSMIC®
112 Barrow Hall
University of Georgia
Athens, GA 30602
(404) 542-3265

Analyzing Static Loading of Complex Structures

Critical loading conditions are determined from the analysis of each structural element.

The Automated Thrust Structures Loads and Stresses (ATLAS) system is a series of programs developed to analyze the elements of a complex structure under static-loading conditions. ATLAS calculates internal loads, beam-bending loads, column- and web-buckling loads, beam and panel stresses, and beam-corner stresses.

ATLAS determines the most critical loading conditions from the analysis of each element. This eliminates the traditional approach of preselecting a limited number of conditions that are arbitrarily designated as critical before analysis. Although written for investigation of the Space Shuttle orbiter fuselage assembly, ATLAS could be adapted for such other complex structures as tall buildings, offshore oil rigs, and aircraft.

There are four main programs: (1) CONDENSE reformats and condenses input data obtained from the Monte Carlo flight tapes containing data on engine thrust, pitch, yaw, and other flight measurements; (2) FILTER significantly reduces the number of conditions to be processed, yet retains the critical load cases that meet selected criteria; (3) GLOBAL calculates the loads on the actuator and gimbal bearings due to engine thrust; and (4) ATLAS sums the loads due to thrust, pitch, yaw, and inertia.

The five extreme positive and negative values are listed for the following: (a) shear panel loads (trim3 and quam4 components), (b) beam-corner stresses, (c) beam-element webbing loads, and (d) axial strut loads. The margins of safety for beam-element webbings and struts are also calculated.

These programs are written in FORTRAN IV and Assembler for batch execution and have been implemented on an IBM 370-series computer with a central-memory requirement of approximately 2,200K of 8-bit bytes for the maximum number of elements (150 trim3, 75 quam4, 450 corners, 150 webs, and 100 struts). Fewer elements require less core. ATLAS was developed in 1983.

The programs were written by Darrell C. Gallear of Rockwell International Corp. for **Johnson Space Center.**
MSC-20896 / TN

FOR ADDITIONAL INFORMATION

CONTACT:
COSMIC®
112 Barrow Hall
University of Georgia
Athens, GA 30602
(404) 542-3265

NASA Tech Brief
National Aeronautics and Space Administration

Computer Software

Variable-Conductance Heat Pipes

It calculates the length of the gas-blocked region and the vapor temperature in the active portion.

In response to a need to accurately and efficiently predict the performance of variable-conductance heat pipes (VCHP's) incorporated in spacecraft thermal-control systems, a computer code VCHPDA has been developed to interact with thermal analyzer programs such as SINDA (Systems Improved Numerical Differencing Analyzer). Given the axial temperature distribution and design specifications of the VCHP, the code is used to calculate the length of the gas-blocked region and the vapor temperature in the active portion of the heat pipe from the simultaneous solution of nonlinear, coupled integro-differential equations governing conservation of noncondensible gas species and thermal energy based on the "flat gas-front" theory.

Historically, the code originated in efforts carried out under the Advanced Thermal Control Experiment program, during which a method to analytically simulate a gas-loaded, variable-conductance heat pipe was developed. A computer subroutine VCHP2 was implemented to numerically solve the analytical model. The VCHP2 code, which interfaced with general thermal models involving heat pipes, was used successfully in steady-state thermal simulation of systems such as the transmitter experiment package (TEP) variable conductance heat pipe system (VCHPS) on the Canadian Communications Technology Satellite (CTS) *Hermes*. Subsequent attempts, however, to utilize VCHP2 for transient thermal analyses yielded unsuccessful results due to numerical instabilities arising during the gas/vapor front-location/vapor-temperature calculations.

As part of efforts to investigate several thermal anomalies that occurred during operation of the CTS spacecraft, the solution scheme in VCHP2 was analyzed in order to uncover the source of the numerical problems. The analysis revealed that the iterative approach used in the subroutine to obtain a convergent solution (starting from an initial, guessed gas length and vapor temperature) was inadequate in view of the nonlinear nature of the model. A new analytical method was formulated which, under most physically realizable operating modes, unconditionally circumvents numerical instabilities.

In addition, two new features were introduced into the VCHP model that permit simulation of the effects of an ice-plug formation and open-artery capacity on the performance of a VCHP system. The appropriate logic for solution of the analytical model was incorporated into the revised version of the VCHP2 subroutine, now called VCHPDA.

The advantages of the VCHPDA code over prior programs are the improved accuracy, unconditional stability, and increased efficiency of the solution resulting from the novel approach and the use of the state-of-the-art numerical techniques for solving the VCHP mathematical model.

The code is a valuable tool in the design and evaluation of advanced thermal-control systems using variable-conductance heat pipes. It is written in FORTRAN IV for use on CDC 600 computers.

This program was written by David Antoniuk of TRW, Inc. for **Lewis Research Center.** *LEW-14075 / TN*

FOR ADDITIONAL INFORMATION

CONTACT:
COSMIC®
112 Barrow Hall
University of Georgia
Athens, GA 30620
(404) 542-3265

Programing Structural Synthesis System

This program aids research in analysis and optimization.

The Programing Structural Synthesis System (PROSSS2) was developed to provide a structural-synthesis capability by combining access to SPAR with the CONMIN program and a set of interface procedures. SPAR is a large general-purpose finite-element structural-analysis program, and CONMIN is a large general-purpose optimization program.

The implementation of the PROSSS2 analysis/optimization process results in a minimized objective function, typically the mass defined in terms of a set of such design variables as the cross-sectional dimensions of a structural member. Also, the member is subject to a set of constraints; for example, the stress must be less than some allowable value.

PROSSS2 is intended to be used in the following three basic ways: (1) as a research tool for the development of optimization techniques that will interface with an efficient analysis program, (2) as a research tool for testing new analysis techniques that will interface with an efficient optimization program, and (3) as an application tool that can be adapted to a wide range of different problems.

With PROSSS2, the analysis and optimization programs are executed repeatedly in a looping manner until the process is stopped by a user-defined termination criteria. This part of the system is referred to as the repeatable part of PROSSS2. However, some of the analysis, such as model definition, need be done only once and can be saved for future use. These parts are performed outside the loop and are referred to as the nonrepeatable part of PROSSS2. Three options are provided for organizing optimization procedures by combining nonlinear or piecewise-linear programing methods with analytic or finite-difference gradients.

In this newest release, PROSSS2 is controlled by SPAR run streams instead of by the control language of the computer. This is accomplished by integration of the entire PROSSS2 program as new processors within the SPAR program. The user supplies PROSSS2 with problem-dependent routines that express the relationships between the structural parameters of interest in SPAR and the design variables used in CONMIN.

PROSSS2 is written in FORTRAN IV for batch execution and has been implemented on a CDC CYBER-series computer. However, the code is machine-independent and can be run with any computer on which SPAR has been implemented. The implementation of PROSSS2 on the CDC requires approximately 51K (octal) of 60-bit words. The PROSSS2 user must have access to the SPAR program. PROSSS2 was developed in 1984.

This program was written by James L. Rogers, Jr., of **Langley Research Center.** *LAR-13408 /TN*

FOR ADDITIONAL INFORMATION

CONTACT:
COSMIC®
112 Barrow Hall
University of Georgia
Athens, GA 30620
(404) 542-3265

NASA Tech Brief
National Aeronautics and Space Administration

Vibration-Response Analysis

The dynamic behaviors of structures are analyzed interactively.

An interactive steady-state vibration-response program, VIBRA, has been developed. Frequency-response analyses are commonly used in evaluating the dynamic behaviors of structures subjected to cyclic external forces. VIBRA calculates the frequency response using a modal-superposition approach. This method is applicable to single or multiple forces applied to a linear, proportionally damped structure in which the damping may be viscous or structural.

VIBRA computes the forced-acceleration response at any selected point on the structure for a given vibratory loading. VIBRA provides tabular output with optional plots of response versus frequency. The interactive capability enables rapid evaluation of the structural response.

VIBRA requires the input of modal data from only the selected response and applied-vibratory-load points. These data may be obtained either from ground vibration measurements or from a natural vibration analysis. VIBRA can use results from any vibration analysis that has output in the form of generalized masses, eigenvalues, and eigenvectors. Thus, VIBRA can be used as a postprocessor for such finite-element codes as NASTRAN.

The user specifies a starting frequency, ending frequency, and frequency step for the VIBRA response analysis. VIBRA output can be plotted on the screen as real acceleration versus forcing frequency, imaginary acceleration versus forcing frequency, acceleration amplitude versus forcing frequency, and phase angle versus forcing frequency. The interactive graphics user has a zoom facility available for detailed examination of the plots. Optionally, the response data are stored for later use.

VIBRA is written in FORTRAN 77 for interactive execution and has been implemented on a CDC CYBER 170-series computer with a central-memory requirement of 120K (octal) of 60-bit words. The graphic output requires the Plot-10 plotting package. The VIBRA program was developed in 1984.

This program was written by Lynn M. Bowman of the U.S. Army Aviation Systems Command for **Langley Research Center.** *LAR-13291 /TN*

FOR ADDITIONAL INFORMATION

CONTACT

COSMIC®
112 Barrow Hall
University of Georgia
Athens, GA 30602
(404) 542-3265

NASA Tech Brief
National Aeronautics and Space Administration
Lyndon B. Johnson Space Center, Houston, Texas

Licensing Opportunity

Three-Axis Load-Cell Assembly

A force-measuring device is both sensitive and rugged.

A load-cell assembly measures the forces applied to an object along each of three orthogonal axes. It was developed for use with a remote manipulator that bends cryogenic ducts. Usually, the required bending forces are low, but occasionally a substantial force must be applied. The device is therefore designed to be rugged and to function over a wide range, having potential applications in automatic testing equipment, industrial robots, and force-measuring equipment.

Previously, load cells were located in and under the remote manipulator. The repeatability and accuracy of measurement were poor, because the forces sensed by the cells also included those caused by the friction and inertia of the manipulator. The problem became worse when smaller ducts, with smaller deflection forces, were used.

The device is placed between the manipulator and the duct or other object to sense the applied loads directly (see Figure 1). Load cells are mounted on the x, y, and z axes (see Figure 2). Linear ball bushings and an intermediate ring assembly separate the forces acting on the axes. A force in the x direction, for example, registers only on the x-axis load cell because its bushings, yoke, and intermediate ring assembly allow the cell to accept force only in that direction. Thus, the crosstalk between the three sensors is very low.

Although they are sensitive to low forces, the load cells can withstand much

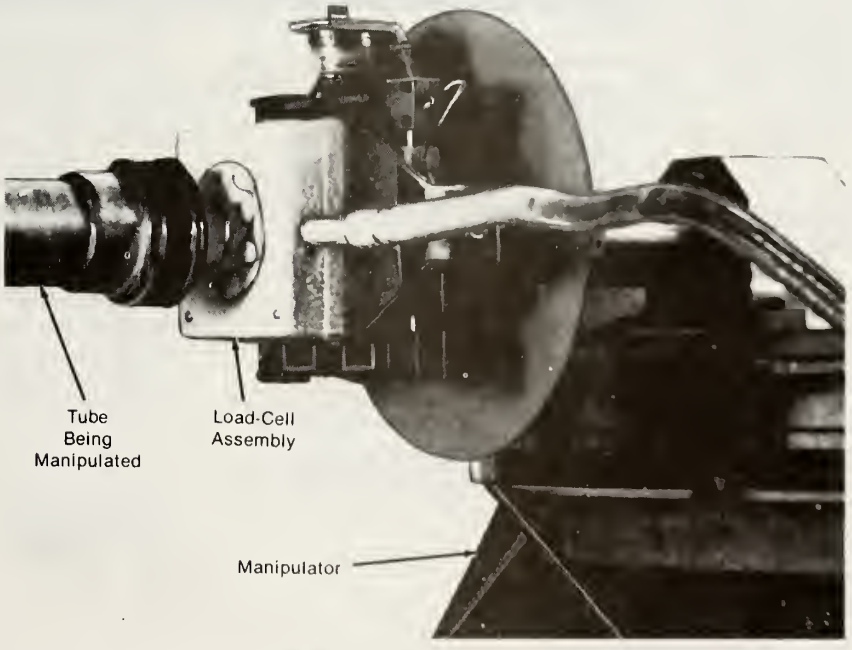

Figure 1. The **Load-Cell Assembly** is placed between a manipulator and the object being manipulated. The load cells thereby measure the forces on the object almost directly, without interference by intervening manipulator forces.

higher forces. Similarly, the ball bushings have low axial friction but can withstand high side loads without being damaged or introducing inaccuracy.

This work was done by Gene R. Rewerts of Ametek, Inc. for **Johnson Space Center.**

Inquiries concerning rights for the commercial use of this invention should be addressed to the Patent Counsel, Johnson Space Center Refer to MSC-20875 / TN

William Chmylak
Lyndon B. Johnson Space Center
Mail Code AL32
Houston, TX 77058
(713) 483-3809

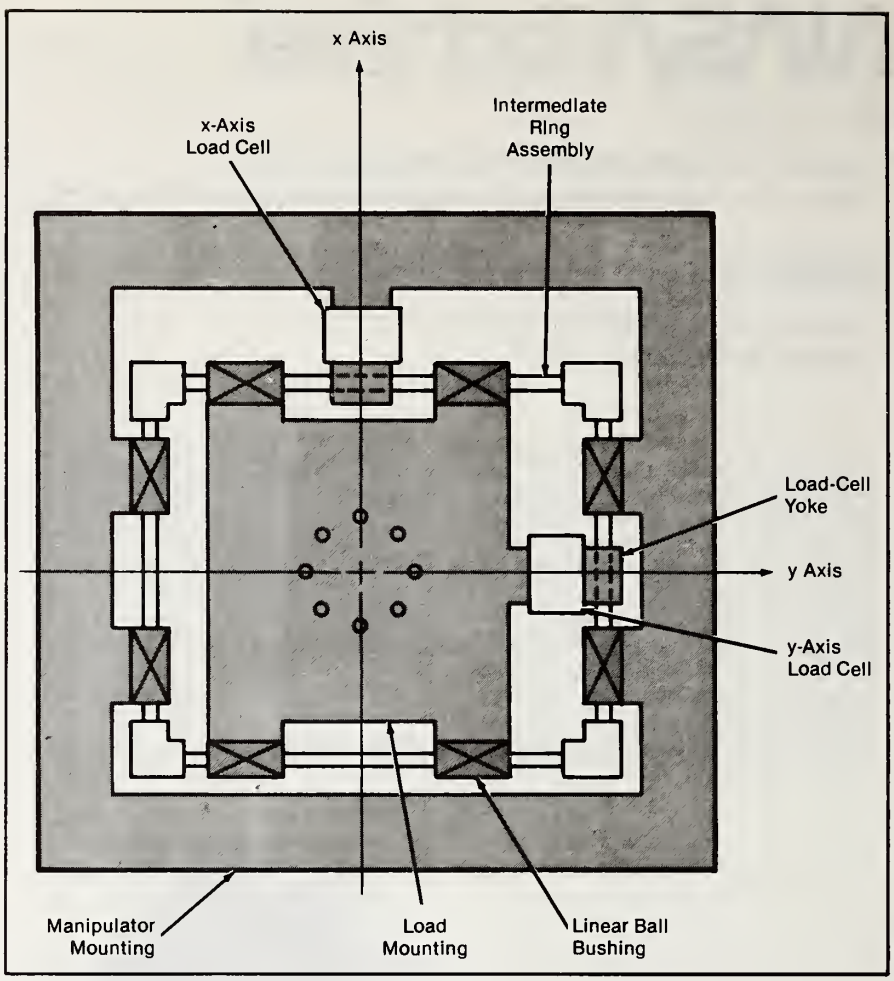

Figure 2. **Load Cells Are Mounted** on three mutually perpendicular axes. The x- and y-axis cells appear in this diagram; the z-axis cell extends out of the page. All cells are similarly equipped with linear ball bushings and intermediate ring assemblies, which isolate the axes from each other.

FOR ADDITIONAL INFORMATION: *Contact: Director, Technology Transfer Division, P.O. Box 8757, BWI Airport, MD. 21240; (301) 621-0100 Ext. 241*

REFER TO THE NUMBER LISTED AT THE END OF THE ARTICLE

NASA Tech Brief
National Aeronautics and Space Administration
Lyndon B. Johnson Space Center, Houston, Texas

Matching Vibration Testing to "Real-World" Conditions

Vibration spectrum of test machine is adjusted to that observed in operation.

A method for vibration testing uses feedback to ensure that a test specimen is exposed to the same vibration spectrum that it would experience in service. In a conventional vibration test, the specimen and its mounting fixture are subjected to a preset excitation spectrum. This spectrum may not cause the correct vibrational response of the specimen because the support fixture may amplify, attenuate, or otherwise alter the vibrational response.

First, the vibrational response of the specimen to random excitation is measured in service. From the in-service spectral response, an arbitrary worst-case spectral response (maximum amplitude as a function of frequency) is constructed from these measurements and is called the "control" spectrum. An estimate is also made of the input spectral setting that ought to cause the shaker table to produce a specimen spectral response like that of the in-service tests.

A test specimen is placed in a test fixture and attached to a shaker (see figure). The shaker is initially operated at one-quarter the full level of the input spectrum to prevent overloading. A short vibration test is run, and the specimen response is compared to the control spectrum. The input spectrum is then adjusted until the response resembles the control spectrum.

This work was done by Albert D. Olsen, Jr., of Beech Aircraft Corp. and Albert V. Keblaitis of Rockwell International Corp. for **Johnson Space Center.**
MSC-20665 /TN

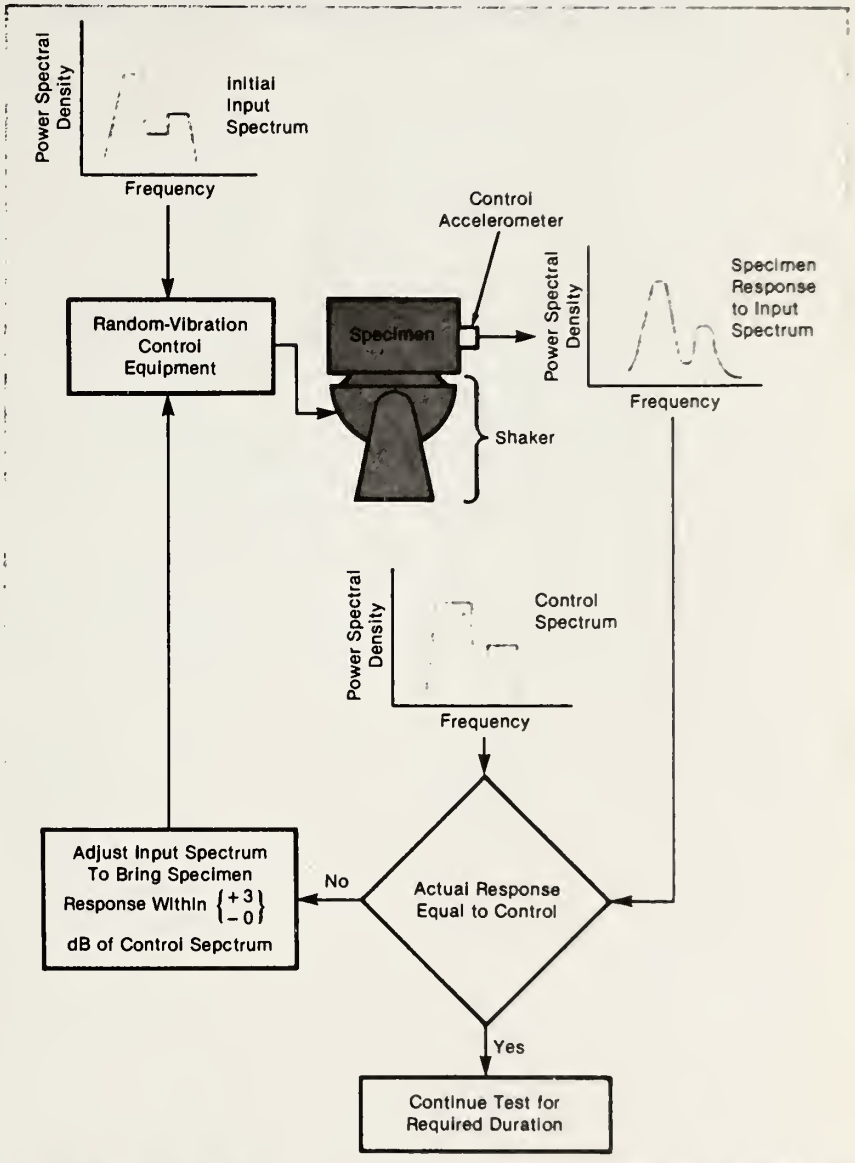

In an Iterative Procedure, the vibrational response of a test specimen is matched to the previously-determined worst-case in-service response. An accelerometer on the test specimen provides feedback.

FOR ADDITIONAL INFORMATION: *Contact: Director, Technology Transfer Division, P.O. Box 8757, BWI Airport, MD. 21240; (301) 621-0100 Ext. 241*
REFER TO THE NUMBER LISTED AT THE END OF THE ARTICLE

Environmental Science & Technology

1089 Disposal of the Pesticide, Coumaphos, Using Microbial and UV-Ozonation Reactions

1090 Aural Nondetectability—A sound propagation and attenuation study yields data needed to predict aural detectability for various conditions.

1091 Surface Coal Gasification—Environmental Studies and Engineering Analysis and Support

1092 Selenium Oxidation and Removal by Ion Exchange

United States Department of Agriculture

Research Technology
Agricultural Research Service

Disposal of the Pesticide, Coumaphos, Using Microbial and UV-Ozonation Reactions

The USDA Animal and Plant Health Inspection Service (APHIS) generates several thousand gallons of concentrated pesticide wastewater annually from its dip vats used to protect cattle and sheep from ticks. The major insecticide used in these vats is coumaphos, a very long-lived compound in soils. A method of decontaminating these wastes before they move into and pollute groundwater has been developed. The method involves the use of a specific microorganism that splits the chemical molecule and a second treatment that uses ozone to destroy one of the major products of microbial actions. When dip vat solutions pretreated with microbes and ozone were added to soils, the coumaphos fragments were rapidly destroyed by soil microbes. These findings will help (APHIS) solve a major problem, and it will enable eventual substitution of a genetically engineered microorganism for the natural microbe used. In addition the ozonation step appears to kill the microbe, thus providing a mechanism for preventing the microbe, engineered or natural, from entering the environment. The method also has potential for broader application for decontamination of other pesticides.

FOR ADDITIONAL INFORMATION: Contact: Dr. Philip C. Kearney, USDA-ARS, Pest, Degrad, Lab. AEQI, Bldg, 050, Rm. 100, BARC-W, Beltsville, MD 20705; (301) 344-3533.

MANUFACTURING TECHNOLOGY NOTE

U.S. ARMY MATERIEL COMMAND

Deputy Chief of Staff for Manufacturing Technology, Alexandria, VA

Project Number: 611102.74A0011 **Filing Code :** 46A009

Aural Nondetectability

A sound propagation and attenuation study yields data needed to predict aural detectability for various conditions.

A study of the parameters that affect the propagation and detectability of sound was made by the U.S. Army Human Engineering Laboratory in order to review the current state of knowledge of sound propagation and detectability, propose new aural detectability limits, and incorporate the latest technical information into design standards. The data, theory, and extensive references in the resulting report could aid efforts to control environmental noise.

This study evaluates the parameters affecting the aural detection of sound, including the following: geometric spreading, atmospheric absorption, ground effect, atmospheric turbulence, refraction due to wind and to temperature gradients (see figure), barriers, foliage, threshold of hearing, psychoacoustic factors, and background noise at the listener's location. Examples are given of the effect on sound propagation of varying the parameters, and several suggestions are offered for field-expedient measures to control or detect sound.

Project officer David C. Hodge
(301) 278-2170 or AV 283-2170.

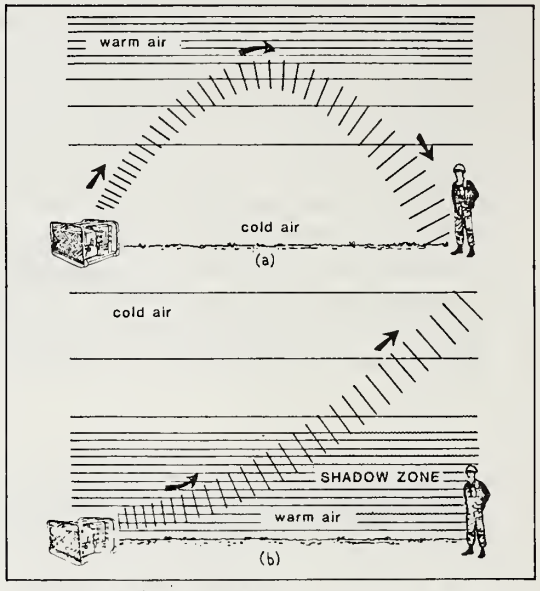

Thermal Gradient Refraction of sound waves, which travel faster as the temperature of the air increases, can increase the ground-level sound propagation at night and decrease the propagation during the day. At night (a), the higher velocity of sound waves in warm upper air causes sound waves to be refracted downward. In the day (b), the higher velocity of sound waves in warm lower air causes sound waves to be refracted upward, producing a shadow zone.

FOR ADDITIONAL INFORMATION:

You can learn more details about this technology by ordering the NTIS report(s):

Proposed Aural Nondetectability Limits for Army Materiel
Order number: AD-A156704/NAA
Price code: A06

Order from:

National Technical Information Service
5285 Port Royal Road
Springfield, VA 22161

This document was prepared under the sponsorship of the U.S. Government. Neither the United States Government nor any person acting on behalf of the United States Government assumes any liability resulting from the use of the information contained in this document, or warrants that such use will be free from privately owned rights.

energygram®

Surface Coal Gasification—Environmental Studies and Engineering Analysis and Support

DOE/TIC/EG-86/046
OFFICE OF SCIENTIFIC AND TECHNICAL INFORMATION

This technical note was based on an Application Assessment Record from the Morgantown Energy Technology Center, Office of Fossil Energy, for the U.S. Department of Energy.

METC
Morgantown Energy Technology Center

Technology Description. The overall goal of the program is to assure that the environmental and health consequences of coal gasification facilities are understood and that adequate control and mitigation measures are available. Specific studies focus upon (1) developing novel, cost-effective methods for controlling process effluents; (2) characterizing process and effluent streams that exist at currently operating gasification facilities; (3) identifying and developing alternative process configurations that reduce or alter potential environmental contaminants; and (4) developing a data base and modeling system for conducting process simulation studies and predicting environmental and health impacts.

The goal of engineering analysis and support is to provide a comprehensive technology data base for the Surface Coal Gasification Program. The objectives are (1) to gather and systematize experimental and theoretical information with the aid of computerized data base management systems, (2) to identify technology strengths and weaknesses, and (3) to define technology needs. This information will be used to solve existing and anticipated operation problems and to provide comparative analyses of competing gasification, cleanup, and utilization technology alternatives.

Significant accomplishments in FY 85 include: (1) completion of environmental sampling and analysis programs at the Mountain Fuel Resources entrained-bed gasifier, the KRW fluidized-bed gasifier, and the DOE/METC entrained-bed reactor; (2) completion of a bibliography on chemical and toxicological data of coal gasification materials; (3) completion of analysis for management of spent Stretford solution; (4) identification of the mechanism for hydantoin formation in gasification quench systems; (5) demonstration of the technical feasibility for decolorizing wastewater using a rotating biological contactor with white rot fungi; and (6) completion of a detailed chemical analysis of GPGA wastewater.

Why Is This Better Than Existing Technology? On the basis of the results, effluent treatment systems capable of meeting existing emission limits for air, water, and solids disposal regulations, as well as workplace safety and health requirements, can be developed. Data will be collected, computerized, and analyzed for ready retrieval by industry to design and construct coal gasification facilities.

Stage of Development. These are ongoing development efforts to collect and analyze data from existing bench-scale units, processing development units, pilot plants, and commercial-scale plants.

Potential Uses and Spinoffs. Data are applicable to existing and prototype plants. The information is also useful in coal liquefaction applications.

FOR ADDITIONAL INFORMATION

DOE report(s):
Morgantown Energy Technology Center
Advanced Environmental Coal Technology Topical Report.
Report number: DOE/METC/SP-194/NAB
Order number: DE83009222/NAB
Price: $11.95
C. J. King, Compiler
Morgantown Energy Technology Center
Proceedings of the Third Biennial Synfuels Wastewater Workshop.
Report number: DOE/METC-84/5/NAB
Order number: DE84009294/NAB
Price: $22.95

Order from
National Technical Information Service
5285 Port Royal Road
Springfield, VA 22161

For additional information, contact
Daniel C. Cicero
Morgantown Energy Technology Center
P.O. Box 880
Morgantown, WV 26507-0880
Telephone No. (304) 291-4725

United States
Environmental Protection
Agency

Water Engineering
Research Laboratory
Cincinnati, OH 45268

Research and Development

EPA

Project Summary

Selenium Oxidation and Removal by Ion Exchange

Strong-base anion exchange was evaluated as a process for the removal of trace quantities of selenium from groundwater. The efficiency of the process was found to depend on the oxidation state of selenium, with the selenate anion, Se(VI), having a greater affinity for the anion-exchange resin than selenite or biselenite anions, Se(IV). Bench-scale experiments with an ion-exchange column compared the effluent concentration histories for synthetic groundwater solutions contaminated with 100 ppb of either Se(IV) or Se(VI). The resin bed capacity for selenium removal was 55% greater with Se(VI). Since Se(IV) is less preferred than the major groundwater anion, sulfate, it was eluted from the column with a chromatographic concentration peak 5.4 times its feed concentration. Se(VI) concentration in the effluent never exceeded its feed concentration.

An analytical method was developed to measure the concentrations of Se(IV) and Se(VI) (i.e., to determine the speciation of selenium) at trace concentration in groundwater. This method uses anion exchange at pH 1.5 to separate undissociated selenious acid (Se[IV]), which passes through the column, from selenate and biselenate anions (Se[VI]), which are retained by the resin. Graphite furnace atomic absorption spectroscopy (GFAAS) is used to measure total selenium in an aliquot of the original groundwater sample and Se(IV) in the anion-exchange column effluent. Se(VI) is determined by difference.

Using this new analytical method as a tool, the oxidation of Se(IV) to SE(VI) at trace concentration in groundwater was studied. The study found that free chlorine can oxidize Se(IV) to Se(VI) in groundwater. In synthetic groundwater containing sulfate, chloride, and bicarbonate at pH 8.3, the reaction is first order in both Se(IV) and free chlorine concentrations, and it can be described by the following rate expression:

$$-r_{Se} = -dC_{Se}/dt =$$
$$(0.21\ L/(min\text{-}mg\ Cl_2))(C_{Cl})(C_{Se})$$

The pH dependence of the reaction was examined in the pH range of 5 to 10. A pH optimum exists between 6.5 and 7.5 in which nearly 70% of the Se(IV) is converted to Se(VI) within 5 min with a chlorine dosage of 5 mg/L. Oxygen was completely ineffective as an oxidant for Se(IV), and potassium permanganate and hydrogen peroxide were much less effective than chlorine.

Introduction

The U.S. Environmental Protection Agency (EPA) National Primary Drinking Water Regulations of 1976 established maximum contaminant levels (MCL's) for 10 inorganic contaminants: barium, cadmium, chromium, lead, mercury, silver, fluoride, nitrate, arsenic, and selenium. Public drinking water supplies contaminated with any one of these substances in excess of the MCL must be treated to remove the contaminant or abandoned.

The MCL for selenium was set at a very low level (0.01 mg/L) because of selenium's suspected carcinogenicity. Selenium contamination of groundwater is fairly common in some regions of the United States, but its removal from these water supplies is not yet practiced. Thus

a continuing need exists for research to evaluate treatment processes for selenium removal. This study is based on an understanding of selenium chemistry and complements the work of previous researchers. The study focuses on the following two-step process for removal of selenium from groundwater:

1. Oxidation of all aqueous selenium to selenate anion, Se(VI), and

2. Strong-base anion-exchange removal of the selenate anion.

Conclusions and Recommendations

The two-step process of oxidation with free chlorine followed by anion exchange appears to be technically feasible and should be considered for removal of selenium to produce potable water from selenium-contaminated groundwater. Further research and development is recommended to develop the optimum process and to adapt the process for optimum operation at specific sites.

Some problems that must be addressed in the next phase of process development include determining the effects of temperature and the presence of other chlorine demands such as TOC, Fe^{2+}, Mn^{2+}, and S^{2-} on oxidation kinetics, countering the effects of residual chlorine from the oxidation process on the anion-exchange resin, determining the optimum anion-exchange resin type and empty bed contact time (EBCT), developing a process control scheme that includes some means (possibly pH changes) of detecting selenium breakthrough, and disposing of spent regenerant.

The analytical method developed to determine the speciation of selenium in groundwater proved to be a useful tool for the study of Se(IV) oxidation and is recommended for measurement of both Se(IV) and Se(VI) in actual groundwaters that are contaminated with selenium. However, the analytical technique should be refined by optimizing the acid used and the sample flow rate.

The full report was submitted in fulfillment of Cooperative Research Agreement No. CR-807939 by the University of Houston-University Park under the sponsorship of the U.S. Environmental Protection Agency.

Joan V. Boegel is now with Metcalf and Eddy, Inc., Boston, MA 02114; and Dennis Clifford is with the University of Houston-University Park, Houston, TX 77004.
***Thomas J. Sorg** is the EPA Project Officer (see below).*
The complete report, entitled "Selenium Oxidation and Removal by Ion Exchange," (Order No. PB 86-171 428/AS; Cost: $11.95, subject to change) will be available only from:
National Technical Information Service
5285 Port Royal Road
Springfield, VA 22161
Telephone: 703-487-4650
The EPA Project Officer can be contacted at:
Water Engineering Research Laboratory
U.S. Environmental Protection Agency
Cincinnati, OH 45268

Manufacturing, Machinery, & Tools

1093 Wound-Elastomer Fabrication of Motor Insulators—Cost are reduced and design flexibility increased in producing insulators with greater strengths.

1094 Directory of Federal Certification Programs Published

1095 Ion Implantation for Corrosion and Wear Resistance

1096 Forging of Discontinuous Metal Matrix Composites

1097 Controlling Arc Length in Plasma Welding—A circuit maintains the arc length on irregularly shaped workpieces.

1098 Ion-Deposited Polished Coatings Polished, dense, adherent coatings are relatively free of imperfections.

1099 Preventing Delamination of Silverized FEP Films—Edge treatment inhibits attack by moisture.

1100 Material for Fast Cutting—Silicon nitride-based tool boosts productivity and reduces costs.

1101 Variable-Friction Secondary Face Seals—Feedback-controlled friction or damping suppresses vibrations.

1102 Spring-Loaded Joule-Thomson Valve—The improved design reduces clogging and maintains a constant pressure drop as the flow rate varies.

1103 Modified Cobalt Drills With Oil Passages—Oil is forced through the drill shanks to lubricate the cutting edges.

1104 Spiral-Groove Ring Seal for counterrotating Shafts—The self-lubricating seal tolerates high sliding speeds.

1105 Designing Power-Transmission Shafting—Consideration of stress and fatigue life gives better designs.

Testing & Instrumentation

1106 Measuring Thicknesses of Coatings on Metals—A digital light sensor and eddy-current sensor measure thickness without contact.

1107 Optical Monitoring of Weld Penetration—Robotic welding can be controlled by a reliable, relatively-noise-free optoelectronic unit.

Other items of interest

1113 Ion-Vapor Deposition Process for Aluminum Coating—This process can supplant cadmium electroplating for corrosion protection.

MANUFACTURING TECHNOLOGY NOTE

U.S. ARMY MATERIEL COMMAND

Deputy Chief of Staff for Manufacturing Technology, Alexandria, VA

Project Number: MMT3XX1126 **Filing Code :** 71H019

Wound-Elastomer Fabrication of Motor Insulators

Costs are reduced and design flexibility increased in producing insulators with greater strengths.

The U.S. Army Missile Command has verified the cost effectiveness and the versatility of the wound-elastomeric-insulator (WEI) method of motor insulator fabrication. This method, which may be applied to any system using a KEVLAR® (or equivalent) wound filament as small as 12 to 15 inches (30.5 to 38.1 cm) in diameter, provides cost reduction, lead-time improvement, and producibility enhancement in motor case fabrication.

In an application of the WEI process to the fabrication of rocket motor insulators, a microprocessor controlled winding machine is used to extrude green elastomer to a precisely controlled thickness and immediately wind it directly onto the case mandrel (see figure); insulator thickness depends upon the number of plies of extruded elastomer laid down. The case is then wound directly onto the insulator in the conventional manner. An automated thickness-profile measuring system was developed to inspect the uncured insulator. Should the insulator be out-of-tolerance, rework can be done before the motor case is wound. The standard case-cure cycle provides an adequate cure for both the casing and the WEI insulator.

Testing of WEI materials resulted in the selection of an insulator that performed as well as, or better than, that presently used. A Pershing II first stage case fabricated by WEI was burst tested at 77 °F(25 °C); the burst pressure attained was the highest ever for this case at this temperature.

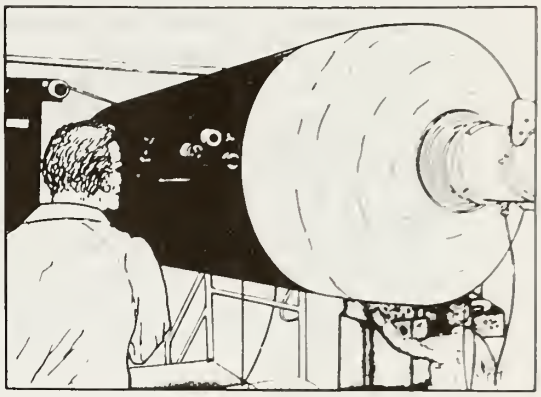

In an application of **The WEI Process,** a green elastomer is extruded to a precisely controlled thickness and then wound directly onto the case mandrel.

FOR ADDITIONAL INFORMATION

You can learn more details about this technology by contacting

Commander
U.S. Army Missile Command
Attn: AMSMI-RD-SE-MT (T. Shaw)
Redstone Arsenal, AL 35898-5270
Telephone No. (205) 876-2147 or AV 746-2147

This document was prepared under the sponsorship of the U.S. Government. Neither the United States Government nor any person acting on behalf of the United States Government assumes any liability resulting from the use of the information contained in this document, or warrants that such use will be free from privately owned rights.

NBS technology update

National Bureau of Standards
U.S. Department of Commerce
Gaithersburg, MD 20899

Directory of Federal Certification Programs Published

Federal Government Certification Programs for Products and Services (SP 714), is a guide for manufacturers, distributors, state and local government officials, consumers and others concerned with the standards and procedures used in federal certification programs. These include manufactured products, agricultural commodities, medical devices and drugs, defense certification programs. These include manufactured products, agricultural commodites, medical devices and drugs, defense procurement, public services including transportation, and the voluntary inspection and uniform grading of such food items as dairy products, meats, and produce. The directory, which contains information on 61 federal certification programs, describes the scope and nature of the program, the testing and inspection practices, standards used, methods of identification and enforcement, reciprocal recognition or acceptance of certification, as well as other relevant information.

FOR ADDITIONAL INFORMATION:

You can learn more details about this technology by ordering the NTIS report(s):

Federal Government Certification Programs.
Order number: PB86-191871/NAC
Price code: A08

Order from:

National Technical Information Service
5285 Port Royal Rd.
Springfield, VA 22161

Ion Implantation for Corrosion and Wear Resistance

A Manufacturing Technology project sponsored by NAVSEA is nearing completion with an end-of-project demonstration scheduled for May 8, 1986 at Spire Corp., Bedford, MA. The project was undertaken to develop the technology necessary to scale up the ion implantation process from a laboratory size feasibility study to a viable high throughput industrial production process and to demonstrate ion implantation as a generic process for corrosion and wear control. The Naval Research Laboratory was responsible for the program, and Spire Corporation had a major subcontract to build and operate the facility.

The Navy has many applications where surface alloying is required to improve the corrosion or wear properties of a part or component. Ion implantation is a new surface modification technique which can be used to precisely alter the composition of the surface region to a depth on the order of four microinches. The advantages of ion implantation are (a) flexibility in that any element can be introduced into any substrate, (b) there are no thermodynamic constraints such as the requirement of an elevated temperature for diffusion or initiation of a chemical reaction, (c) no refinishing of the part is required and (d) there is no discrete interface to fail since implantation occurs below the original surface.

The ion implantation process involves creation of ions in a source, focusing of the ions through a series of magnetic and electrostatic lenses, and acceleration of the ions through a potential gradient typically of the order of 150 kilovolts, all in a vacuum environment. Ion implanters are available commercially from the semiconductor industry but require modification of the ion source to produce high current beams of metal ions. A complete engineering analysis and design of the end station and work piece handling system was required to develop a facility suitable for processing of metallic components. This has been accomplished and engineering solutions to the problems of heat removal, sputtering at non-normal angles of incidence, and surface contamination in vacuum have been successfully implemented.

Demonstration projects have included the implantation of gas turbine engine bearings and helicopter hinge pin bearings with chromium to improve the corrosion resistance of these components, which are subject to pitting corrosion when lubricants become contaminated with chloride in the marine environment. Geometries implanted have included inner races, outer races, and rolling elements for both roller and ball geometries. Another demonstration project was the implantation of beryllium alloy components of gyroscope bearings with boron to improve the wear resistance and operational characteristics of the bearing. A third demonstration project was the implantation of tungsten carbide-cobalt drills with nitrogen to improve the cutting characteristics and reduce the spread in failure life for printed circuit board applications.

This project has provided the critical impetus needed to make ion implantation available as a viable industrial technology for the surface treatment and modification of critical components of Naval equipment subject to degradation by corrosion and wear.

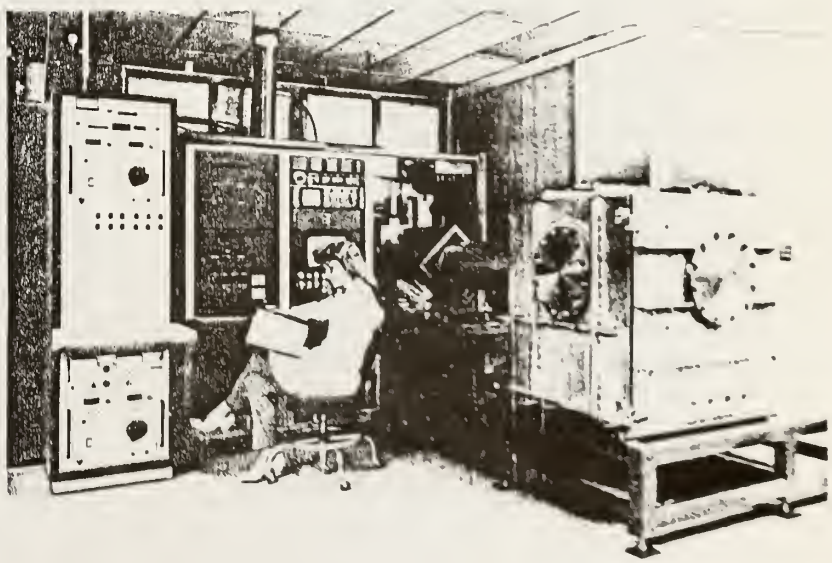

ION IMPLANTATION EQUIPMENT

Specific accomplishments of the project include:

- The first comprehensive engineering analysis of the process requirements.
- The design and construction of the first end station and fixturing optimized for high throughput industrial production.
- The operation of the facility under industrial conditions for a period of eight months.
- The development of a computer code to calculate implanted atom concentration profiles.
- The successful demonstration of ion implantation processing for several components for which service lifetime can be extended by 200% or more with attendant decreases in life cycle costs.

Arrangement are being made to make the facility, located at Spire Corporation, available for feasibility studies of implantation applications without charge for beam time for a period of five years. Production runs of components will be provided by Spire Corporation as a commercial enterprise.

For further information contact:
Commanding Officer
Naval Research Laboratory
Attn: Dr. Fred A. Smidt (Code 4670)
Washington, DC 20375-5000
Telephone: (202) 764-4800;
AV 297-4800

Forging of Discontinuous Metal Matrix Composites

Under NAVSEA sponsorship, McDonnell Douglas Astronautics has developed improved forging processes for shaping discontinuous metal matrix composites (DMMC). Aluminum matrix reinforced materials have been under development by the DOD for the past decade due to their attractive strength to weight, stiffness to weight, and increased long term mechanical stability vis-a-vis unreinforced aluminum. The latter property has resulted in DMMC's being chosen as the material to be used for hatch cover doors in the guidance platform for the Navy's D-5 missile, representing the first introduction of these materials into fleet systems.

During the development and evaluation of metal matrix composite technology, it was demonstrated that this family of reinforced aluminum structural materials could be shaped using most conventional metal working processes. However, due to increased flow stresses, sensitivity to tensile loads in unwrought material, and the abrasive action of the hard reinforcing media (SiC or B_4C), modifications to secondary processing techniques were crucial to making these materials cost effective candidates for replacing conventional metals. Exploratory development programs sponsored by NAVSEA focused on systems studies and hardware demonstrations of DMMC materials in missile, torpedo, and antenna applications. The high specific stiffness of SiC reinforced aluminum makes this composite material a potential candidate for reduction of structural weight in applications that are stiffness critical or deflection limited and where unreinforced aluminum is the primary structural material.

Figure 1 shows a prototype radar antenna which has all major structural and microwave components made from 25 v/o SiC/6061 aluminum. This antenna was fabricated and tested under a previous project and is one of the most complex hardware items ever made from DMMC. The microwave components include sixty-four feedhorns (shown in Figure 1 with the radome removed) connected to a "C" band waveguide. Cost and time constraints in the original fabrication program prevented cost efficient manufacture of the feedhorns and other components. For the antenna shown, the feedhorns, were forged to net shape but had to be extensively machined on all outer surfaces to attain the required configuration. The abrasive nature of this material results in high machining and tooling costs and the achievement of near net shape from secondary processing is needed to make these materials attractive for fleet use.

A manufacturing technology project (M0303) was initiated to reduce feedhorn cost via attainment of nearer net shape forgings. The team of McDonnell Douglas and Chentech designed multi-strike forging tooling and developed the process which resulted in the feedhorn forging shown in Figure 2. Net internal and external shape was attained on all but two sides of the horn. This represents a significant gain in precision forging of DMMC and it is believed that full net inner and outer configuration could be

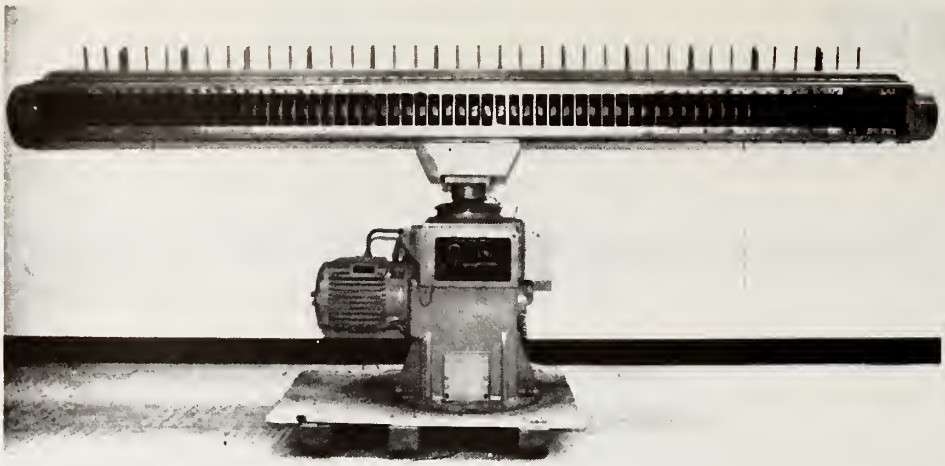

FIGURE 1. PROTOTYPE RADAR ANTENNA

FIGURE 2. FORGING SEQUENCE FOR FEEDHORNS

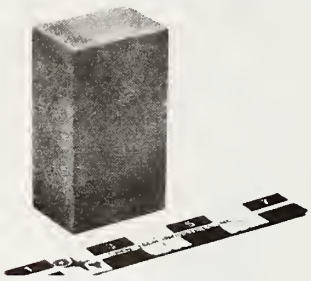

(STARTING BLOCK)

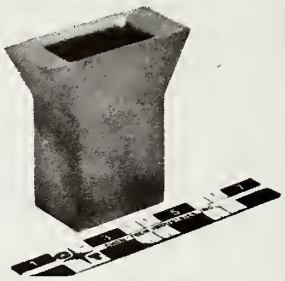

(1ST STRIKE)

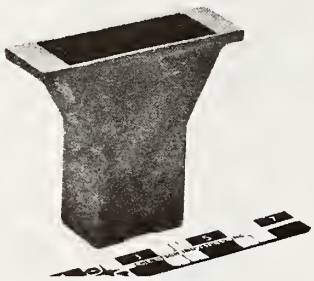

(2ND STRIKE)

(FINAL STRIKE)

achieved with additional investment of time and funding. The results of this project were demonstrated by McDonnell Douglas on March 20, 1986.

This program was significantly aided by the successful billet improvement program reported on earlier. The DMMC materials made using ARCO's improved outgassing techniques provided minimum porosity feedstock for the forging program and resulted in parts with excellent mechanical properties. The gains provided by these and other MANTECH manufacturing science programs have materially aided the development of DMMC technology and hastened their eventual emergence as high performance structural materials for diverse fleet applications.

For more information contact:
Commanding Officer
Naval Surface Weapons Center — White Oak
Attn: Mr. John Tydings
Silver Spring, MD 20903-5000
(202) 394-2488; AV 290-2488

NASA Tech Brief
National Aeronautics and Space Administration
Lyndon B. Johnson Space Center, Houston, Texas

Licensing Opportunity

Controlling Arc Length in Plasma Welding

A circuit maintains the arc length on irregularly shaped workpieces.

A control adapter circuit maintains a constant arc length during plasma arc welding of irregularly contoured parts. The circuit can be added to plasma arc welding machines with just a few wiring changes. Welds made with the circuit are cleaner and require less rework than do welds made without it. The beads are smooth and free of inclusions.

The circuit (see figure) samples the ac arc voltage, then half-wave rectifies and filters it to reduce the ripple. The resulting dc measurement signal is applied to a comparison amplifier, which compares it to a reference voltage that represents the commanded arc length. The amplifed comparison signal is applied to a power amplifier that drives a motor and gear train to adjust the electrode position and therefore the arc length.

This work was done by William F. Iceland of Rockwell International Corp. for **Johnson Space Center.**

Inquiries concerning rights for the commercial use of this invention should be addressed to the Patent Counsel, Johnson Space Center Refer to MSC-20900. /TN

William Chmylak
Lyndon B. Johnson Space Center
Mail Code AL32
Houston, TX 77058
(713) 483-3809

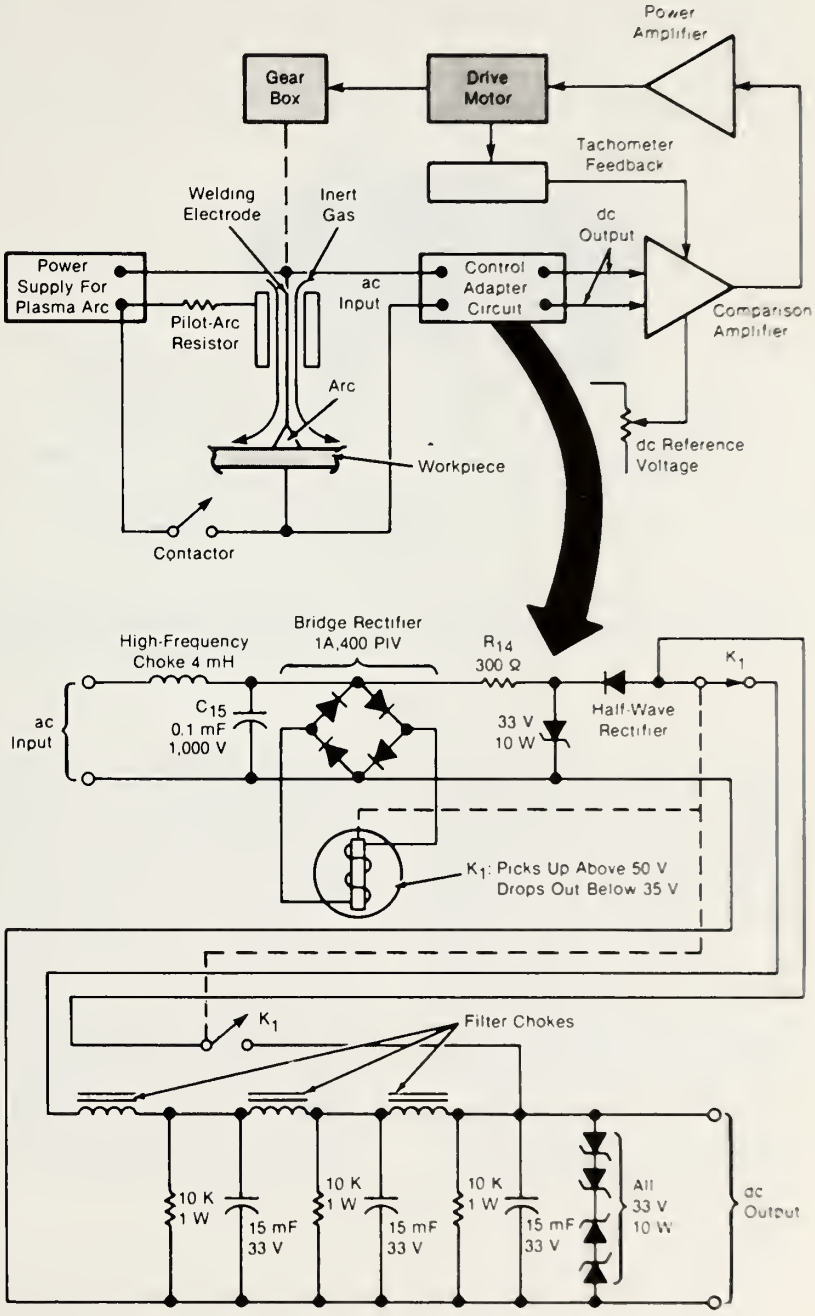

The **Length of a Plasma Arc** is continuously adjusted by the control circuit to maintain the commanded value. After a pilot arc has been established, the contactor is closed and transfers the arc to the workpiece. The control circuit then half-wave rectifies the ac arc voltage to produce a dc control signal proportional to the arc length.

FOR ADDITIONAL INFORMATION: *Contact: Director, Technology Transfer Division, P.O. Box 8757, BWI Airport, MD. 21240; (301) 621-0100 Ext. 241*
REFER TO THE NUMBER LISTED AT THE END OF THE ARTICLE

NASA Tech Brief
National Aeronautics and Space Administration
Lewis Research Center, Cleveland, Ohio

Ion-Deposited Polished Coatings

Polished, dense, adherent coatings are relatively free of imperfections.

A process has been developed to provide a highly-polished and adherent dense coating to a substrate that is free of voids, contaminants, and inclusions. A broad-beam ion source is used to sputter-polish while a vapor or sputter deposition is occurring simultaneously on the substrate surface. Prior techniques removed material from the surface, exposing subsurface voids and contaminants. No simultaneous fill of voids occurred and therefore the surface was not free of defects since these were removal processes.

The new process consists of using a broad-beam ion source in an evacuated chamber to ion-clean a rotating surface that allows the grazing incidence of the ion beam. This sputter cleans off absorbed gases, organic contaminants, and oxides of the mirror surface. In addition to the cleaning, surface protrusions will be sputter-etched away.

Once the surface has been ion-cleaned, a variety of vacuum-deposition techniques can be used to deposit adherent coatings on the cleaned mirror surface. Figure 1 depicts grazing-incidence ion polishing with simultaneous, normally incident vapor or sputter deposition. The simultaneous sputter polishing and vacuum deposition must be done in a manner so that the sputter-etch rate is slightly lower than the deposition rate on the mirror surface. This allows pits or depressions in the mirror surface to fill in quickly because the grazing-incident ion beam does not have a view factor to sputter-etch these areas which are receiving near-normal incident vapor or sputter deposition. At the same time, protrusions, bumps, and other convex surface asperities have a sputter-etch rate higher than surrounding smooth flat surfaces. This is due to the relative angles at which the sputter-etching ions and the deposition material arrive.

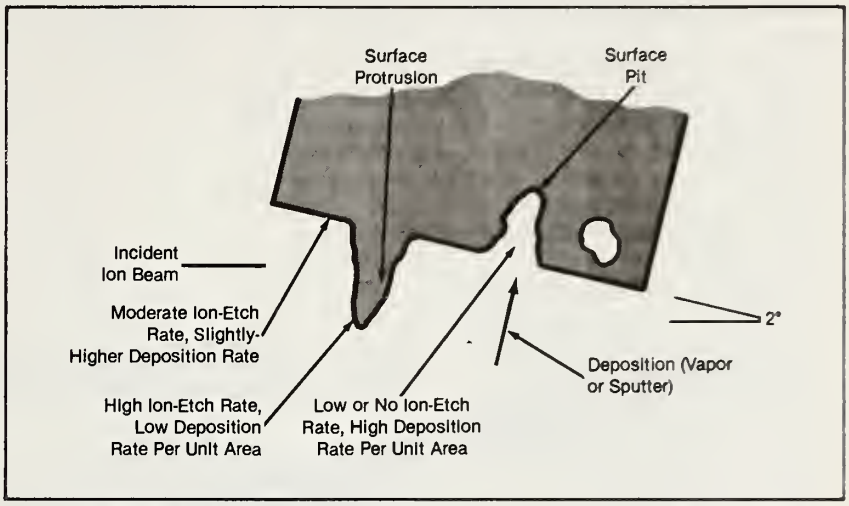
Surface Protrusion
Surface Pit
Incident Ion Beam
Moderate Ion-Etch Rate, Slightly-Higher Deposition Rate
High Ion-Etch Rate, Low Deposition Rate Per Unit Area
Low or No Ion-Etch Rate, High Deposition Rate Per Unit Area
Deposition (Vapor or Sputter)
2°

Figure 1. **Grazing-Incidence Ion Polishing** is conducted simultaneously with deposition by normally incident vapor or a sputtering beam.

Figure 2 depicts the processes of simultaneous ion sputter, polishing, and deposition. The process leads to a smooth deposited and polished surface in a similar manner analogous to the macroscopic process of multiple painting and sanding operations for wood finishing. The net deposition resulting quickly becomes a smooth mirror-surface deposit that slowly builds up free from surface irregularities, such as defects, voids, or protrusions. The process is stopped when the desired deposit thickness is achieved. Both the ion-beam sputter polishing and the deposition should be stopped simultaneously when the desired coating thickness is achieved.

Eleven other adaptations to the process are the following:

1. The mirror material can be metals, metal carbides, metal oxides, certain polymers, and most inorganic compounds.
2. The deposition can be produced by vapor deposition from electron-

beam evaporators, heated boats, filaments, or by ion-beam, dc or RF sputtering from the same or another deposition system.

3. The substrate surface angle θ can be varied from 0° to ≅ 10° with respect to the incident ions, depending on the degree of polishing desired.
4. The surface can be cooled or heated as desired to improve the quality of the coating.
5. The ion energy can be varied from a few hundred to a few thousand electronvolts.
6. The sputtering ions can be a variety of gas species, such as Ar, Xe, Ne, and N.
7. The duration of initial sputter-etch cleaning can be varied from seconds to hours, depending upon the thickness desired.
8. The ion beam can be of various diameters, from centimeters to meters, depending upon the substrate diameter.
9. The deposited coating can be a variety of materials, such as metals, metal oxides, and metal nitrides. The deposited materials can also be a different material than the substrate.
10. The rotation rate of the substrate can be varied as desired to produce the best-quality surface coating.
11. Further coatings can be applied by the same process if one wants to switch materials for the outer substrate surface.

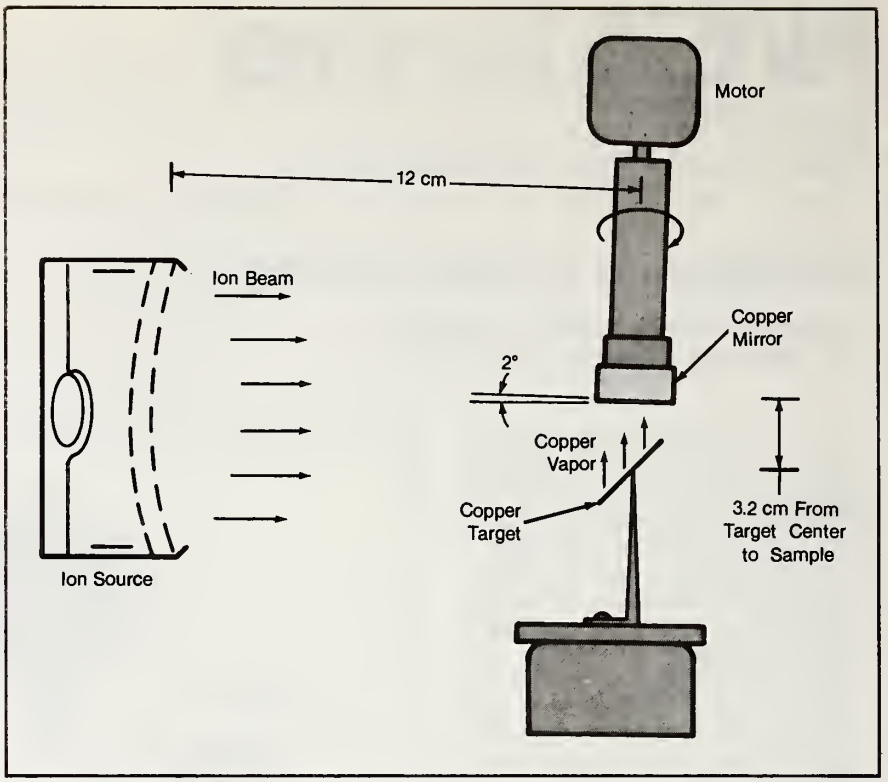

Figure 2. **Ion Sputter Polishing** and deposition give a smooth deposited and polished surface, in a manner analogous to that of the repeated painting and sanding of wood.

The process is particularly adaptable to the polishing of various substrates for optical or esthetic purposes.

This work was done by Bruce A. Banks of **Lewis Research Center.** *Further information may be found in NASA TM-81679 [N81-19278/NSP], "Simultaneous Ion Sputter Polishing and Deposition" [A03] A copy may be purchased [prepayment required] from the National Technical Information Service, Springfield, Virginia 22161. LEW-13545 /TN*

FOR ADDITIONAL INFORMATION: *Contact: Director, Technology Transfer Division, P.O. Box 8757, BWI Airport, MD. 21240; (301) 621-0100 Ext. 241*

REFER TO THE NUMBER LISTED AT THE END OF THE ARTICLE

NASA Tech Brief
National Aeronautics and Space Administration
Lyndon B. Johnson Space Center, Houston, Texas

Preventing Delamination of Silverized FEP Films

Edge treatment inhibits attack by moisture.

A novel procedure overcomes delamination of a silver-coated fluorinated ethylene/propylene (FEP) film on an aluminum substrate. FEP presents special difficulties with regard to metalization because it is formulated to actually prevent adhesion.

The delamination of untreated assemblies is apparently due to attack by moisture that migrates through the silicone adhesive between the silver and the FEP. The conclusion that failure was not a result of residual stress — perhaps from processing or simply from differential thermal expansion of the laminated layers — was reached after an extensive test program.

The new technique prevents delamination by sealing the edges where delamination starts. To ensure adhesion, the surface to be sealed is carefully prepared. The edges are abraded lightly with sandpaper to provide a roughened surface for mechanical bonding to the edge-sealing material. A bead of flexible epoxy about one-sixteenth inch (1.6 mm) wide is applied with a syringe so that the edges of the metalization, FEP layer, and film-to-substrate adhesive are covered (see figure).

The method is easy to implement, even in the field as a repair procedure. It withstands a variety of environmental tests, including heat and vacuum testing for 24 hours, moisture testing at 95 percent relative humidity for 5 days, and 3 weeks total water immersion at room temperature. Untreated laminates, in contrast, deteriorated seriously during such tests.

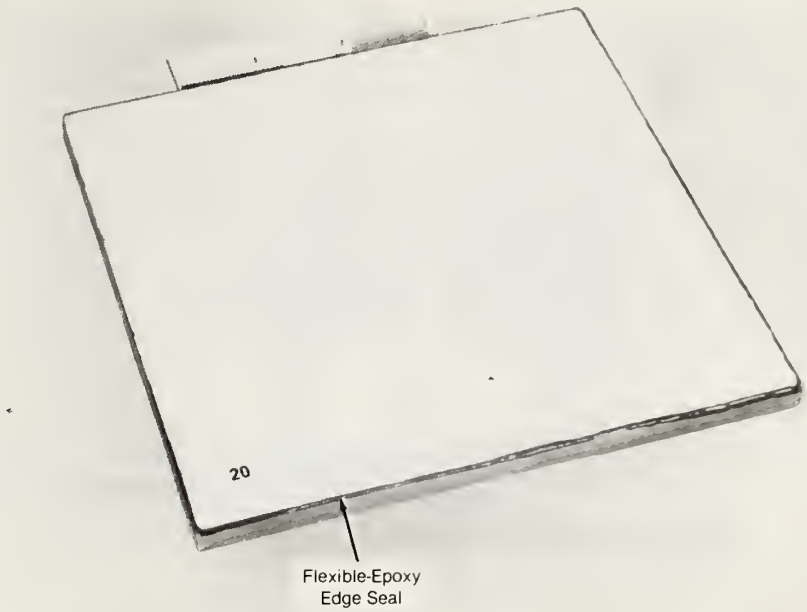

Samples of Aluminum/FEP/Silver Laminate survive humidity tests and other environmental tests when the edges of the layers are covered by an epoxy bead.

This work was done by Larissa Domnikov, Judy May, and Roberto Gallego of Hughes Aircraft Co. for **Johnson Space Center.**

MSC-20460 /TN

FOR ADDITIONAL INFORMATION: *Contact: Director, Technology Transfer Division, P.O. Box 8757, BWI Airport, MD 21240; (301) 621-0100 Ext. 241*

REFER TO THE NUMBER LISTED AT THE END OF THIS ARTICLE

NASA Tech Brief
National Aeronautics and Space Administration
Marshall Space Flight Center, Alabama

Material for Fast Cutting

Silicon nitride-based tool boosts productivity and reduces costs.

A new material for cutting tools increases the productivity of machining processes. The material, called Iscanite (or equivalent), is based on silicon nitride and contains more than 90 percent silicon. It combines impact resistance close to that of coated carbides with heat and wear resistance close to those of aluminum oxide ceramics.

Tools made of Iscanite (or equivalent) can operate at higher cutting speeds. For equal pressure on the workpiece, an Iscanite (or equivalent) tool will therefore remove more material than will a conventional tool. The new material makes it unnecessary to use high pressure to increase the removal rate and therefore greatly reduces workpiece slippage, vibration, and tool breakage. Iscanite (or equivalent) tools last longer and therefore reduce the amount of cutting time lost to indexing, gauging, and adjustments.

The material is made by a hot-pressing technique that yields a product having full density. The material can be used for cutting on old or new machine tools and makes it possible to exploit fully the power and speed of a machine.

This work was done by Andrew Perez of Rockwell International Corp. for **Marshall Space Flight Center.**
MFS-29130 /TN

FOR ADDITIONAL INFORMATION: *Contact: Director, Technology Transfer Division, P.O. Box 8757, BWI Airport, MD 21240; (301) 621-0100 Ext. 241*
REFER TO THE NUMBER LISTED AT THE END OF THIS ARTICLE

NASA Tech Brief
National Aeronautics and Space Administration
Lewis Research Center, Cleveland, Ohio

Variable-Friction Secondary Face Seals

Feedback-controlled friction or damping suppresses vibrations.

A variable-friction secondary seal has been conceived to control the vibration and stability of the primary seal ring over a wide range of conditions. By varying the friction force or damping applied to the primary seal ring, the vibration can be controlled to provide stable operation.

Self-acting face seals are a special type of face seal that operate with a very-thin liquid or gaseous film between the primary seal faces. In addition to the primary sealing face, face seals have a secondary seal, typically in the form of piston rings or elastomeric O-rings. The purpose of the secondary seal is to seal the secondary leak path in the face-seal assembly. Face seals are subject to instability due to the vibration of the primary seal ring. This results in excessive seal-face wear or failure.

Previous devices for producing the damping of primary-seal-ring vibration were of a static nature; i.e., the friction force was optimized for one seal-operating condition only. The disadvantage was that instabilities were encountered when seal conditions deviated from the design condition or when the seal was perturbed by transients.

As a means of alleviating this situation and allowing control over a wide range of conditions, the variable-friction secondary seal was conceived. The components of the "variable-friction secondary seal" (see figure) are the bladder and secondary seal ring, which has an axial split line. Operationally, variable friction and consequently variable damping are achieved by introducing air or hydraulic pressure through the stem into the bladder, which causes the bladder to expand into the secondary-seal ring. This changes the radial force and, consequently, the friction damping applied to the carrier.

In the event that the seal film becomes unstable or the primary ring begins to vibrate, the bladder pressure is changed to mitigate the instability or vibration. The bladder pressure can be changed manually or by means of a feedback control system, which senses primary-ring vibration amplitude. The control system then changes the bladder pressure to minimize or limit the primary-ring vibration amplitudes within stable boundaries. The secondary-seal material may be selected to provide many different friction coefficients, and coatings may be applied to the secondary-seal ring to optimize the friction coefficient and sliding interface.

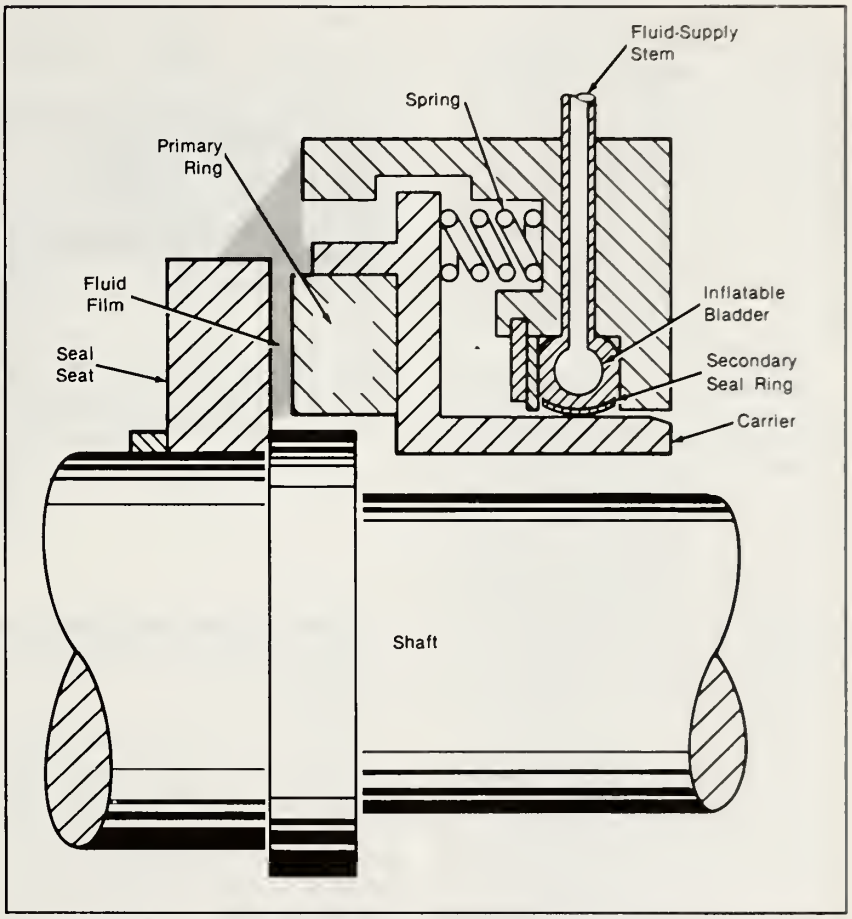

The Friction Damping Applied to the Carrier is varied by changing the pressure of air or fluid in the bladder.

Advantages of the "variable-friction secondary seal" are that face-seal stability can be controlled as a function of primary-ring vibration amplitudes, and also the friction can be remotely changed to achieve acceptable vibration amplitudes for a large range of seal-operating conditions without compromising the secondary-seal performance. The concept is also useful in seal testing in which the dynamic stability of face seals is under evaluation.

This work was done by Eliseo DiRusso of **Lewis Research Center.**
LEW-14170 /TN

FOR ADDITIONAL INFORMATION: *Contact: Director, Technology Transfer Division, P.O. Box 8757, BWI Airport, MD 21240; (301) 621-0100 Ext. 241*
REFER TO THE NUMBER LISTED AT THE END OF THIS ARTICLE

NASA Tech Brief
National Aeronautics and Space Administration
NASA's Jet Propulsion Laboratory, Pasadena, California

Spring-Loaded Joule-Thomson Valve

The improved design reduces clogging and maintains a constant pressure drop as the flow rate varies.

A spring-loaded Joule-Thomson (J-T) valve permits optimal cooling-power regulation of a J-T refrigerator by allowing independent adjustment of the flow rate and pressure drop through the valve. Because the spring-loaded J-T valve maintains a constant pressure drop, an upstream room-temperature throttle valve can adjust the flow rate precisely for any given upstream pressure. In addition, the new valve is relatively invulnerable to frozen gas contaminants, which can clog fixed-orifice J-T valves.

Conventional J-T expansion valves have fixed orifice openings; the pressure drop through these openings depends on the helium flow rate. Moreover, any trace amount of frozen gas contaminants could block such openings, drastically changing the cooling power of the refrigerator.

The new valve operates very much like a variably-loaded check valve. The orifice is regulated by a steel ball pushed by adjustable spring tension against a soft brass seat (see figure). The steel ball is raised off the seat whenever the force of the upstream pressure exceeds the spring force. Thereafter, a nearly-constant pressure drop is maintained as long as the gas flows by the spring-loaded ball. An increase in the flow rate merely lifts the ball further, the pressure drop being almost unaffected. Contaminants that freeze out on the ball or seat lift the ball slightly further, but do not clog the valve permanently, as in a fixed-orifice J-T valve.

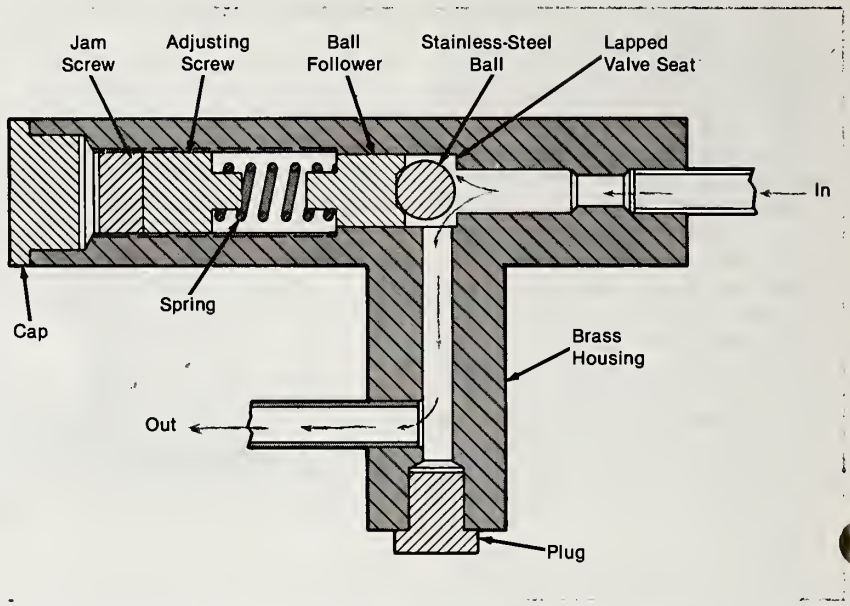

In this **Spring-Loaded Joule-Thomson Valve** the pressure drop is regulated by the spring pushing the stainless-steel ball against a soft brass seat. The pressure drop remains nearly constant, regardless of the helium flow rate and of any gas contaminants frozen on the valve seat.

The metal-to-metal seat is more attractive for cryogenic applications than plastic seating materials, which tend to deform more than metals at low temperatures. Also the ball-and-socket approach is better than valve-poppet/O-ring designs, because a ball-and-socket design is self-centering. The new design also allows for external adjustment of the flow rate by means of a room-temperature throttle valve upstream of the J-T valve. Because the spring stiffness varies with temperature, the pressure drop at liquid-helium temperatures (typically 4.5 K) is about 4 percent higher than at room temperature.

The valve was tested on a cryogenic refrigerator used for maser receivers. At the throttle valve, the pressure dropped from 282 psia (1.94×10^6 N/m^2) to 262 psia (1.81×10^6 N/m^2); and at the spring-loaded J-T valve, from 262 psia (1.81×10^6 N/m^2) to 20 psia (1.38×10^5 N/m^2) while the temperature at the J-T valve was maintained at 4.5 K.

This work was done by Jack A. Jones and Michael J. Britcliffe of Caltech for **NASA's Jet Propulsion Laboratory.**
NPO-16546 /TN

FOR ADDITIONAL INFORMATION: *Contact: Director, Technology Transfer Division, P.O. Box 8757, BWI Airport, MD 21240; (301) 621-0100 Ext. 241*
REFER TO THE NUMBER LISTED AT THE END OF THIS ARTICLE

NASA Tech Brief
National Aeronautics and Space Administration
Marshall Space Flight Center, Alabama

Modified Cobalt Drills With Oil Passages

Oil is forced through the drill shanks to lubricate the cutting edges.

Drill bits have been cooled and lubricated by oil forced through the drill shanks and out holes adjacent to the bits. This cooling technique increases drill-bit life and allows increased drill feed rates.

The particular application involved the removal of inertia-weld nuggets from the bottoms of holes 10 in. (25.4 cm) long with 0.188 in. (0.47 cm) diameter. The nugget material is left after inertia welding of Haynes 188 (or equivalent) posts (containing the holes) to Inco 718 (or equivalent) stubs. The nuggets are irregularly shaped with inconsistent material properties.

Carbide drill bits tend to break from the surface irregularities, making cobalt a better cutting tool material. However, cobalt drill bits dull rapidly without adequate cooling. The drill diameter is only 0.010 in. (0.025 cm) less than that of the hole. The conventional cooling method fails to get coolant to the cutting surface of the drill at the bottom of the hole.

The solution to the problem is shown in the figure. The drill shank is joined with a tube having three exit holes 120° apart near the shank end. Cooling oil is forced through the tube and out the exit holes toward the bit.

This work was done by E. E. Hutchison and D. Richardson of Rockwell International Corp. for **Marshall Space Flight Center.** *MFS-29137 /TN*

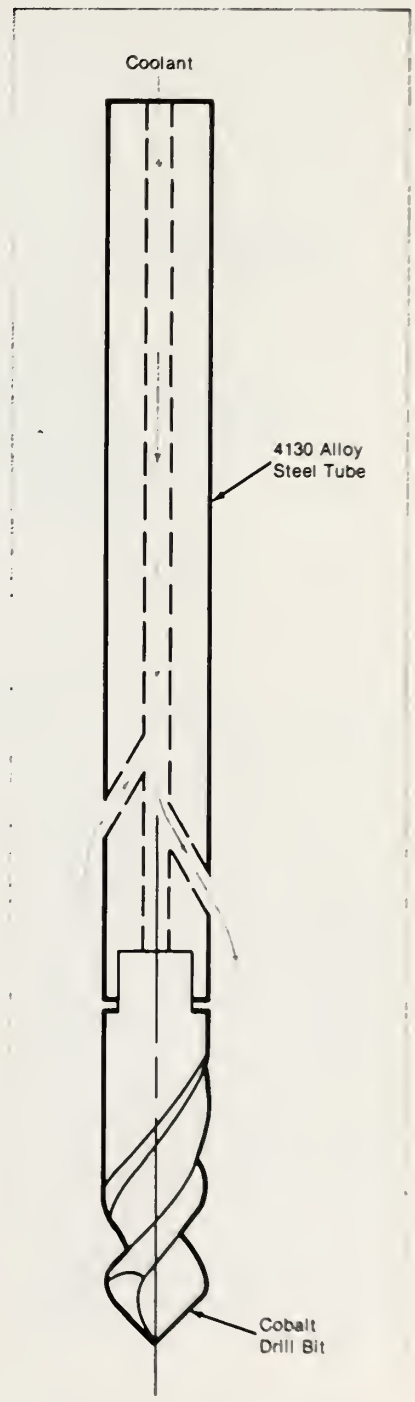

During Drilling the Bit Is Cooled by oil forced through the shaft and out holes near the bit.

FOR ADDITIONAL INFORMATION: *Contact: Director, Technology Transfer Division, P.O. Box 8757, BWI Airport, MD 21240; (301) 621-0100 Ext. 241*
REFER TO THE NUMBER LISTED AT THE END OF THIS ARTICLE

NASA Tech Brief
National Aeronautics and Space Administration
Lewis Research Center, Cleveland, Ohio

Spiral-Groove Ring Seal for Counterrotating Shafts

The self-lubricating seal tolerates high sliding speeds.

The spiral-groove intershaft ring seal is a new seal concept that has potential application in sealing fan-bleed air between two counterrotating shafts in advanced gas-turbine engines. This is a difficult sealing application for any contacting-type seal because the counterrotating shafts set up very high sliding speeds for the seal. In addition to the high sliding speed, the seal must accommodate axial translation due to relative axial motion between the two shafts.

The intershaft ring-seal application is an excellent example of the need for applying self-acting, gas-lubricating bearing technology to contacting-type seals. Application of a self-acting geometry in the form of spiral grooves to the faces of the ring-seal housing will maintain a thin air film of relatively high stiffness between the seal ring and the housing, thereby enabling the seal to operate in a noncontacting mode over the entire engine-operating range. The seal could then operate at high sliding speeds, accommodate axial translations, and have leakage rates consistent with contacting-type seals.

When spiral grooves are employed in a seal as a film-generating mechanism, the following are generally required to calculate the axial-force equilibrium: (1) film load-capacity curves (lift force as a function of film thickness), (2) minimum film thickness over the operating range, and (3) optimization of the spiral-groove geometry to maximize the lift force for a given seal-envelope size and operating condition. Figure 1 shows the intershaft seal concept. The housing, which contains the carbon ring, rotates with the inner shaft. The carbon ring is bounded on its outside diameter by the outer shaft,

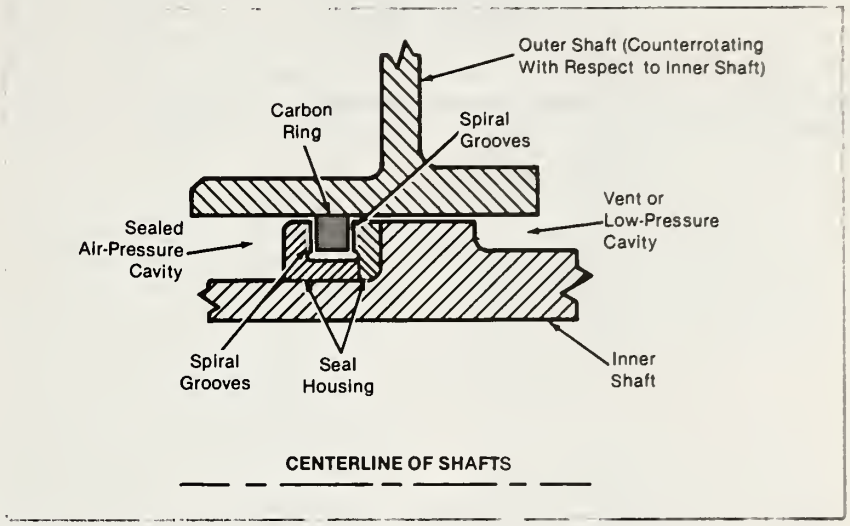

Figure 1. The **Intershaft Seal** includes spiral grooves that generate lubricating gas films.

which counterrotates with respect to the inner shaft. As the shafts rotate, the carbon ring expands into the outer shaft and assumes the speed of the outer shaft. The relative sliding speed between the carbon ring and the inner shaft can approach 255 meters per second (835 feet per second).

It should be noted that the carbon ring may require a radial split line to limit hoop stresses due to rotation and to assure that the carbon ring will rotate with the outer shaft. Relative axial translations between the inner and outer shafts of up to 0.64 centimeter (0.25 inch) due to thermal expansion are possible over the design operating range. This translation causes the carbon ring to approach one of the two housing faces. The spiral grooves on the housing faces generate a very high lift force as the carbon ring approaches either face, thereby maintaining a fluid film between the carbon ring and the housing face.

Figure 2 is a schematic drawing of the seal showing it in a neutral position (equal clearance on either side of the carbon). The total axial clearance between the carbon ring and the housing face is only 0.0203 millimeter (0.0008 inch) or 0.0102 millimeter (0.004 inch) per side when the seal is centered in the housing. The airflow through the seal is shown; P_1 is the high pressure, and the pressure drop from P_1 to P_2 occurs across the seal dam. The porting shown is designed such that the spiral grooves are bounded by the sealed pressure (P_1) at both the outside and inside diameters; hence, there is no pressure difference across the spiral grooves. This is known as a pressure-balanced spiral-groove concept. The

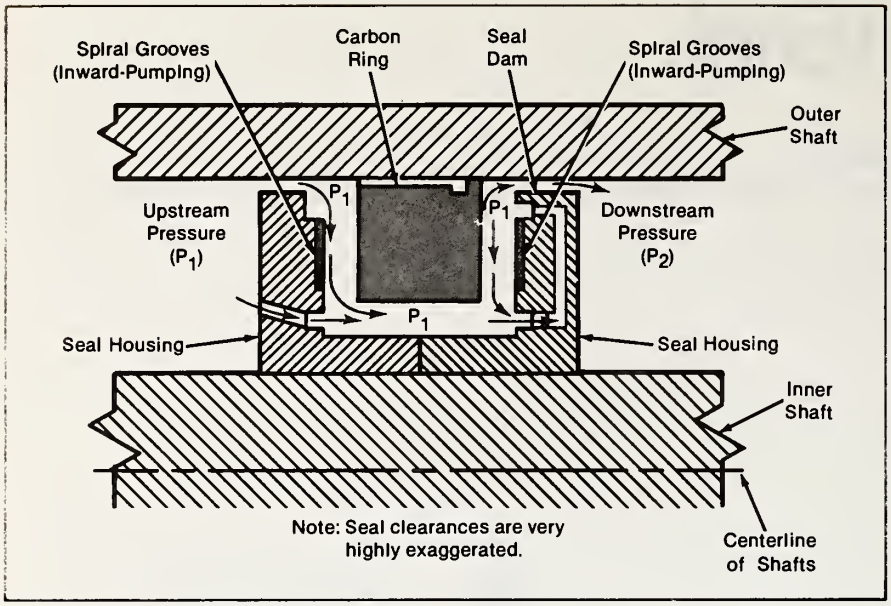

Figure 2. In the **Pressure-Balanced Spiral-Groove Concept,** the spiral-groove flow is isolated from the seal-leakage flow.

pressure-balanced concept isolates the spiral-groove flow from the seal-leakage flow so that the spiral-groove performance is not subject to any ill effects due to seal-leakage flow.

Transients such as pressure and thermal expansion that occur over the engine-operating range will change the axial-force equilibrium of the seal, thus causing the carbon seal ring to approach one of the housing faces. As the clearance between the carbon seal ring and one of the housing faces approaches zero clearance, the spiral grooves generate a very high lift force. The lift force increases exponentially with reduction in clearance until a clearance is achieved at which axial-force equilibrium is restored. The forces that enter into the axial-force equilibrium are pressure-area forces on the carbon ring, friction force between the carbon ring and the outer shaft (produced by relative axial translations of the shafts), and the lift force generated by the spiral grooves.

This work was done by Eliseo DiRusso of **Lewis Research Center.** *Further information may be found in NASA TP-2142 [N83-25712/NSP], "Design Analysis of a Self-Acting Spiral Groove Ring Seal for Counter-Rotating Shafts" [A02] A copy may be purchased [prepayment required] from the National Technical Information Service, Springfield, Virginia 22161.*
LEW-14248 /TN

FOR ADDITIONAL INFORMATION: *Contact: Director, Technology Transfer Division, P.O. Box 8757, BWI Airport, MD 21240; (301) 621-0100 Ext. 241*
REFER TO THE NUMBER LISTED AT THE END OF THIS ARTICLE

NASA Tech Brief

National Aeronautics and Space Administration

Lewis Research Center, Cleveland, Ohio

Designing Power-Transmission Shafting

Consideration of stress and fatigue life gives better designs.

Power-transmission shafting is a vital element of all rotating machinery. A shafting-design procedure has been developed based on fatigue-strength considerations. This method not only accounts for the effects of static and constant-amplitude fluctuating loads but will provide shaft-diameter estimates for variable-amplitude-loading duty cycles.

A stress-life approach is adopted for limited-life designs, restricted to the intermediate-to-high cycle-fatigue-life region. A local notch strain-life analysis is recommended for short-lived designs. In the absence of actual component-fatigue data, the S-N (stress-life) characteristics of the shaft in bending can be approximated by a straight line connecting the true fracture-strength coefficient with the corrected fatigue limit of the shaft on log/log coordinates. The figure shows that this approximation works reasonably well for a variety of steels, based on fatigue data found in the open literature. The predictions appearing in these figures are an estimate of the fatigue limit based on the ultimate tensile strength of the steel. Knowledge of the true fatigue limit for the particular steels in question would be expected to enhance the accuracy of the prediction.

The method requires the use of the fatigue limit of the shaft to be designed, which is almost always different from the fatigue limit of the highly-polished, notch-free test specimen, commonly listed in material-property tables. Typical values of fatigue-life-modifying factors are used to correct the fatigue limit of the test specimen for service factors that are known to affect fatigue strength. These factors include surface condition, size, reliability, temperature, stress concentration, press-fitted collars, residual stress, and corrosion corrections. For example, residual stress due to certain manufacturing processes can have major effects (both beneficial and negative) on shaft fatigue life. This is clearly illustrated in the lower part of the figure, which shows that the introduction of compressive residual stress in the notched region of the test specimen through shot peening has essentially eliminated the notch effect almost entirely.

Shafting material, rigidity, and critical speed are also considered, as are surface finish, dimensional tolerance, and material-strength properties of commonly-used commercial transmission-line shafting. Recommended gear and bearing maximum-shaft-misalinement values are also addressed. Critical speed considerations are used along with a Rayleigh-Ritz method to calculate, as a first approximation, the fundamental or first critical frequency of a shaft/bearing system using either completely-rigid or laterally-flexible bearing supports.

A longstanding objective in the design of power-transmission shafting is to eliminate excess shaft material without compromising operational reliability. This shafting-design method allows the designer to assess the impact of key operating and design variables and shaft-material selection on fatigue life and shaft size. The method lends itself to the computer-aided design of both aerospace and industrial shafting.

This work was done by Stuart H. Loewenthal of **Lewis Research Center.** *Further information may be found in NASA RP-1123 [N84-27041/NSP], "Design of Power-Transmitting Shafts." [A03] . A copy may be purchased [prepayment required] from the National Technical Information Service, Springfield, Virginia 22161.*

LEW-14240 /TN

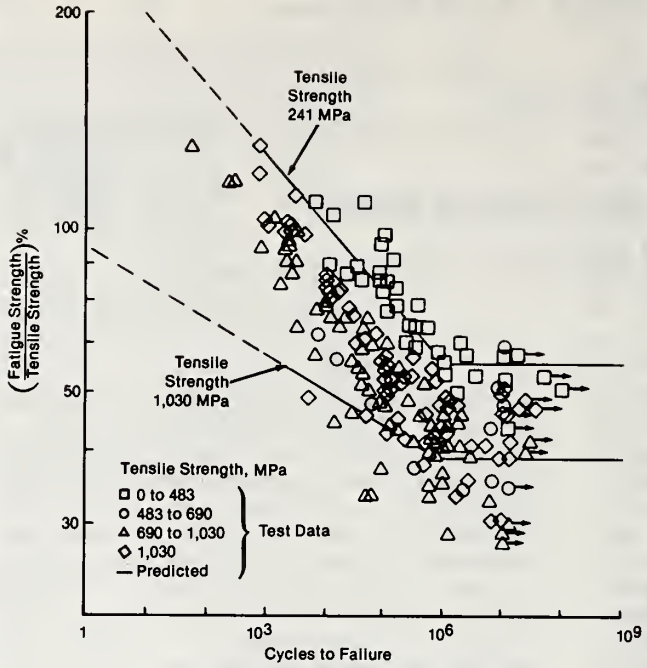

COMPARISON WITH TEST DATA FOR STEELS OF DIFFERENT TENSILE STRENGTH

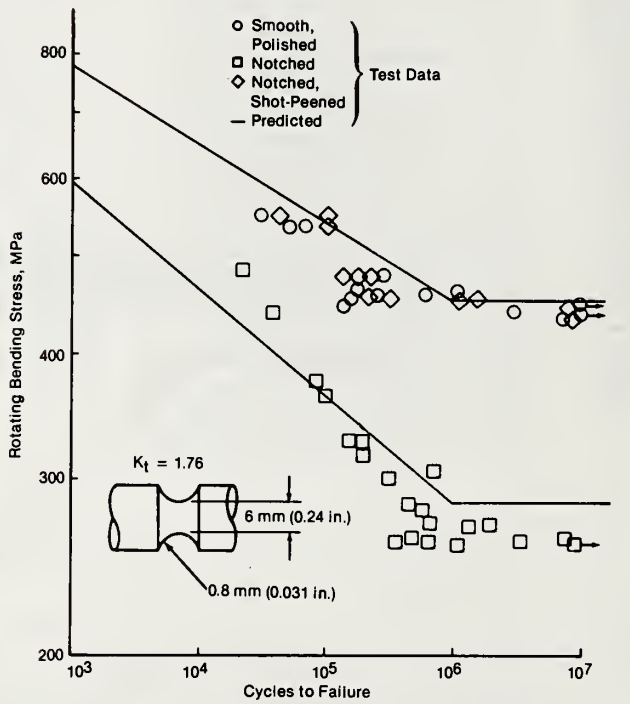

COMPARISON WITH TEST DATA FOR NOTCHED SPECIMENS

The **Stress/Life Characteristic** of a shaft is approximated for design purposes by straight lines based on previously published data. The straight-line predictions shown here are estimates of the fatigue limit based on the ultimate tensile strength of steels.

FOR ADDITIONAL INFORMATION: *Contact: Director, Technology Transfer Division, P.O. Box 8757, BWI Airport, MD 21240; (301) 621-0100 Ext. 241*

REFER TO THE NUMBER LISTED AT THE END OF THIS ARTICLE

NASA Tech Brief
National Aeronautics and Space Administration
Marshall Space Flight Center, Alabama

Measuring Thicknesses of Coatings on Metals

A digital light sensor and eddy-current sensor measure thickness without contact.

Using laser-beam reflections and eddy-current sensing, an instrument measures the thicknesses of nonconductive coatings on metal substrates. When the capabilities of available components are fully exploited, the instrument will be able to measure coatings from 0.001 to 6 in. (0.0025 to 15 cm) thick with an accuracy of 1 part in 4,000. The instrument can readily be incorporated in automatic production and inspection systems. For example, it can be used to inspect thermal-insulation layers, paint, and protective coatings. It can also be used to control the application of coatings to preset thicknesses.

The eddy-current-sensing portion of the instrument maintains a reflected-light triangulation sensor at a fixed distance from the surface of the substrate as the substrate moves under it. The light sensor determines the angle and therefore the perpendicular distance of the laser-beam spot on the coating surface. With the laser kept at a fixed distance above the substrate by the eddy-current sensor, the angle to the laser spot is thus a function of the coating thickness. A microcomputer computes this thickness from the light-sensor angle measurement.

The eddy-current sensor and the light sensor are mounted together on a precise translation stage that moves toward or away from the coated substrate (see figure). The output of the eddy-current sensor is converted to a digital signal and is compared with the required sensor-to-substrate separation stored in the computer memory. The computer calculates the direction and magnitude of the separation error and sends a signal to the stepping motor that drives the translation

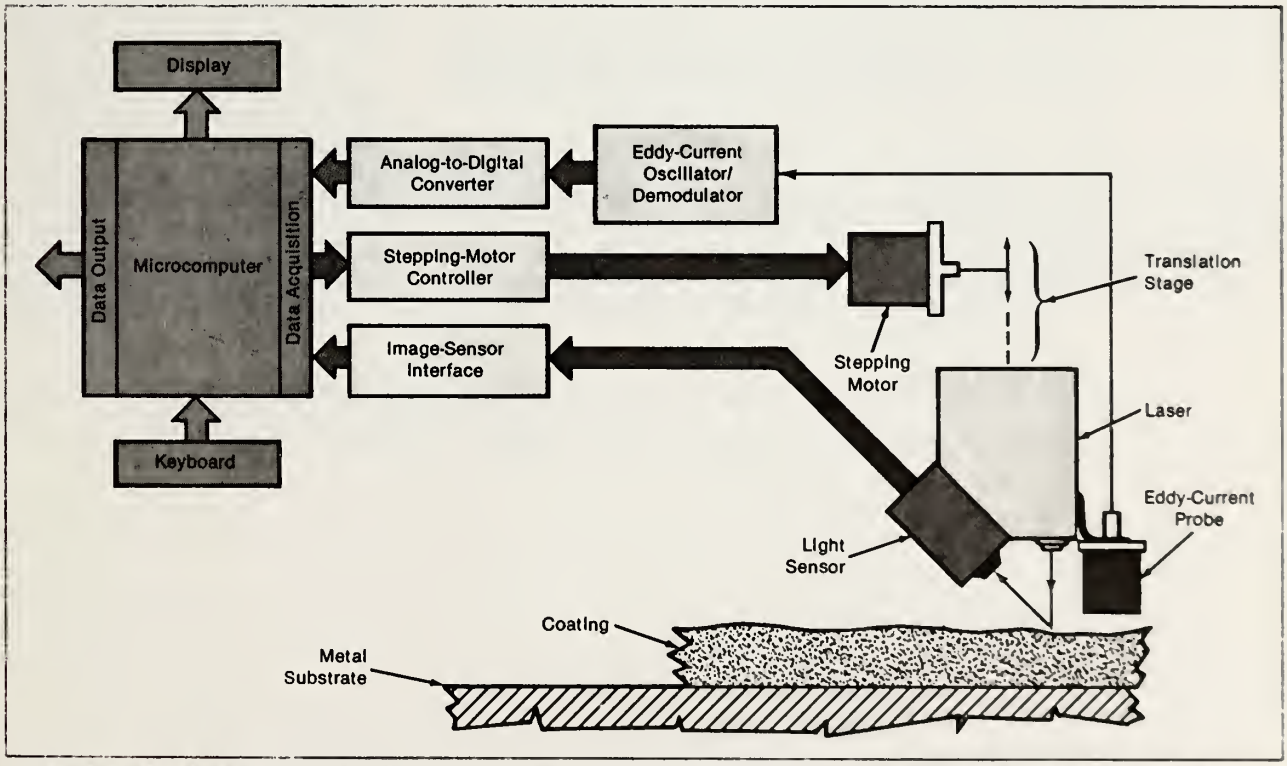

The Surface of a Coating reflects a laser beam to an optical sensor. The position of the reflected spot on the sensor is used by the microcomputer to calculate the coating thickness. The eddy-current sensor maintains a constant distance between the optical sensor and the metal substrate.

stage. This adjusts the position of the sensors accordingly.

The light source is a helium/neon laser with a 1-mW output. The light sensor is an array of light-sensitive memory cells. When struck by photons, each cell discharges at a rate proportional to the product of light intensity and length of exposure. Before each measurement, the array is first refreshed with digital ones. Light is then focused on it to discharge the cells selectively. An image focused on the array is thus converted into a pattern of ones and zeros. The array is then read in the manner of an ordinary memory chip, and the angle information is extracted.

In addition to its other functions, the microcomputer can be used to control the movement of the sensors over the specimen surface. From a series of thickness measurements, it can also determine the waviness of the coating surface from the valleys and peaks of the thickness values and the distance between them.

This work was done by Glenn M. Cotty, Jr., of Martin Marietta Corp. for **Marshall Space Flight Center.** *MFS-28126 /TN*

FOR ADDITIONAL INFORMATION: *Contact: Director, Technology Transfer Division, P.O. Box 8757, BWI Airport, MD 21240; (301) 621-0100 Ext. 241*

REFER TO THE NUMBER LISTED AT THE END OF THIS ARTICLE

NASA Tech Brief
National Aeronautics and Space Administration
Marshall Space Flight Center, Alabama

Optical Monitoring of Weld Penetration

Robotic welding can be controlled by a reliable, relatively-noise-free optoelectronic unit.

A system is being developed to monitor weld penetration optically and produce a signal for controlling an arc welder. The system is aimed for automatic welders, robot welders in particular. Made from small, low-cost components and utilizing optical fibers to conduct the signals, the system is immune to the electromagnetic interference that is common in industrial environments.

The monitor directs collimated light from a small diode laser at the molten pool of metal beneath the arc (see figure). A filter intercepts the reflected beam to suppress extraneous light, including light from the welding arc. A position-sensitive detector at a distance from the pool intercepts the beam reflected by the pool.

If the weld penetrates the workpiece completely, the curvature of the pool surface suddenly changes. This causes a sudden deflection of the reflected light beam, and consequently a displacement of the beam spot on the detector. Signal-processing circuitry determines the amplitude and rate of beam displacement to detect penetration and to generate control signals for the robot to regulate welding parameters.

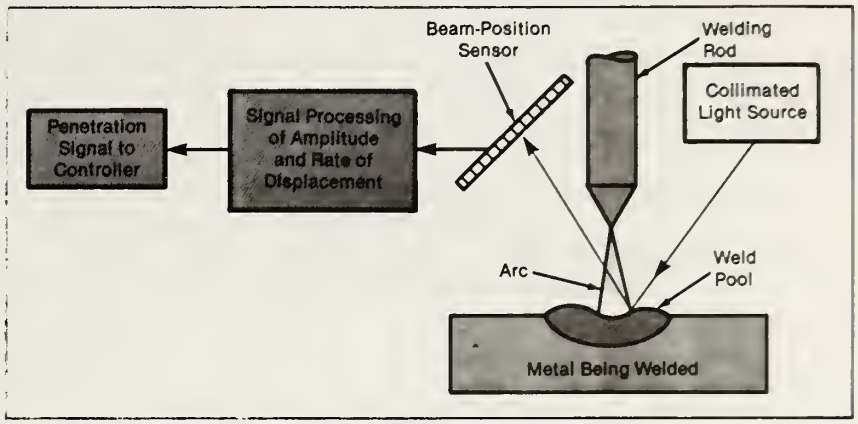

Bounding Off the Meniscus of a Pool of Molten Metal, a laser beam impinges on a position-sensitive photodetector. The beam diameter can be adjusted for the width of the weld. Optical filters screen out the light from the arc.

The monitor is insensitive to changes in weld current, welder speed, and the thermal properties of the welded metal except as they affect weld penetration. The monitoring principle is adaptable to other types of welding, including tungsten/inert-gas, laser, and electron-beam techniques.

This work was done by Jonathan Maram of Rockwell International Corp. for **Marshall Space Flight Center.**
MFS-29107 /TN

FOR ADDITIONAL INFORMATION: *Contact: Director, Technology Transfer Division, P.O. Box 8757, BWI Airport, MD. 21240; (301) 621-0100 Ext. 241*
REFER TO THE NUMBER LISTED AT THE END OF THE ARTICLE

1108 Ultralow-loss Optical Fibers Developed

1109 Antifouling Polyurethane Synthesized

1110 Leather Production from Pigskins

1111 Hydraulic Fluid, Chlorotrifluoroethylene, Evaluated For Nonflammability

1112 Powder Metallurgy Allous - Properties

1113 Ion-Vapor Deposition Process for Aluminum Coating—This process can supplant cadmium electroplating for corrosion protection.

1114 Rigid, Straight Composite Anodes for Chromium Plating—Improving anode straightness provides more even plating, thus reducing finishing costs.

1115 Crystal-Growing Crucible To Suppress Convection—A platform under the growth region can stabilize the melt for a more uniform crystal growth.

1116 Heat- and Radiation-Resistant Lubricants for Metals—Protective and lubricating coatings are formed in situ.

1117 Fundamentals of Alloy Solidification—The potential benefits of microgravity processing are discussed.

1118 Si3N4-Based Ceramic With Greater Hot Strength—Zyttrite-doped material outperforms MgO-doped material above 1,200° C

Software

1119 Fatigue-Crack-Growth Structural Analysis Elastic and plastic deformations are calculated under a variety of loading conditions.

Testing & Instrumentation

1120 Technique for Predicting Glass Crack Growth Rates

1121 Sensor Developed to Improve Quality Control of Processed Metals

1122 Compression-Failure Mechanisms in Composite Laminates—Failure mechanisms are observed using transparent fiberglass/epoxy birefringent materials.

1123 Comparative Thermal-Conductivity Test Technique—Approximate thermal conductivities are determined rapidly.

Other items of interest

1053 Positive-Index Guiding in CDH-LOC Lasers—A nonabsorbing passive region has beam-guiding capability.

1079 Acoustic/Magnetic Stress Sensor—This high-resolution sensor is fast, portable, and does not require permanent bonding to the structure.

1095 Ion Implantation for Corrosion and Wear Resistance

1096 Forging of Discontinuous Metal Matrix Composites

1099 Preventing Delamination of Silverized FEP Films—Edge treatment inhibits attack by moisture.

1100 Material for Fast Cutting—Silicon nitride-based tool boosts productivity and reduces costs.

1106 Measuring Thicknesses of Coatings on Metals—A digital light sensor and eddy-current sensor measure thickness without contact.

Ultralow-loss Optical Fibers Developed

The Naval Research Laboratory (NRL) reports a major milestone in the development of ultralow-loss optical fibers. The new fibers are expected to lead to optical fibers capable of transmitting data thousands of miles (transoceanic and transcontinental) without repeaters.

Conventional fiber-optic telecommunication systems require costly repeaters every 30 miles or so to amplify the signal. NRL's new fluoride optical fibers have an inherent transmission loss so low that one strand, with a diameter the size of ordinary sewing thread, has the potential to carry 10,000 telephone calls from coast to coast at one time. This compares to four calls for a conventional copper wire.

Optical fibers currently in use, such as those in telecommunications systems, are based on silica glass. Although these fibers have a high transparency and can be fabricated relatively cheaply, their transmission range is limited due to the need for repeaters or amplifiers.

Since this limitation is fundamental to the material, researchers around the world have been searching for alternative materials for optical fibers that potentially can transmit data thousands of miles without repeaters.

The principal goal of scientists at NRL is pioneering the development of fiber communications for transoceanic use. However, because they must be powered and represent a possible source of failure, the use of repeaters in undersea optical fiber telecommunication systems are undesirable. Additionally, sub-oceanic repairs are costly and time-consuming.

Because NRL's new fluoride glasses can transmit light with several orders of magnitude lower loss than silica, they are ideal for long distance data transmission systems and other applications. It is expected that the NRL development of fluoride optical fibers will provide improved capabilities far beyond those of current systems because the novel fibers can transmit in the infrared.

Possible applications requiring extremely long fiber lengths and ultralow-loss infrared transmissions include repeaterless telecommunications systems and acoustic and magnetic fiber sensor systems. Applications of the new fibers that involve medium fiber lengths and average infrared transmission include laser surgery and cauterization, infrared medical diagnostics, infrared power delivery systems for powering equipment by non-electrical means, and for microwelding and cutting, remote temperature sensing, chemical sensing systems for carbon monoxide, carbon dioxide and methane, and many others.

The new development was announced at a recent Optical Fiber Communication Conference in Atlanta, Ga. The group was told that the ultralow-loss fluoride fibers represent a major achievement because the 1 decibel/kilometer mark has long been recognized as the first major milestone to realizing ultralow-loss propagation.

It is predicted that NRL's rapid progress in producing improved fibers will continue because of new purification and processing techniques recently developed at NRL.

For Additional Information, Contact:
Navy Domestic Technology Fact Sheet Reader Reply Service
Code E211
Naval Surface Weapons Center
Dahlgren, VA 22448-5000
(703) 663-8921
Refer to 110502/TN

Antifouling Polyurethane Synthesized

A polyurethane with antifouling properties has been successfully synthesized at the David Taylor Naval Ship R&D Center (DTNSRDC). This material will permit increased use of polyurethanes in the Fleet where the advantages of this class of resins, such as castability, durability, and water immersion resistance, can be fully realized along with the added property of fouling resistance.

Numerous attempts to create this material in the past have been thwarted by the rapid catalytic action that the primary antifouling ingredient (tri-n-butyltin, contaminated with dibutyltin compounds) exerts on the polyurethane synthesis reaction.

This caused runaway polymerization, resulting in end-products with very limited potlife (the time between mixing and solidification of the material). The success of the present effort was achieved by using a highly purified tri-n-butyltin ester of a copolymer of acrylic acid with methyl methacrylate in the polymerization of the antifouling polyurethane.

It is believed that the purification process of the organotin ester, which involved successive distillations, removed the dibutyltin contaminants, which were responsible for the previously unsuccessful attempts.

While additional work is necessary before Fleet applications can be made, it is anticipated that these new urethanes will function as long term antifoulants.

For Additional Information, Contact:
Navy Domestic Technology Fact
Sheet Reader Reply Service
Code E211
Naval Surface Weapons Center
Dahlgren, VA 22448-5000
(703) 663-8921
Refer to 110402/TN

United States Department of Agriculture

Research Technology
Agricultural Research Service

Leather Production from Pigskins

Making a silk purse out of a sow's ear may be impossible, but a pig's skin can be made into high-quality leather using a method developed by Agricultural Research Service scientists.

William J. Hopkins, a leather chemist with the agency, says simple, inexpensive processes recently developed at the Animal Biomaterials Research Unit in Philadelphia preserve hides in a nearly fresh state for up to 2 weeks until they can be made into leather. They treat pigskins with acid sulfite solutions or sulfur dioxide. The most common way of treating pigskins is with a salt solution, but there are disadvantages to that method.

Salting down, or brining, shrinks pigskins more than other kinds of hides and reduces the quality of the leather that can be made from them.

But the processes developed by Hopkins lessen hide shrinkage and reduce pollution from salt solutions.

Pigskin makes good leather, according to the Pigskin Council of America, which says it is soft but strong, stretches less than cowhide, and easily takes colorful dyes.

Despite the virtues of pigskin, the council estimates that only about 6 percent—fewer than 5 million—of the 80 million hogs slaughtered each year in the United States are skinned for possible leathermaking.

Most of the pigskins are used in food or converted to fat or protein for industrial and agricultural uses, according to Stephen H. Feairheller, who leads the Unit.

Mindful of the failure to capitalize on an abundant hog industry product, agency scientists are seeking ways to make pigskin processing more economically attractive to the industry.

For example, Hopkins wants to develop a stable air-dried hide product that would offer tanneries yet another alternative to salting pigskins. Other researchers have looked at ways to remove excess fat from pigskins so they can be more easily made into leather.

Chemist William Hopkins with treated pigskins.

William A. Hopkins is at the USDA-ARS Eastern Regional Research Center, 600 Mermaid Lane, Philadelphia, PA 19118. ■

U.S. Air Force
Technology Note

HYDRAULIC FLUID, CHLOROTRIFLUOROETHYLENE, EVALUATED FOR NONFLAMMABILITY

The Air Force has completed a series of aircraft braking tests of a new, nonflammable hydraulic fluid called chlorotrifluoroethylene, or CTFE. This new fluid, developed at Aeronautical Systems Division (ASD) and its Air Force Wright Aeronautical Laboratories (AFWAL), is expected to eliminate fire hazards associated with hydraulic fluids in modern-day aircraft.

ASD's 4950th Test Wing conducted the braking tests using an instrumented C-135 aircraft on which one pair of wheels was modified with seals and special components compatible with CTFE. The CTFE system performed as expected. In fact, no fire occurred even when a fitting cracked during a landing causing a spray of CTFE over the brakes at a temperature of 1,100 degrees F.

Steps leading to testing CTFE began about a decade ago. Researchers knew about CTFE in the early 1970s, but characteristics of the fluid prevented extensive testing because of its non-compatibility with either existing fluids or gydraulic systems.

CTFE is roughly twice as dense as Mil-H-5606 hydraulic fluid, which has been used widely in Air Force aircraft since the 1940s. Additionally, CTFE cannot be used with existing seals and, at present, is 15 times as expensive as 5606--although its cost should decrease dramatically with increased production.

FOR ADDITIONAL INFORMATION: Contact: Mike Wallace at the Department of the Air Force, Headquarters Aeronautical Systems Division (AFSC), Wright-Patterson Air Force Base, Ohio 45433-6503; (513) 255-2725. Refer to PAM 86-107.

Powder Metallurgy Alloys - Properties

Results obtained during a cooperative test program involving 12 different aerospace laboratories, conducted to determine the properties of three first generation high strength powder metallurgy aluminum-base alloys, are described in a Technical Report prepared by members of the Air Force Wright Aeronautical Laboratories. The alloys studied were 7091 and 7090, both produced by Alcoa, and IN6021, produced by Novamet. Several different product forms were investigated and testing was conducted by the participating aerospace companies. Properties reported include tensile, compression, bearing, and shear properties, fracture toughness, smooth and notched bar fatigue properties, fatigue crack growth behavior, and corrosion behavior. Sufficient tests were conducted in some cases to obtain preliminary estimates of design allowable properties. Values reported for tensile and yield strength in the longitudinal and long transverse directions for the nine different materials evaluated are shown in Table 3.

TABLE 3. SUGGESTED DESIGN ALLOWABLE TENSILE PROPERTIES (FOR USE IN COST BENEFIT ANALYSES ONLY)

Powder Metallurgy Alloy	Product Form	Temper	Tensile Strength, ksi		Yield Strength, ksi	
			Long	L. Trans.	Long.	L. Trans.
7091	Forging	-T7E78	76.8	64.9	68.4	64.9
	Extrusion	-T7E69	82.7	76.5	74.1	66.7
	Plate	-T7E69	78.5	79.1	73.3	72.7
	Sheet	-T7E69	77.4	79.0	72.6	69.3
7090	Forging	-T7E80	78.6	77.2	70.1	67.1
	Extrusion	-T7E71	87.5	83.1	81.5	75.1
	Plate	-T7E71	85.6	86.3	79.8	80.7
IN9021	Forging	—	80.3	83.2	70.5	72.1
	Extrusion	—	88.3	86.3	83.1	74.2

FOR ADDITIONAL INFORMATION:

You can learn more details about this technology by ordering the NTIS report(s):

Petrok, G.J., Molas, M. A., "The Mechanical Property Data Base From a Cooperative Program on First Generation PM Aluminums", Final Report No. AFWAL-TR-85-4052, Air Force Wright Aeronautical Labs, WPAFB, OH, August 1985.
Order number: AD A159779
Price code: A14

Order from:
National Technical Information Service
5285 Port Royal Rd.
Springfield, VA 22161

MANUFACTURING TECHNOLOGY NOTE

U.S. ARMY MATERIEL COMMAND

Deputy Chief of Staff for Manufacturing Technology, Alexandria, VA

Project Number: MMT6XX8113 Filing Code : 491085

Ion-Vapor Deposition Process for Aluminum Coating

This process can supplant cadmium electroplating for corrosion protection.

The U.S. Army Armament, Munitions, and Chemical Command has established a cost-effective ion-vapor deposition (IVD) process for coating steel and other metals with aluminum for corrosion protection. This process can supplant electroplating by cadmium, which can cause hydrogen and solid-metal embrittlement, and which is environmentally hazardous. Compared with physical-vapor deposition and chemical-vapor deposition, the IVD process for aluminum provides the best adhesion and the most uniform coating thickness.

The basic equipment required for the IVD are a steel vacuum chamber, a vacuum pumping system, an evaporation source, and a high-voltage power supply (see figure). After the system is pumped down to about 10^{-4} torr (10^{-2} Pa), the chamber is then backfilled with an inert gas to about 10μm (1 Pa), and a high negative potential is applied between the parts being coated and the evaporation source. The gas becomes ionized and creates a glow discharge around the parts to be coated. The positively charged gas ions bombard the surface of the parts and give them a final cleaning.

Commercially available aluminum wire (1100 alloy) is then evaporated by continuously feeding it into resistance-heated crucibles. Part of the aluminum vapor is ionized as it passes through the glow discharge. Bombardment by the inert gas ions accelerates the aluminum vapor toward the part surface, resulting in denser coatings and improved coating adhesion. The ionization also provides better throwing power and allows complex shapes to be more uniformly plated. The total coating cycle requires about 45 minutes.

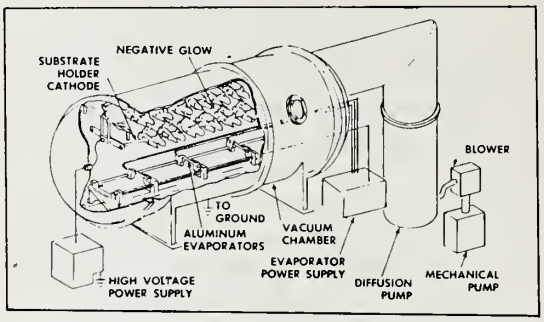

Ion Vapor Depositon provides uniform and strongly adherent coatings for metal components.

FOR ADDITIONAL INFORMATION

You can learn more details about this technology by contacting:

Commander
ARDEC
Attn: SMCAR-AET-M (C. Feng)
Bldg. 355 Metals Branch
Picatinny Arsenal
Dover, NJ 07801-5001
Telephone No. (201) 724-5746 or AV 880-5746

This document was prepared under the sponsorship of the U.S. Government. Neither the United States Government nor any person acting on behalf of the United States Government assumes any liability resulting from the use of the information contained in this document, or warrants that such use will be free from privately owned rights.

MANUFACTURING TECHNOLOGY NOTE

U.S. ARMY MATERIEL COMMAND

Deputy Chief of Staff for Manufacturing Technology, Alexandria, VA

Project Number: MMT6XX8152 Filing Code : 71E031

Rigid, Straight Composite Anodes for Chromium Plating

Improving anode straightness provides more even plating, thus reducing finishing costs.

The U.S. Army Armament, Munitions, and Chemical Command has developed a rigidly straight composite anode for use in the electrochemical deposition of chromium; the currently used copper electrodes lose their straightness and consequently cause off-side plating. In addition to producing more-uniform deposits during plating, the composite electrodes are lighter, and hence more transportable, than copper electrodes.

The goal of the command was to use unidirectional graphite filaments to develop a composite anode that would have specific strengths and specific moduli 33 and 9 times as high as those of copper, respectively. (See figure.) When simply supported at its ends, the finished anode was to have a mid-span deflection (due to its own weight) that was not permanent and not to exceed 0.5 in. (1.27 cm), and it was to withstand three times its finished weight. The anode was to be capable of enduring a current density of 90 A/dm^2 for four hours.

The specified electrodes are fashioned from Union Carbide VSC-32 graphite fiber (or equivalent) and an epoxy matrix of DOW 324 (or equivalent) using the hand lay-up method, and in particular the tape form, since it provides a uniform component and a controllable fiber volume. In the thermal-expansion molding technique selected, 2-in. (5.1-cm) wide graphite/epoxy tape was hand laid-up into the steel mold, the silicone rubber mold was inserted and capped with the aluminum plate, and the entire assembly was then oven cured. During curing, the silicone expanded, thereby pressuring the unidirectional composite at the inside diameter.

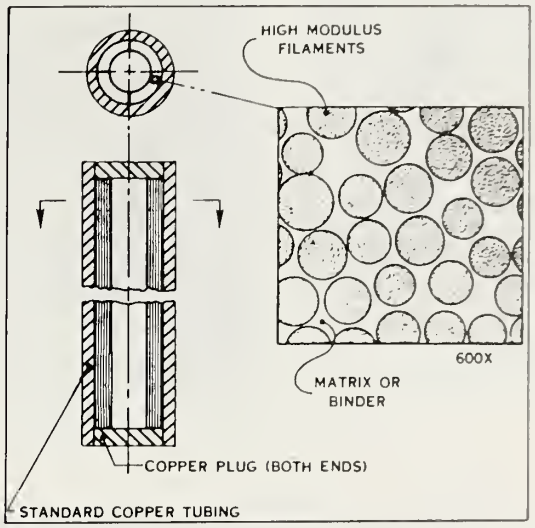

A **Lightweight Composite Anode** resists bending and consequently produces plating more even than that produced using standard copper electrodes.

FOR ADDITIONAL INFORMATION

You can learn more details about this technology by contacting

Commander
Watervliet Arsenal
Benet Weapons Laboratory, Research Branch
Attn: SMCAR-CCB-R (Dr. G. D'Andrea)
Bldg. 115
Watervliet Arsenal, NY 12189-4050
Telephone No. (518) 266-5296 or AV 974-5296

This document was prepared under the sponsorship of the U.S. Government. Neither the United States Government nor any person acting on behalf of the United States Government assumes any liability resulting from the use of the information contained in this document, or warrants that such use will be free from privately owned rights.

NASA Tech Brief
National Aeronautics and Space Administration
NASA's Jet Propulsion Laboratory, Pasadena, California

Crystal-Growing Crucible To Suppress Convection

A platform under the growth region can stabilize the melt for a more uniform crystal growth.

A proposed crucible for growing silicon webs or boules can suppress thermal convection near the solidification interface. Thermal convection must be suppressed because it causes nonuniform crystal growth. In the new crucible (see figure), there would be a platform just below the growth interface so that the melt would be too shallow to support convection.

The new crucible design is derived from the theory of stability of a heated fluid. The instabilities that give rise to convection occur when the gravitational forces due to thermally induced density gradients exceed frictional forces in the fluid. The critical depth for the onset of the pertinent instability can be calculated from the heat flux through the surface of the melt, the volume coefficient of thermal expansion, the thermal conductivity, the thermal diffusivity, and the kinematic viscosity.

All of these quantities except the heat flux are properties of the molten material and are available in standard reference works. The heat flux can be evaluated in terms of the system configuration and operating conditions. For example, if the crucible operates in a vacuum, the heat flux equals the net thermal radiation from the melt surface. If the operation is in a gaseous environment, conduction and convection also contribute to the heat flux.

The width of the platform is approximately the width of the crystal plus twice the critical depth. The platform height is such that the melt depth under the crystal-growth region is less than the critical depth. The thermal resistance of the quartz platform material is considerably greater than that of the molten silicon: This contributes further to stability by reducing the heat flux through the melt, thereby decreasing the thermal gradient that drives convection.

This work was done by Robert Richter of Caltech for **NASA's Jet Propulsion Laboratory.** *NPO-16597 / TN*

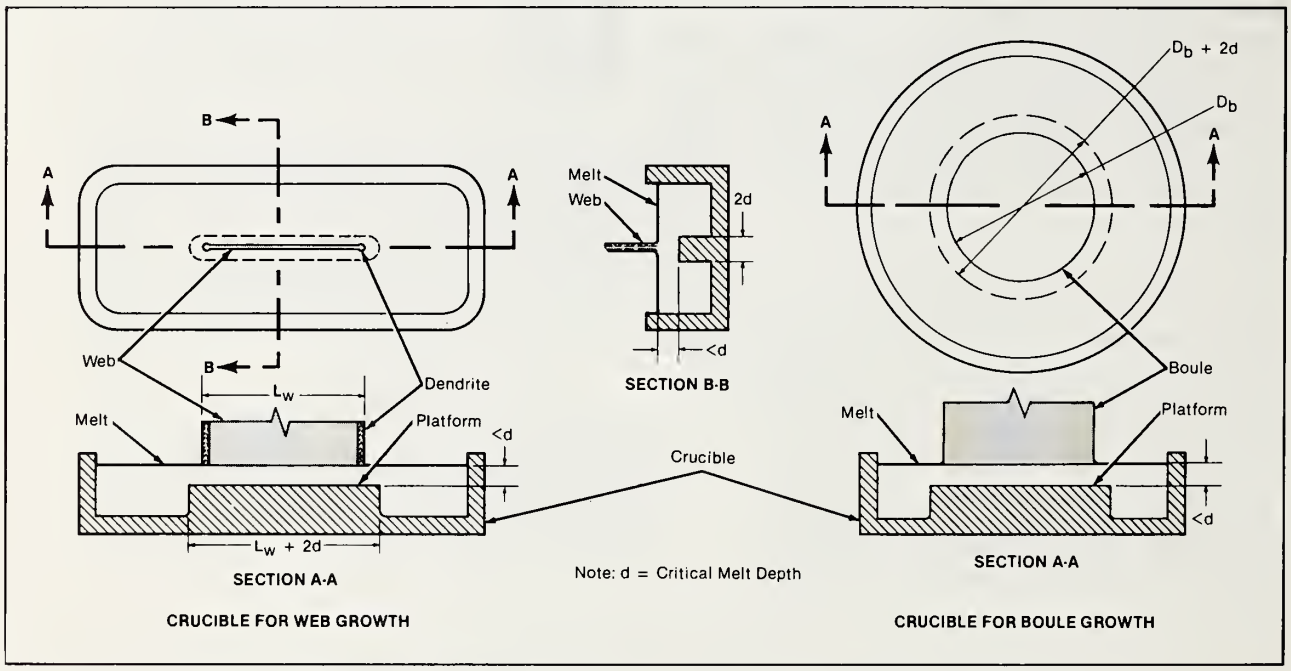

The **Improved Crucible for Growing Silicon Crystals** would include a platform just below the growth interface.

FOR ADDITIONAL INFORMATION: *Contact: Director, Technology Transfer Division, P.O. Box 8757, BWI Airport, MD. 21240; (301) 621-0100 Ext. 241*
REFER TO THE NUMBER LISTED AT THE END OF THE ARTICLE

NASA Tech Brief
National Aeronautics and Space Administration
NASA's Jet Propulsion Laboratory, Pasadena, California

Heat- and Radiation-Resistant Lubricants for Metals

Protective and lubricating coatings are formed in situ.

A class of high-performance lubricants is under investigation at NASA's Jet Propulsion Laboratory. These lubricants are useful as additives to oils and greases in gears, transmissions, motors, and other machines where rubbing loads between metal parts may be severe. Because of their low volatility and lack of requirement for air or moisture, these lubricants should also be useful in vacuums.

One type of additive includes orthophthalonitrile and its derivatives. The additive would ordinarily be dissolved or suspended in a base fluid. Under high mechanical loads that cause lubricating fluid films to become thin, metal parts rub together. The orthophthalonitrile reacts with metal-surface asperities at high frictional temperatures to form lubricating films of metal phthalocyanine. These compounds are also formed with the hot metal fragments torn from the asperities. Bearing surfaces are thereby better protected from scoring, and fragments are rendered less harmful to the base fluids.

On heating to 250 to 260 °C, the additive also forms metal-free phthalocyanine, which is extremely thermally stable and an efficient lubricant. The phthalocyanine molecular structure is planar like that of graphite. However, it is even more effective than graphite as a lubricant because metal-free phthalocyanine can form extremely stable bonds to metal. At high temperatures in air, it does not form corrosive compounds as does molybdenum disulfide.

Without modification, orthophthalonitrile is not a suitable additive to conventional motor oils because of its low solubility in aliphatic compounds. One way of making soluble additives is to synthesize orthodinitriles substituted with aliphatic groups. Other potential substituents are cyclohexanes, linear polyethers, and fluorocompounds.

Very little of the precursor compounds to the formed solid pthalocyanine lubricant is needed. Moreover, since the additives can probably be synthesized from inexpensive materials, their low cost and high performance should make them suitable for commercial use.

Other chelating/lubricating additives are under consideration. Molecules can be tailored to confer solubility on the additives. Candidate molecular groups includes pyridino, sulfhydro, pyrrole, phenoyl, cyano, indolino, amino, keto, diketo, nitroso, hydroxylamino, thiophene, and carboxyl.

This work was done by Emil A. Lawton of Caltech for **NASA's Jet Propulsion Laboratory.** *NPO-16341/TN*

FOR ADDITIONAL INFORMATION: *Contact: Director, Technology Transfer Division, P.O. Box 8757, BWI Airport, MD. 21240; (301) 621-0100 Ext. 241*
REFER TO THE NUMBER LISTED AT THE END OF THE ARTICLE

NASA Tech Brief
National Aeronautics and Space Administration

Fundamentals of Alloy Solidification

The potential benefits of microgravity processing are discussed.

A symposium was held at the Lewis Research Center in September of 1984. It dealt with the subject of microgravity and some basic metallurgical factors involved in the production of metals. General metallurgical areas of interest were metal solidification and processing. The five specific areas covered included (1) the undercooling of liquids, (2) porosity, (3) microstructure, (4) solidification, and (5) segregation.

Metallurgy today is characterized by processes that have evolved over the years in the unit gravity of Earth. Future processing will not be confined to Earth and may take place in a low or microgravity environment such as might be found on satellites, Space Shuttle-type vehicles, or a future space station. Because of this new access to a space environment, renewed interest is being generated in the role of gravity on basic metallurgical phenomena.

Fourteen individual papers were presented at this symposium entitled "Fundamentals of Alloy Solidification Applied to Industrial Processes." The authors represented material experts in government, academia, and industry. The underlying theme of this symposium was the possible benefits of microgravity processing and its beneficial effects on industry processing. Information contained in the conference publication is of such a nature that it would readily lend itself to inclusion in educational programs at the college level.

This work was done by F. Harf of **Lewis Research Center.** *Further information may be found in NASA CP-2337 [N84-34589/NSP], "Fundamentals of Alloy Solidification Applied to Industrial Processes," [A03] A copy may be purchased [prepayment required] from the National Technical Information Service, Springfield, Virginia 22161.*
LEW-14229 /TN

FOR ADDITIONAL INFORMATION: *Contact: Director, Technology Transfer Division, P.O. Box 8757, BWI Airport, MD. 21240; (301) 621-0100 Ext. 241*
REFER TO THE NUMBER LISTED AT THE END OF THE ARTICLE

NASA Tech Brief
National Aeronautics and Space Administration
Lewis Research Center, Cleveland, Ohio

Si_3N_4-Based Ceramic With Greater Hot Strength

Zyttrite-doped material outperforms MgO-doped material above 1,200° C

A new ceramic material has been produced by the addition of 10 weight percent zyttrite (yttria-stabilized zirconia) to Si_3N_4 (silicon nitride) that offers significantly-improved high-temperature properties (nearly double those of MgO-doped Si_3N_4 ceramic, as shown in the figure). The work also showed that by using controlled Si_3N_4 powder with 10 weight percent zyttrite, a significant improvement in room-temperature strength can be achieved.

Advanced ceramic materials that are of great interest for a variety of high-temperature structural applications are silicon nitride (Si_3N_4) and silicon carbide (SiC). Si_3N_4 and SiC ceramics have potential for use in aircraft and automobile engines and in electric-power generating systems. These ceramics combine high thermal conductivity and low coefficients of thermal expansion and consequently have high thermal-shock resistance. Because of their high refractory nature, these ceramics are capable of operating at temperatures in the range of 2,500° to 3,000° F (1,370° to 1,650° C). However, for sintering to full density, sintering aids are required that often form a glassy phase at the grain boundaries. In Si_3N_4, a glassy phase is responsible for strength loss at high temperatures.

With the new ceramic material, time-dependent flexure tests showed very little strength degradation at 1,400° C (2,552° F).

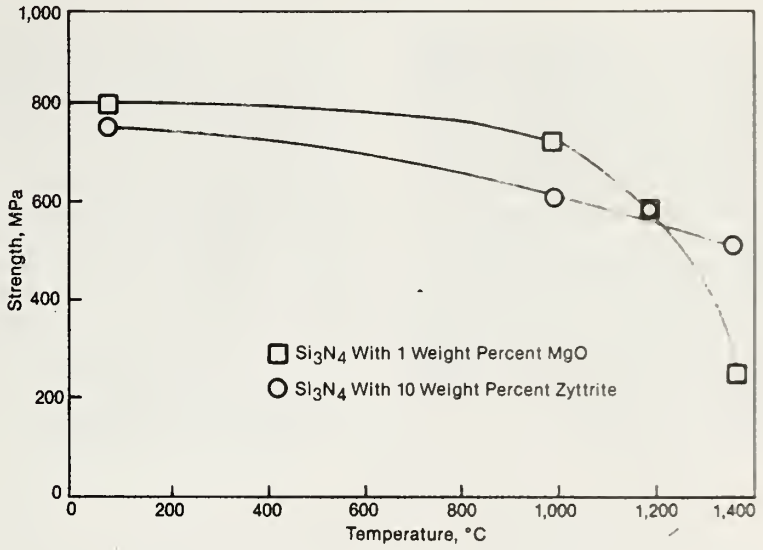

The **Four-Point-Bending Strengths** of two Si_3N_4-based ceramics are compared at different temperatures.

The creep resistance at 1,350° C (2,462° F) was one to two orders of magnitude better than Si_3N_4 materials containing MgO and Y_2O_3 as sintering aids. Further, the Weibull modulus "m" (for 30 test bars) was estimated to be 17, which is relatively high for Si_3N_4 materials, and the oxidation resistance at 1,370° C (2,500° F) in air compared favorably to the oxidation resistance of silicon carbide material. These improved properties strongly suggest that the 10-weight percent zyttrite/Si_3N_4 material has a strong potential for high-temperature applications.

This work was done by Sunil Dutta and Bruno Buzek of **Lewis Research Center.**
LEW-14193 / TN

FOR ADDITIONAL INFORMATION: *Contact: Director, Technology Transfer Division, P.O. Box 8757, BWI Airport, MD. 21240; (301) 621-0100 Ext. 241*
REFER TO THE NUMBER LISTED AT THE END OF THE ARTICLE

Fatigue-Crack-Growth Structural Analysis

Elastic and plastic deformations are calculated under a variety of loading conditions.

The prediction of fatigue-crack-growth lives can be made with the Fatigue-Crack-Growth Structural Analysis (FASTRAN) computer program. As cyclic loads are applied to an initial crack configuration, FASTRAN predicts crack length and other parameters until a complete break occurs. The loads may be tensile or compressive and of variable or constant amplitude. FASTRAN incorporates linear-elastic fracture mechanics with modifications for load-interaction effects caused by crack closure. FASTRAN is considered a research tool, because of lengthy calculation times.

Surface cracks, surface cracks at holes, and corner cracks at holes in a three-dimensional body can be modeled. The representation is based on the Dugdale model, with alterations to allow plastically deformed material along crack surfaces as the crack advances. Plane stress and plane strain conditions are simulated in FASTRAN by using a constraint factor on tensile yielding to account for three-dimensional effects. FASTRAN has successfully predicted crack growth in metallic-alloy sheet materials under aircraft-spectrum loading.

FASTRAN is written in FORTRAN IV for batch execution and has been implemented on a CDC CYBER 170-series computer under NOS 1.4 with a central-memory requirement of approximately 200K (octal) of 60-bit words. The program was developed in 1981.

This program was written by J. C. Newman, Jr., of **Langley Research Center.** *LAR-13412 /TN*

FOR ADDITIONAL INFORMATION

CONTACT:
COSMIC®
112 Barrow Hall
University of Georgia
Athens, GA 30602
(404) 542-3265

energygram®

Technique for Predicting Glass Crack Growth Rates

DOE/TIC/EG-36/009
OFFICE OF SCIENTIFIC AND TECHNICAL INFORMATION

This technical note was based on research conducted by Sandia National Laboratories for the U.S. Department of Energy.

Sandia National Laboratories

Results of experiments and mathematical modeling have enabled researchers at Sandia National Laboratories to predict how rapidly glass and ceramic materials will crack when exposed to various stresses, humidity, and chemical environments.

Their new abilities are expected to help designers produce more reliable optical fibers, solar collector covers, underwater windows, insulators for high-performance batteries, and many other items made of glass or ceramics.

The researchers believe this understanding can eventually be used to identify ways of treating glasses with thin coatings—possibly polymers—that slow or stop crack growth. Techniques of reliably healing cracks that develop in glass may be an eventual result of the work.

Key to the new predictive capability is the use of model chemical compounds, which are small clusters of silicon and oxygen atoms tailored to simulate the physical characteristics of glass. In glass, the silicon-oxygen-silicon bonds located at crack tips are highly distorted, due to the strains being applied to them, and they behave differently from normal bonds that make up bulk glass. The model chemical compounds are tailored to simulate this same difference.

The scientists observe and analyze crack-causing chemical reactions to their model chemical compounds. On the basis of these results, they predict the nature and growth rate of chemical attack on actual crack tip bonds and then test pieces of glass in a variety of chemical environments to determine how closely actual crack growth parallels those predictions.

Researchers are extrapolating long-term behavior of up to 10 years in the future. Prior to verification of their model chemical compounds, the accuracy of glass behavior predictions for periods of longer than several months was questionable.

FOR ADDITIONAL INFORMATION

For additional information, contact:
Public Information Division
Sandia National Laboratories
Albuquerque, NM 87185
Telephone No.: (505) 844-8065
or (505) 844-7767

NBS technology update

National Bureau of Standards
U.S. Department of Commerce
Gaithersburg, MD 20899

Sensor Developed to Improve Quality Control of Processed Metals

A new ultrasonic sensor for measuring the depth and properties of treated steels and metal alloys has been developed at NBS to improve quality control of processed metals. The sensor, which uses ultrasonic waves to make very precise measurements of both the depth and mechanical properties of surface-modified layers, eliminates the need to destroy finished products by cross-sectioning materials to determine the effectiveness of processes used to modify metal surfaces and the quality of the component. The sensor was developed by two guest workers, from Johns Hopkins University, Dr. Moshe Rosen, professor of materials science, and graduate student Bret J. Elkind, and NBS scientist Dr. Haydn N.G. Wadley. The sensor has been evaluated in a series of laboratory tests at NBS to verify its accuracy and performance. The researchers anticipate the new ultrasonic sensor will become an important measurement tool for manufacturers using nondestructive evaluation techniques to improve the quality control of their products.

FOR ADDITIONAL INFORMATION: Contact: Dr. Hayden Wadley, National Bureau of Standards, A-167, Materials Bldg., Gaithersberg, MD 20899; (301) 921-2956.

NASA Tech Brief

National Aeronautics and Space Administration

Langley Research Center, Hampton, Virginia

Compression-Failure Mechanisms in Composite Laminates

Failure mechanisms are observed using transparent fiberglass/epoxy birefringent materials.

The efficient use of composites in aircraft structural components requires a thorough understanding of the failure mechanisms of these materials. The opaqueness of graphite/epoxy laminates prevents direct observation of the mechanisms involved in the initiation and propagation of damage. Although destructive failure-assessment methods are available, the sequence of failure within the laminate is difficult to determine using these methods.

An in situ nondestructive technique was developed to observe failure as it develops and as it propagates within the laminate. This technique is based on the use of a transparent fiberglass/epoxy birefringent material. The transparency allows visual observation of the location of initial laminate failure and of the subsequent failure propagation; the birefringence allows the laminate stress distribution to be observed during the test and also after the test if permanent residual stresses occur.

Two $(+45_4/-45_4)_{2s}$ fiberglass/epoxy specimens, each with a single, centrally-located circular hole, were tested. The specimens were fabricated from commercially-available glass cloth preimpregnated with epoxy resin. Specimens were nominally 6.0 by 3.0 by 0.11 in. (15.2 by 7.6 by 0.28 cm), and the hole diameters were 0.19 and 0.50 in. (0.48 and 1.27 cm).

The specimens were tested by slowly applying a compressive end load to simulate a static loading condition. The ends were machined flat and parallel to permit uniform compressive loading. Loaded edges were clamped by fixtures during testing while unloaded edges were supported by knife-edge restraints to prevent the specimen from buckling as a wide column. The polarizer and analyzer were oriented at $+45°$ and $-45°$, respectively, to the load axis.

Experimental results shown in Figures 1 and 2 illustrate the value of the birefringent material for observing the failure of composite specimens. The specimens in Figure 1 were loaded and then unloaded. When these unloaded specimens were illuminated with polarized light, the isochromatic fringe patterns indicated that plastic deformation had occurred.

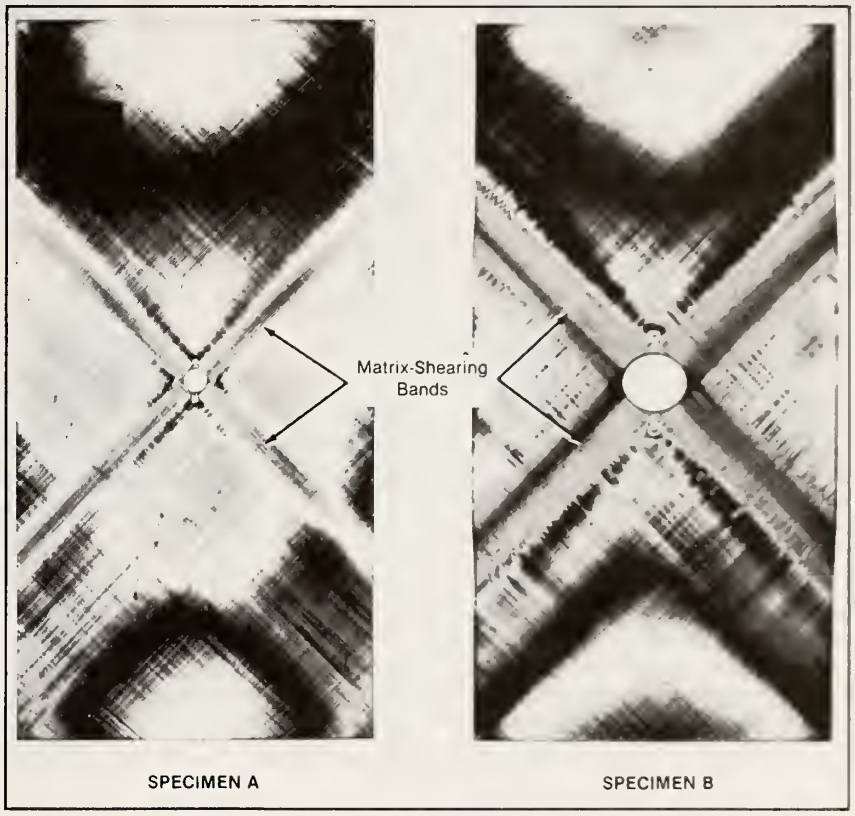

Figure 1. **Polarized Light Reveals** matrix-shearing bands in damaged regions of the specimen.

The pattern on specimen A indicates that high stresses exist in bands oriented at $\pm 45°$ to the load axis. For this uniaxially loaded laminate, the in-plane shear stress is a maximum on elements oriented 45° to the applied load, resulting in high stresses in the epoxy matrix between fibers. The high stresses in the bands in specimen A are caused by in-plane fiber/matrix shearing in these regions and are identified as matrix-shearing bands in the figure. While the specimen was being loaded, these bands initiated at the hole boundary and grew toward the specimen edges.

Specimen B was loaded further into the plastic range than was specimen A. This specimen also has matrix-shearing bands, but the isochromatic fringes are not observed in the region of these bands. While the specimen was being

loaded, severe internal damage occurred within the bands, disrupting the light path and destroying the birefringence. The damage was caused by local delamination and in-plane shearing failure mechanisms.

When this specimen is illuminated with white light (Figure 2), the damage in the matrix-shearing bands is indicated by the ±45° dark bands. The damage is most severe at the two locations where the hole boundary intersects the horizontal centerline of the specimen: the locations where damage initiated.

Closer inspection of the damaged regions reveals a fiber-kinking mechanism. The kinking results from a +45° layer partially restraining the in-plane shearing occurring in an adjacent −45° layer, or vice versa. The fiber kinking occurs without fiber breakage due to the flexibility in the matrix provided by extensive shear failures.

The transparency and birefringence properties of the fiberglass/epoxy material enable regions of high stress to be located and the mechanisms of local failure and of failure propagation to be identified within the laminate. This fiberglass/epoxy material may also be useful for studying stress fields and for identifying failure initiation and propagation mechanisms in a wide variety of composite structures.

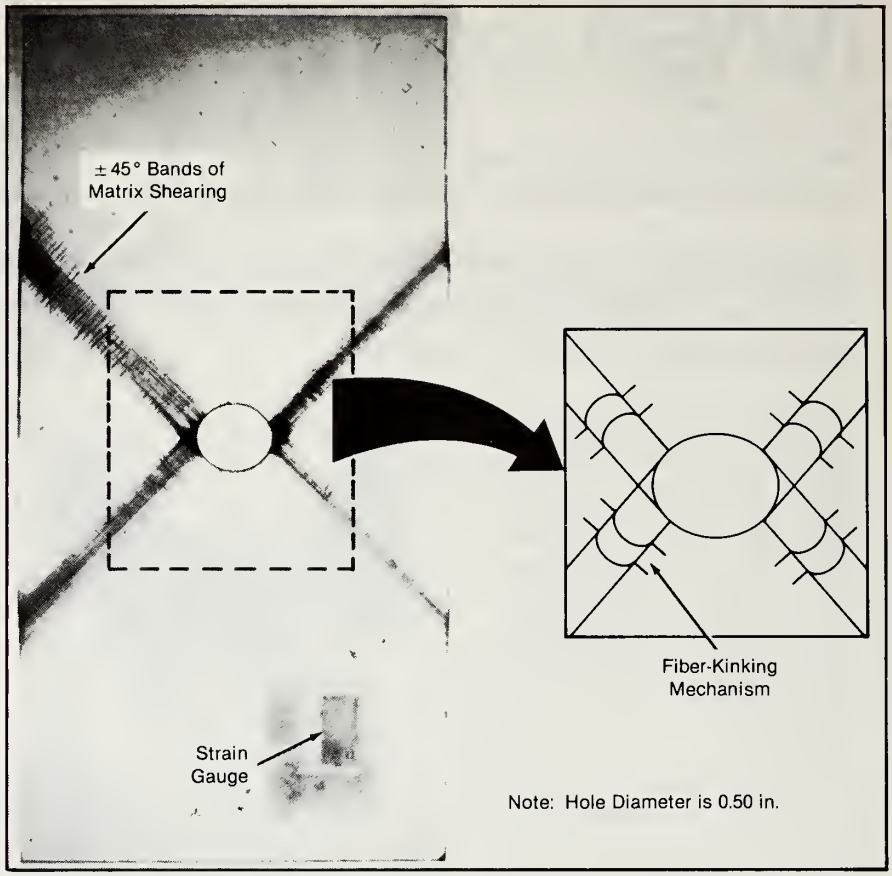

Figure 2. **White Light Reveals** matrix-shearing bands plus a fiber-kinking mechanism.

This work was done by Mark J. Shuart, Jerry G. Williams, and Paul A. Cooper of **Langley Research Center.** *Further information may be found in:*

NASA CR-165709 [N81-26183/NSP], "Development of Orthotropic Birefringent Materials for Photoelastic Stress Analysis" [$10], and

NASA TM-86306 [N84-20259/NSP], "Investigating Compression Failure Mechanisms in Composite Laminates with a Transparent Fiberglass-Epoxy Birefringent Material" [$7].

Copies of these reports may be purchased [prepayment required] from the National Technical Information Service, Springfield, Virginia 22161.

LAR-13345 / T N

FOR ADDITIONAL INFORMATION: *Contact: Director, Technology Transfer Division, P.O. Box 8757, BWI Airport, MD. 21240; (301) 621-0100 Ext. 241*

REFER TO THE NUMBER LISTED AT THE END OF THE ARTICLE

NASA Tech Brief
National Aeronautics and Space Administration
Lyndon B. Johnson Space Center, Houston, Texas

Licensing Opportunity

Comparative Thermal-Conductivity Test Technique

Approximate thermal conductivities are determined rapidly.

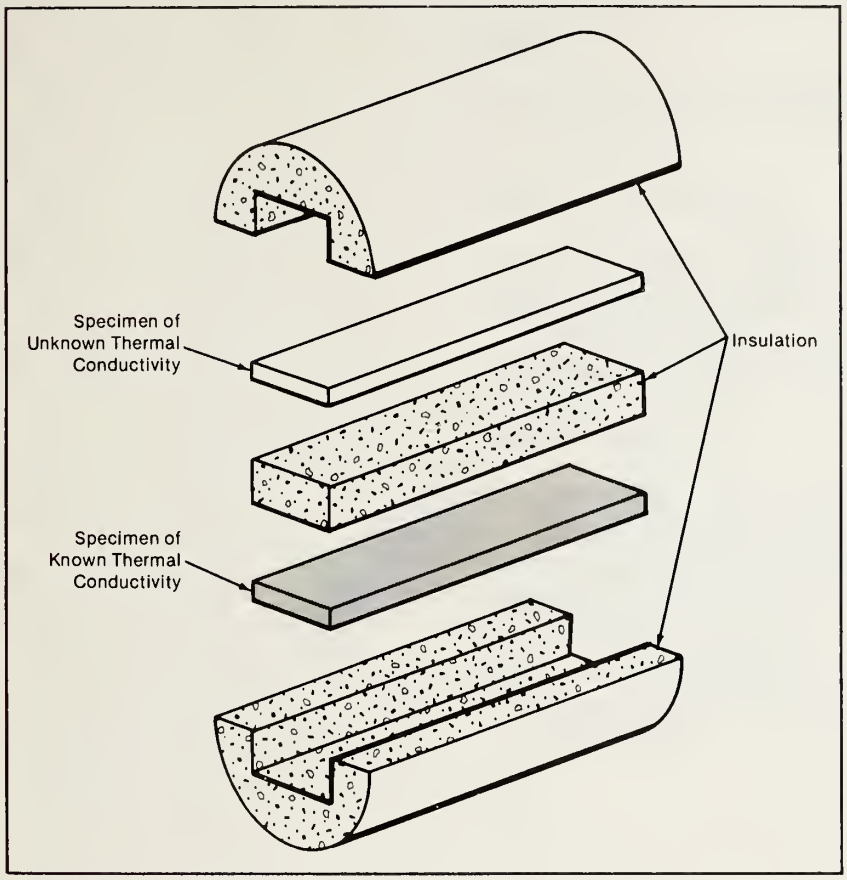

The Two Specimens, the conductivities of which are to be compared, are placed in an assembly with insulation. One end of the assembly is then placed in a furnace. The temperature of the furnace, of each end, and of the center of each specimen are then recorded.

The thermal conductivity of a material can be estimated conveniently in a test procedure that compares it to a material of known conductivity. This procedure can be used to rate quickly the candidate materials for applications in which thermal conductivity is a prime consideration. Once the selection has been reduced to one or two candidates, formal thermal-conductivity test methods can be used to verify the results of the inexpensive comparative technique.

An exploded view of the test arrangement is shown in the figure. The two 1- by 6-in. (2.5- by 15-cm) test specimens, one of known thermal conductivity, are well separated by insulation and then wrapped in insulation. This assembly is then partially inserted into a tube furnace so that one end of each specimen is exposed to the furnace temperature, and the other end is open to the atmosphere. Thermocouples are attached to both ends and to the middle of each sample. The thermocouple readings are monitored for 15 to 30 min.

The steady-state conduction equations for each specimen are ratioed and solved for the conductivity ratio (candidate sample to known sample). The heat-flow ratio — needed for this calculation — is determined using the temperatures of the heated ends of the specimens to calculate the convective and radiant interchanges between the specimens and the furnace. The data-reduction procedure can be programed into a hand-held calculator. Originally applied to advanced carbon/carbon composite materials at temperatures above 3,000° F (1,600° C), this procedure should be applicable to a wide variety of materials and a wide range of temperatures.

This work was done by Charles N. Webster and James K. Willis of LTV Aerospace Corp. for **Johnson Space Center.**

Inquiries concerning rights for the commercial use of this invention should be addressed to the Patent Counsel, Johnson Space Center
Refer to MSC-20980 / TN

William Chmylak
Lyndon B. Johnson Space Center
Mail Code AL32
Houston, TX 77058
(713) 483-3809

FOR ADDITIONAL INFORMATION: *Contact: Director, Technology Transfer Division, P.O. Box 8757, BWI Airport, MD. 21240; (301) 621-0100 Ext. 241*
REFER TO THE NUMBER LISTED AT THE END OF THE ARTICLE

Medicine & Biology

1124 Starch Ampicillin Agar for the Quantitative Detection of Aeromonas Hydrophila

1125 Protein Identification Service Available

1126 Adjustable Headband for Earphones—A new headband is designed for comfort and convenience.

Software

1127 Psychological Tests to Determine Environmental Effects Computerized

Testing & Instrumentation

1128 High-Definition X-Ray Detector

1129 Detection of Double Stranded RNA by Immunoblot Electrophoresis

1130 Measuring PCB Levels in Blood

Other items of interest

1045 Small-Portion Water Dispenser—Pressure is regulated and flow is timed to control the amount dispensed.

1077 A Simplified Model of Thermal Comfort in Buildings

1089 Disposal of the Pesticide, Coumaphos, Using Microbial and UV-Ozonation Reactions

1090 Aural Nondetectability—A sound propagation and attenuation study yields data needed to predict aural detectability for various conditions.

United States Department of Agriculture

Research Technology
Agricultural Research Service

Starch Ampicillin Agar for the Quantitative Detection of Aeromonas Hydrophila

Recently, public health officials have been increasingly concerned about the role that the bacterium, Aeromonas hydrophila may play in causing human diseases. They have established that contaminated water supplies can be a source of the microorganism. However, little is known about the role foods may play in transmitting the disease-causing microorganism, in part due to the lack of suitable methods for detecting A, hydrophila in foods. This information is particularly vital because the microorganism can grow at refrigeration temperatures normally used to safeguard foods. To rectify this problem an effective method (Starch Ampicillin Agar) for detecting the microorganism in foods was developed and found that A, hydrophila is present in a wide variety of retail fresh foods of animal origin. The development of this detection method, and the accompanying evaluation of food products, provides public health investigators with much needed information for evaluating the importance of foodborne A, hydrophila as a cause of human disease.

Interest in Aeromonas hydrophila as a foodborne and human pathogen is increasing. Isolation media from the clinical laboratory were evaluated for food use and found either not to give quantitative recovery of A, hydrophila or did not permit ready differentiation of A, hydrophila from the background microflora. A new medium was developed which permitted quantitative recovery of A, hydrophila from foods. The medium consisted of phenol red agar base (Difco), soluble starch (10 g/liter), and ampicillin (10mg/liter). All foods surveyed contained A, hydrophila. Foods sampled included red meats, chicken, raw milk, and seafood (fish, shrimp, scallops, crab and oysters). The count of A, hydrophila at the time of purchase ranged from 1 X 10**2/g (lower limit of detection) to 5 X 10**5/g. In most instances the count of A, hydrophila increased during 1 week's storage at 5 deg C. The starch ampicillin agar developed permitted rapid quantitative recovery of A, hydrophila from foods, and permitted this recovery in the presence of very large numbers of competing microflora.

FOR ADDITIONAL INFORMATION: Contact: Dr. Samuel A. Palumbo, USDA-ARS, ERRC, 600 E. Mermaid Lane, Philadelphia, PA 19118; (215) 233-6524.

NIH
Research & Technology

Federal
Technology
Resource

U.S. Department of Health and Human Services Public Health Service National Institutes of Health

PROTEIN IDENTIFICATION SERVICE AVAILABLE

On the basis of their sequence, partial sequence, or amino acid composition, proteins such as enzymes and hormones are identified and analyzed at the Protein Identification Resource of the National Biomedical Research Foundation at Georgetown University in Washington, D.C.

They are analyzed with the aid of a computer system and the protein sequence data base developed at the resource, which is supported by the Biomedical Research Technology Program of the NIH Division of Research Resources. Investigators can perform some of their own analyses at the resource or can send data for analysis from anywhere in the world by using a microcomputer or computer terminal and a modem.

Many protein structures contain information required to understand the causes of diseases and to develop rational approaches to treatment. For example, research based on known sequences of the surface regions of viral coat proteins may enable scientists to synthesize peptide antigens that could be used to immunize people against viruses.

Scientists at the resource recently used the computer system to determine that a gene of vaccinia virus, a large DNA virus, produced a protein similar to epidermal growth factor and transforming growth factor alpha. The identified gene had structural and functional similarities to the growth factors that cause cells to grow and divide.

The main field of interest at the resource is the identification of newly sequenced proteins. The resource maintains the world's largest collection of protein sequence information. After entering the sequence of an unidentified protein, scientists at the resource can use several computer programs to search the protein against a data base of known sequences. One of these programs compares complete sequences. It is designed to locate regions of similarity between a test protein and sequences contained in the data base. Proteins tentatively identified can be further characterized by other programs, if needed.

The SEARCH program can be used to identify a protein sequence. The program compares information about a segment of specific length to all known protein segments of the same length, identifying the parts, if any, that are the same or similar.

Another computer program, ALIGN, can be used to verify that proteins are related, even distantly. The program can also generate statistics based on the comparison of random rearrangements of the sequences. It relies on an algorithm that requires the specification of two parameters and a comparison matrix.

Proteins may also be compared on the basis of amino acid composition, which is easier and quicker to determine than the sequence of a protein.

Newly identified proteins are placed in groups of related sequences, which are organized into hierarchical categories. These categories include families, subfamilies, and entries. Families are less than 50 percent different, subfamilies are less than 20 percent different, and entries are less than 5 percent different. Researchers are also trying to classify functional regions of proteins called domains. Information about domains is included in the feature table of an entry.

If a relationship cannot be found, a published sequence is entered into the data base as a new type of protein.

Scientists at the resource believe that it is easier to compare protein sequences than nucleic acid sequences. They have also developed a scoring matrix to use in comparing protein sequences. The mutation data (MD) matrix is based on changes found in closely related protein sequences, which reflect similarities in the chemical functions of the amino acids.

The computer system can also display hydrophobicity profiles that scientists use to predict secondary protein structures or possible potential antigenic sites.

The Protein Sequence Query (PSQ) Program provides rapid access to the data base. Entries may be located and retrieved by biological source, sequence length, molecular weight, and amino acid composition. These programs also contain routines that can splice and edit sequences, search for open reading frames, and search for restriction enzyme cut sites. The protein sequence data base also contains more than 5 000 citations of the published literature. Information can be retrieved by author, journal, or

other reference citation.

Scientists can browse through the Protein Sequence Information System at the facility or by accessing the online system. Some information about nucleic acid sequences that code for protein sequences can be retrieved from the nucleic acid sequence data base (NAQ). Tapes containing all the protein sequences and literature references and most of the programs are also available.

The resource staff collaborates with other investigators on new computer programs that can perform additional analyses or that facilitate retrieval and make access to the data base easier. They also train investigators to access and use the computer system to perform searches and other analyses. A newsletter providing information on new computer programs and data is published occasionally.

—Barbara Proujan

For more information about the Protein Identification Resource, contact:
Kathryn Sidman, Technical Services Coordinator
Protein Identification Resource
National Biomedical Research Foundation
Georgetown University Medical Center
3900 Reservoir Road, N.W.
Washington, D.C. 20007
Telephone: (202) 625-2121.

Dr. Lois T. Hunt, senior research scientist at the Protein Identification Resource in Washington, D.C., explains how data analysis indicated a match between a protein made by vaccinia virus and epidermal and transforming growth factors found in rodents and humans.

Protein Identification Resource

NASA Tech Brief
National Aeronautics and Space Administration
John F. Kennedy Space Center, Florida

Licensing Opportunity

Adjustable Headband for Earphones

A new headband is designed for comfort and convenience.

A new headband holds an earphone and microphone on the wearer's head securely and comfortably. A wearer can easily adjust it for his or her own head size and can readily readjust it for greater comfort without removing it.

Unlike conventional headbands, which are essentially springs that clamp on the head over in an arc, the new headband contacts the head, lightly but firmly, at only two points, eliminating the headaches and soreness often caused by the conventional models. Moreover, the new headband can be adjusted more precisely to the individual's needs. Whereas a wearer would ajust the width of a conventional headband in a coarse way by bending it, the new headband can be adjusted finely by a tensioning device.

The new band consists of a pair of steel head-clamping spring strips joined by the tensioning screw (see figure). A cushioned side support is mounted on the end of one strip, and a cushioned earphone and the microphone are mounted on the end of the second strip. The band is reversible; that is, the earphone can be worn on either the left or the right ear. The side support can be replaced by a second earphone for stereo listening or by an ear mute for use in noisy surroundings.

The wearer adjusts the tension, tightening or loosening the knurled-head screw. This screw and a small, compressed coil spring cooperate to slide the head-clamping springs toward or away from each other. The wearer adjusts it while it is still on the head by turning the knurled head, thereby compressing or loosening the spring. Various alternatives to the coil-spring adjuster are available, such as a bidirectional rotatable cylinder on a threaded shaft, a thumbscrew on sliding strips, or a rack-and-pinion arrangement.

This work was done by Pierce C. Toole, Howard E. Chalson, and Stephen Bussey of **Kennedy Space Center.**

Inquiries concerning rights for the commercial use of this invention should be addressed to the Patent Counsel, Kennedy Space Center

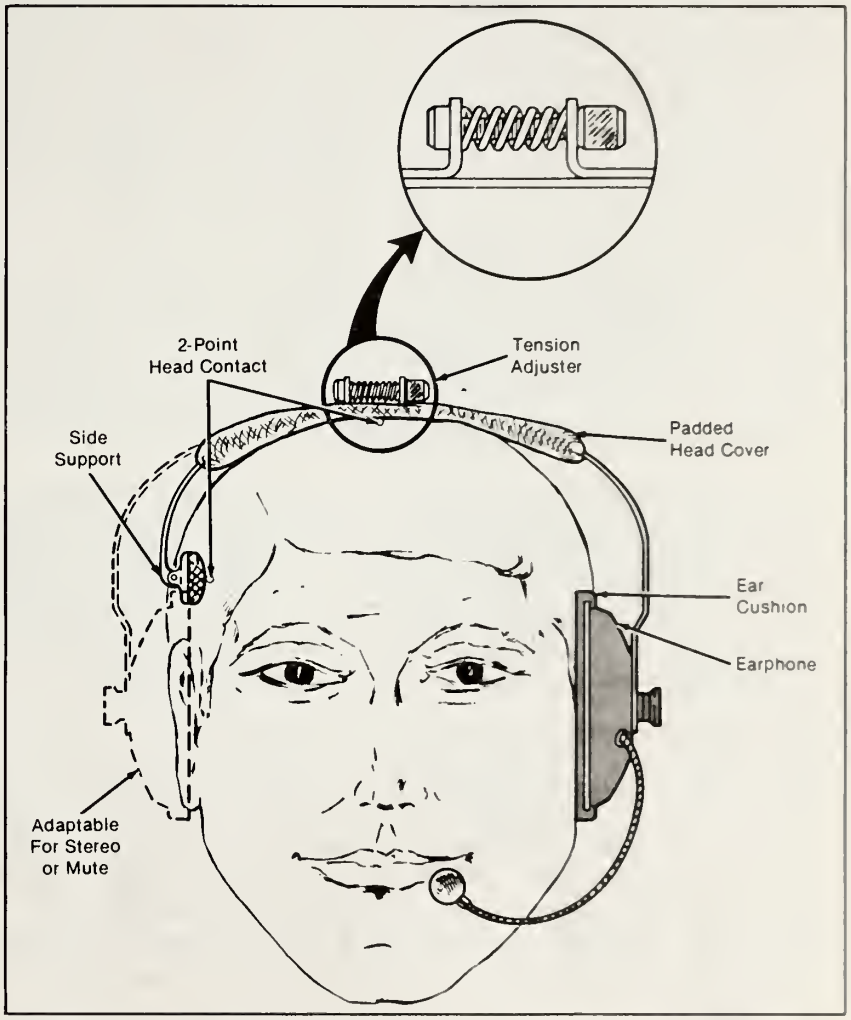

The **Headband Contacts the Head** at only two points; at the top and above one ear and at the padded side support. It accommodates standard earphones and microphones

Refer to KSC-11322 / TN

U. Reed Barnett
John F. Kennedy Space Center
Mail Stop PT-TPO-A
Kennedy Space Center, FL 32899
(305) 867-3017

FOR ADDITIONAL INFORMATION: *Contact: Director, Technology Transfer Division, P.O. Box 8757, BWI Airport, MD. 21240; (301) 621-0100 Ext. 241*

REFER TO THE NUMBER LISTED AT THE END OF THE ARTICLE

Walter Reed Army Institute of Research

Psychological Tests to Determine Environmental Effects Computerized

Psychologists use a number of test batteries to help them gauge such diverse human attributes as intelligence, mental and motor skills, and psychological well-being. Some test batteries are designed as screening tests, to measure absolute ability and to compare individuals, while others are used to follow a single individual over time, to compare the way he or she responds to the same tasks when subjected to different environmental conditions or physiological states. Members of the Department of Behavioral Biology have developed a computerized test battery that falls into the latter category.

The test has already been used in various versions for studying the effects of sleep deprivation, heat stress, physical fatigue, physical conditioning, hypoxia, nicotine, atropine and sickle cell disorders. It has generally been used with normal, healthy, motivated young adults with a high school or college education. The battery does not require touch typing skills, but does require the ability to read and figure above the grade school level.

Some of the tasks in the test are interchangeable and can be added or left out depending on the constraints and purpose of each study. Most tasks were chosen because they met multiple criteria: (1) they represent a reasonable sample of elementary skills thought to underlie many real-world tasks; (2) they can be administered briefly and repeatedly; (3) they can be performed on a computer; and (4) they are either known or expected to be sensitive to physiological, psychologic or environmental variables.

Some of the simplest tasks involve visual recognition; in one task, two or more target letters are presented at the top of the display screen, along with a string of 20 letters in the middle of the screen. The subject is asked to determine as quickly as possible whether the string contains the target letters. A more taxing task test is short-term memory. Nine random digits are displayed simultaneously in a row across the center of the screen for one second. The screen then goes blank for three seconds, after which eight of the original nine digits are re-displayed in a different random order, and the subject enters the missing digit.

The test battery measures subjective parameters as well; in one task, subjects are presented with 65 adjectives and asked to respond on a five point scale the extent to which the adjectives reflect their current feelings.

The test battery is designed to be run on any personal computer compatible with the IBM PC or Apple II series.

FOR ADDITIONAL INFORMATION: Contact: Walter Reed Army Institute of Research, Attn: SGRD-UWS (Mr. Paul Klein), Washington, D.C. 207-5100; (202) 576-2580.

energygram®

High-Definition X-Ray Detector

DOE/TIC/EG-86/082
OFFICE OF SCIENTIFIC AND TECHNICAL INFORMATION

This technical note was based on research conducted by Lawrence Berkeley Laboratory for the U.S. Department of Energy.

Lawrence Berkeley Laboratory

Technology Description. An X-ray imaging detector for making digital heart angiograms has been designed jointly with Stanford University. The detector takes advantage of the abrupt difference in the absorption of X-rays in iodine at energies slightly above and below the K absorption edge (33.17 keV). Iodine is introduced into the heart arteries noninvasively and twice scanned by monochromatic X-rays, in one scan the X-rays being about 10 eV above the K edge and the second scan being 10 eV below. The images of bone and overlying tissue are essentially identical in the two images and cancel when the logarithmic difference of the two images is derived, leaving a well-defined image of the coronary arteries. A novel linear array of 300 silicon detectors, each with individual readout, detects X-rays from a fan-shaped beam scanned across the heart.

Why Is This Better Than Existing Technology? Images can be produced with an exposure about 1/100 that of conventional X-ray imaging. Coronary arteries of 1 mm diameter are readily imaged.

Stage of Development. An operating system is being utilized.

Potential Uses and Spinoffs. Medical radiography.

FOR ADDITIONAL INFORMATION

DOE report(s):
A Multi-Element Silicon Detector for X-ray Flux Measurements.
Report number: LBL-12746/NAB
Order number: DE82004841/NAB
Price: $9.95
300-Element Silicon-Lithium Position-Sensitive Imaging Detector
Report number: LBL-19641/NAB
Order number: DE86005232/NAB
Price: $9.95

Order from:
National Technical Information Service
5285 Port Royal Road
Springfield, VA 22161

For additional information, contact
Jack T. Walton and Albert C. Thompson
Lawrence Berkeley Laboratory
Berkeley, CA 94720
Telephone No. (415) 486-5631 and (415) 486-5590

Schematic layout of system for performing digital angiography using synchrotron radiation.

United States Department of Agriculture

Research Technology
Agricultural Research Service

Detection of Double Stranded RNA by Immunoblot Electrophoresis

The study of double-stranded RNA found in virus infected cells is becoming a valuable tool in virus detection and characterization. A variety of techniques need to be developed which can more fully characterize these molecules. An immunoblot procedure was developed which can detect double-stranded RNA modecules from a mixture of nucleic acids (single and double-stranded RNA and DNA) which had been electrophoretically separated in an agarose gel. The use of immunoblotting in detecting double-stranded RNA molecules has been demonstrated. This procedure can be used in place of, or in addition to, commonly used double-stranded RNA characterization procedures.

The procedure permits the serological detection of double-stranded RNA (dsRNA) which has been electrophoretically transferred from agarose gels to Zeta-Probe blotting membranes. Cucumber mosaic virus replicative forms of RNAs 1-3 and cassava (Manihot esculenta) clone "Secundina" dsRNAs can be routinely detected from 1.0 g of leaf tissue. This procedure allows for the detection and size estimation of dsRNAs in crude nucleic acid preparations.

FOR ADDITIONAL INFORMATION: Contact: Dr. Clifford J. Gabriel, USDA-ARS, U.S. Plant Intro. Res. St, 11601 George Palmer Hwy, Glenn Dale, MD 20769; (301) 344-3003.

NBS technology update

National Bureau of Standards
U.S. Department of Commerce
Gaithersburg, MD 20899

Measuring PCB Levels in Blood

Tests for amounts of polychlorinated biphenyls (PCBs) in blood samples can be checked for accuracy with a standard reference material (SRM) now available from NBS. Such tests are important for determining exposure of persons who work with toxic PCB compounds--employees in the chemical industry or emergency personnel who clean up chemical spills, for example. SRM 1589 is in the form of freeze-dried human blood serum "spiked" with 106 nanograms of Aroclor 1260 per gram of serum. (Aroclor 1260 is a mixture of PCBs found in some transformer oils). The SRM, which must be reconstituted with 10 milliliters of distilled water, is intended for use in the calibration of analytical instruments and validation of a laboratory's measurement procedure for PCBs in blood. It also may be used as a primary standard against which secondary reference materials may be compared. Certified to be accurate within a 1 percent range, the SRM costs $163 per three-vial set.

FOR ADDITIONAL INFORMATION: To order SRM 1589, Polychlorinated Biphenyls (as Aroclor 1260) in Human Serum, or for more information about the more than 900 SRMs the bureau offers for sale, contact the Office of Standard Reference Materials, B311 Chemistry Building, National Bureau of Standards, Gaithersburg, MC 20899; (301) 921-2045.

Natural Resources Technology & Engineering

1131 Raindrops Affect Radar Echoes of the Sea

1132 Selecting Water Spray Pressures for Optimum Dust Control

Software

1133 Mine Stench Fire Warning Computer Model

Other items of interest

1053 Positive-Index Guiding in CDH-LOC Lasers—A nonabsorbing passive region has beam-guiding capability.

Raindrops Affect Radar Echoes of the Sea

A scientist at the Naval Research Laboratory (NRL) has determined that raindrops can affect radar echoes of the sea. Field and laboratory data indicate that splashes produced by raindrops can, under certain conditions, increase sea clutter detected by radar.

The results of the research have a bearing on the interpretation of sea clutter encountered by conventional radar systems and from microwave sensing instrumentation. The applications of interest to the Navy are for distinguishing target signals from backscatter and for sensing physical conditions of wind and sea.

Experiments were conducted from a cliff overlooking the Chesapeake Bay. Backscatter measurements were taken before, during, and after several rainstorms and for a variety of wind and water conditions. Analysis of the data has indicated that with initially calm sea and wind conditions, the splashing of raindrops on the water can greatly increase the surface backscatter.

In laboratory experiments, ultrahigh-resolution radar techniques and split-screen video were used to capture the scattering effects of various phases of splashes. Results of the laboratory experiments confirmed the results of the field experiments and provided a guideline for an ongoing analytical model of the rain splash effect.

NRL studies also suggest that this phenomenon can affect a wide range of illumination angles and, therefore, might be applicable to radar on airplanes as well as on surface ships.

For Additional Information, Contact:
Navy Domestic Technology Fact
Sheet Reader Reply Service
Code E211
Naval Surface Weapons Center
Dahlgren, VA 22448-5000
(703) 663-8921
Refer to 110504/TN

Technology News

From the Bureau of Mines, United States Department of the Interior

No. 244,

Selecting Water Spray Pressures for Optimum Dust Control

Objective

Control respirable dust in underground coal mines through selection of optimum water spray pressures.

Approach

Through underground trials at longwall and continuous mining operations, the relationship between operating water spray pressure and respirable dust levels at the machine operator's location was determined.

Defining the Application

Water sprays are used for two significantly different control applications. On longwall mining machines, sprays are commonly installed both on the body of the machine and on the cutting drum. Sprays on the body of the machine are used to redirect dust which has already become airborne away from the machine operator. Each spray acts as a small fan, directing the primary airflow over and around the machine and towards the face, away from the operator. The energy of this system is directly related to the spray pressure. Higher pressures move more air, but care must be taken not to cause turbulence and boilout into the walkway. Sprays mounted on the drum are effective at suppressing the respirable dust at the bit/coal interface and preventing it from becoming airborne. Again, these sprays must not impart excessive energy to the dust particles thus stirring up more dust than they suppress. While mounting sprays on the shearer drum is standard industry practice, there is no reliable technology available to successfully mount water sprays on the cutting drum of continuous miners. Instead, sprays are mounted on the machine body, close to the drum, and directed at the cutting head. This allows the water to reach the bit/coal interface and mix with the cut material. Here again, care must be exercised to prevent these sprays from imparting excessive energy to the dust particles and stirring up more dust than they suppress. These sprays can also cause dust "rollback" from the face, toward the operator, if operated at too high pressures.

For methane control however, air movement and turbulence are desired; higher water spray pressures can be used without stirring up dust if a specific water spray system, called the spray fan system, is used (see *Technology News* No. 162). On the other hand, when only concerned with dust control, higher pressures and associated air movement and turbulence should be avoided.

Test Results

Longwall—Shearer Clearer System

An optimum external water spray system developed for longwall shearers has been tested at a number of underground coal mining operations. Water sprays strategically-mounted on the shearer body divide the primary airflow into a dusty split confined to the face and a clean air split over the operator (see *Technology News* No. 221). The minimum operating spray pressure for external sprays designed to move air is approximately 150 psi, measured at the nozzle. At face velocities of approximately 350 fpm, increasing shearer clearer spray system pressure from 100 to 150 psi can reduce dust levels around the shearer by as much as 70%. Note that this applies only to external spray systems designed to direct dusty air away from the shearer operators. Increasing the operating pressure of a poorly-designed external spray system will actually increase dust exposure.

Longwall—Drum Sprays

Drum sprays are the most effective system for reducing respirable dust generated by the machine. Here, increasing drum water flowrate can reduce dust

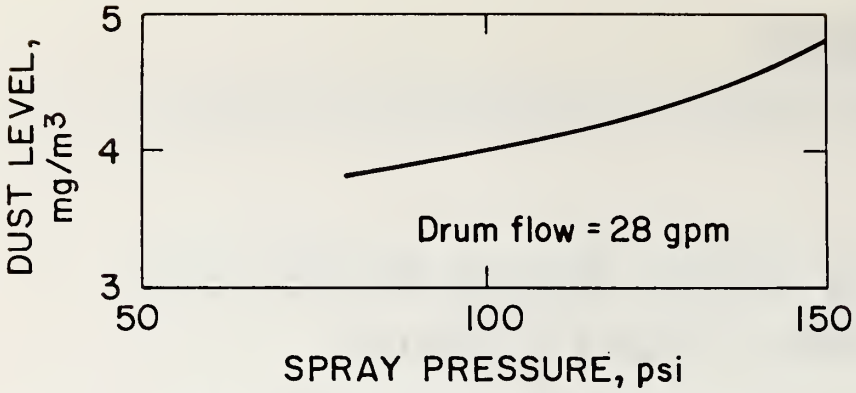

Effects of drum spray pressure on respirable dust levels.

levels but increasing drum spray pressure increases dust exposures. With the flowrate to the drum held constant at 28 gpm, the operating pressure was increased from about 75 to 115 psi. This pressure increase raised dust levels around the machine by 25%. When pressure was increased from 80 to 150 psi, dust levels in the walkway also increased on about 25% (see figure). Thus, the optimum drum spray pressure appears to be from 70 to 100 psi. Increased water flowrate should be achieved by increasing the nozzle orifice size rather than the operating spray pressure.

Continuous Miner—Anti-rollback system

Although high pressure sprays knock dust down more effectively, they can increase dust rollback to the miner operator. An optimum external water spray system for continuous mining machines was tested at a number of underground operations (see *Technology News* No. 225). A moderate spray pressure of 100 psi measured at the nozzle appears to be a practical maximum. A well designed external water spray system, operating at 100 psi and 28 gpm, can reduce dust levels at the operator by 40%, as compared to a conventional system operated at 150 psi and equal waterflow. Spray type and orientation, as well as face airflow, must be considered when designing a spray system. A system that causes rollback at 3,000 cfm may not do so at 6,000 cfm.

Recommendations

In summary, to move air and redirect the dust away from the operator, the spray pressure should be at least 150 psi. To suppress dust before it becomes airborne, spray pressure should be kept below 100 psi. These pressures are operating pressures at the spray nozzle, and should be measured with a tee connector inserted into the spray block with the spray at one end of the tee and the pressure gage at the top. The most appropriate sprays for dust control on continuous mining machines are flat-fan nozzles; for external air moving qualities (shearer clearer), hollow cone nozzles; and for longwall shearer drum sprays, solid stream nozzles.

For More Information

Further information can be obtained by contacting the Technical Project Officer, Robert A. Jankowski, at the Bureau of Mines, Pittsburgh Research Center, P.O. Box 18070, Pittsburgh, PA 15236, or calling 412-675-6691. *Technology News* Nos. 112, 113, 118, 150, 155, 162, 221, and 225, and RI 8963 also contain additional information. Single copies are available by writing to the Bureau of Mines, Branch of Technology Transfer, 2401 E. Street, NW, Washington, D.C. 20241 or by calling 202/634-1224.

Technology News

From the Bureau of Mines, United States Department of the Interior

No. 251

Mine Stench Fire Warning Computer Model

Objective

Enable mine personnel to determine the effectiveness of and to optimize the mine fire stench warning system without resorting to costly trial and error fire drills.

Approach

The mine fire stench warning system is used by underground metal/nonmetal mines to warn mine workers of a fire or other emergency. Stench is released directly into the mine ventilation and/or compressed air lines, and its repulsive odor warns miners to evacuate the mine or to follow other established emergency procedures. Unfortunately, since most deep metal mines have complex ventilation systems, some areas of the mine may receive nauseatingly high concentrations of stench while other areas, in more remote locations, may receive no warning or greatly delayed warning at best. The Bureau of Mines, through research, endeavored to solve this problem with a computer modeling system designed to calculate the distribution of odorant by the stench warning system.

How It Works

The mine's normal ventilation is first established either as measured quantities that are entered as input data for the program or calculated within the program from flow production factors such as fans and natural ventilation, as well as flow impedance associated with wall friction. The advantage of the latter approach is that as new drifts are opened, doorways closed, and fans added, a prediction can be made of the new mine ventilation. The ventilation calculations are made within the program by first representing the mine network as a collection of closed paths. Then the conservation of energy is applied to the air flow around each path, while frictional wall losses are used to establish pressure drops along airways. At each junction (airway intersection within the mine network), conservation of mass is applied to relate the airflow rates. Temperature variations within the mine are used to calculate natural ventilation head loss as part of the conservation of energy around each path. Fan head losses are determined from the fan characteristic curve and are entered into the energy balance. The real-time capability of the program is utilized to project the time-dependent spread of stench from a warning system throughout the mine complex. This evaluation proceeds by associating control volumes with specific contaminant concentrations. Each control volume is transported with the airflow. At

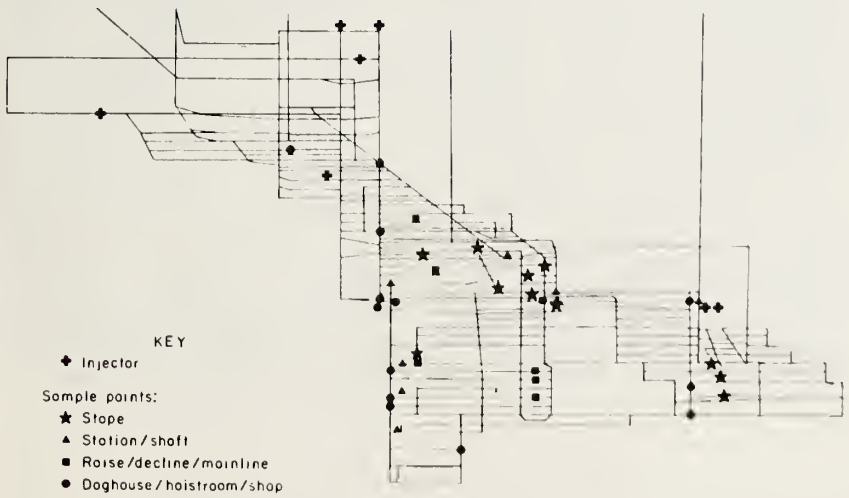

Configuration of sampling points and location of stench injectors at a mine used to validate the computer model.

junctions where control volumes meet, perfect mixing is assumed and a new control volume (a new contaminant concentration) is formed. The contaminant sources are specified at fixed locations in the network, and for finite time durations.

Test Results

Validation tests of the computer model were conducted at a large South Dakota gold mine. The mine's ventilation and stench system were first modeled, then the computer-predicted stench travel times were compared to actual stench arrival times reported by miners to their shift bosses (sampling points) during a routine stench/fire evacuation drill at the mine. The mine's stench system utilized tetrahydrothiophene stench agent and six Bureau-developed stench injectors (as described in *Technology News* no.138, "Improved Mine Stench Fire Warning System"). The ventilation network, injector locations, and sampling points are shown in the diagram.

Initial comparison of measured and predicted arrival times provided poor correlation so the field data were broken down into four subgroups for further analysis. The subgroups were chosen to differentiate between sampling points in areas of well defined ventilation (subgroups one and two) and sampling points in areas where ventilation might be somewhat uncertain (subgroups three and four). Subgroups one consisted of 13 sample points in station and shaft areas; subgroup two consisted of 7 sample points located in raises, declines, and mainlines; subgroup three consisted of 12 sample points located in stopes; subgroups four consisted of 8 sample points located in doghouses, hoistrooms, and shops.

The closest correlations were observed in the first two subgroups. In general, the best correlations occurred where network branches corresponded to single airways in the mine. Where a number of parallel airways were represented in the computer simulation by a single network branch (as was common for subgroups three and four), prediction of arrival time in a particular airway was less precise. Of the twenty sample points in subgroups one and two, two were found to be in error. The first error was due to a report of stench detection at a time which coincided with the release of stench, even though the closest injector was over 4800 feet away. The second error was attributed to failure to report detection until 20 minutes after sample points further downstream had reported detection. Correlation for the remaining 18 points was 0.509. This correlation is very good considering the iterative nature of a model of this type, and the fact that imprecise measurements made in the mine are being compared to the mathematical precision of a computer.

The computer model proved to be very useful. Analysis of data from subgroups 3 and 4 and outliers from subgroups 1 and 2 located three areas of the mine that were inaccurately modeled due to errors in the input data. This analysis suggests a second potential use of the computer model—that is, as an inexpensive method for refining ventilation flow data. Large discrepancies between predicted and measured arrival times indicate errors in computer model input data (ventilation parameter measurement errors or network reduction errors). Although less precise than using tracer gases such as SF_6, this method is much less expensive since the data are a byproduct of normal mine evacuation drills. Using this method to correct input data errors after each stench drill, convergence between predicted and measured values is expected.

Patent Status

The Bureau of Mines does not plan to patent or copywrite this computer model.

For More Information

The computer program and in-mine tests are described in *Mine Ventilation,* Chapter 1, Section 4, "Mine Stench Fire Warning Computer Model Development and In-Mine Validation Testing", by S. J. Ouderkirk, W. H. Pomroy, J. C. Edwards, and J. Marks, A. A. Balkema Publishers, Accord, MA, 1985. For more details, including information on how to obtain copies of the program, contact the principal investigator for this work, William H. Pomroy, Twin Cities Research Center, Bureau of Mines, 5629 Minnehaha Ave. So., Minneapolis, MN 55417 or telephone (612) 725-3469.

1134 Synchrotron Ultraviolet Radiation Facility (SURF II)

1135 High Current Metal Ion Source (MEVVA)

1136 Three-Dimensional Radiative-Transfer Equation—Progress is made toward the interpretation of radiometric observations.

Software

1137 Software to Calculate Activities of Alpha Emitters

Testing & Instrumentation

1138 Schlieren Photography of Combustion Processes—Individual burning granules can be examined in detail.

1139 Ball-and-Socket Mount for Instruments—Jaws engage an instrument precisely but release it readily.

1140 Recording Interferograms Holographically—Images of experiments are stored for later analysis.

1141 Solid-Sorbent Air Sampler—Portable unit takes eight 24-hour samples.

Other items of interest

1061 Laser-Induced Optical Degradation—The performance of irradiated optical systems is modeled.

1072 Lithium-Counterdoped Solar Cells—Resistance to damage by energetic electrons is increased.

1078 Detoxification of Halon Fire-Extinguishant Products—Ammonia compounds absorb toxic hydrogen halides as they are produced.

NBS technology update

National Bureau of Standards
U.S. Department of Commerce
Gaithersburg, MD 20899

Synchrotron Ultraviolet Radiation Facility (SURF II)

NBS has updated the 10-year-old SURF II Users' Guide, which provides technical information for researchers using the bureau's Synchrotron Ultraviolet Radiation Facility (SURF II). The new guide reflects several major improvements to SURF II, which now includes eight beamlines; high-flux grazing-incidence and normal-incidence monochromators; a spectrometer calibration facility; a very-high-resolution spectrograph; and a far-uv diode calibration facility. SURF II has an operating energy of 300 MeV, and a maximum electron beam current well in excess of 100 mA. SURF II is the most precisely calibrated electron storage ring in the United States--electron beam current can be measured to within 2 percent, and absolute radiation flux is known to within a few percent. It is ideally suited to calibrations and fundamental radiometric studies.

FOR ADDITIONAL INFORMATION: Interested researchers should contact Dr. Robert Madden, A251 Physics Building, National Bureau of Standards, Gaithersburg, MD 20899; (301) 921-2031.

energygram®

High Current Metal Ion Source (MEVVA)

DOE/TIC/EG-86/043
OFFICE OF SCIENTIFIC AND TECHNICAL INFORMATION

This technical note was based on research conducted by Lawrence Berkeley Laboratory for the U.S. Department of Energy.

Lawrence Berkeley Laboratory

Technology Description. The Metal Vapor Vacuum Arc (MEVVA) high-current ion source produces beams of metallic ions at currents up to one ampere. In the operation of the source, a vacuum arc is created between a cathode and an anode. The cathode can be any electrically conducting solid. Intense concentrations of current form at minute regions on the cathode and thus vaporize and ionize cathode material and give rise to a dense plasma, which plumes toward the anode and provides a path for the current. A central aperture in the anode allows plasma to pass through, and an axial magnetic field guides the charged particles to extraction electrodes.

Beams of Li, C, Al, Si, Ti, Cr, Fe, Co, Ni, Cu, Nb, Mo, Ta, Au, Pb, and U ions have been produced by the MEVVA source, with an extraction voltage of up to 60 kV and an ion current of up to one ampere. The source is simple and reliable. It is also possible to combine conducting and nonconducting materials (for instance La and B) in the cathode to obtain an ion beam containing both materials.

Why Is This Better Than Existing Technology? In conventional sources, beams of several tens of milliamperes, maximum, are obtainable.

Stage of Development. Units have been built and operated. A patent is pending.

Potential Uses and Spinoffs. Ion implantation in semiconductor technology and surface treatment of materials.

FOR ADDITIONAL INFORMATION

For additional information, contact:
I. G. Brown
Lawrence Berkeley Laboratory
53-103
Berkeley, CA 94720
Telephone No.: (415) 486-4174

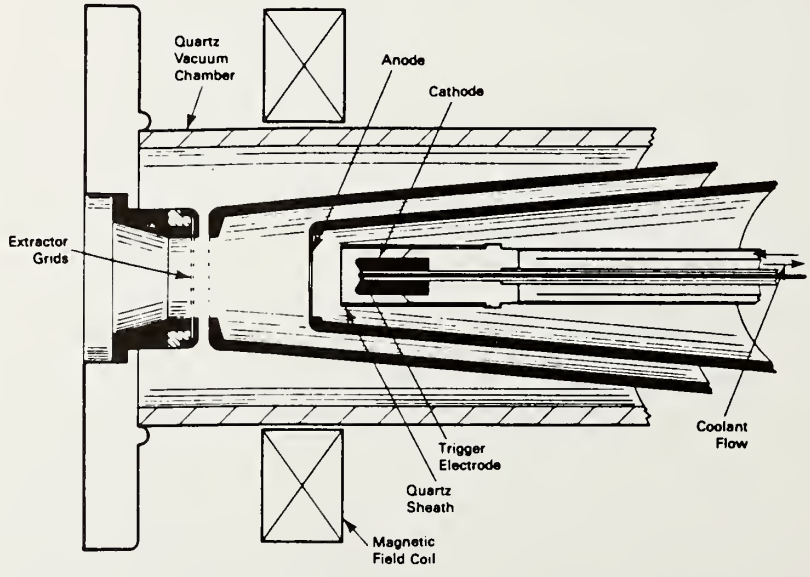

Simplified, cutaway view of the MEVVA II ion source.

NASA Tech Brief
National Aeronautics and Space Administration

Three-Dimensional Radiative-Transfer Equation

Progress is made toward the interpretation of radiometric observations.

A theoretical paper discusses the equation of radiative transfer in a three-dimensional, inhomogeneous, scattering medium illuminated from above and bounded below by a laterally-inhomogeneous, reflective plane. A representation of the radiation field with full three-dimensional variability is derived by use of a spatial Fourier transform and matrix-operator techniques developed previously for the one-dimensional version of the problem. The equations should be useful for radiometric measurements from aircraft and spacecraft.

Initially, the problem is stated generally in terms of spatial integrals expressing the radiation incident upon, generated within, reflected from, and passing through, a horizontal planar layer. The horizontal spatial dependence of all quantities is approximated as periodic for discretization of the Fourier wave-number spectrum. In practical problems, such an approximation does not give rise to errors as long as an appropriate buffering zone is constructed within the primary pattern to prevent contamination by the adjacent repetitions of the pattern. The periodicity assumption makes it convenient to take the two-dimensional Fourier transform of the radiative-transfer equation in the horizontal plane.

Explicit expressions for the reflectivity and transmissivity operators and emission functions for an infinitesimally thin layer bounded by the z and $z + \Delta z$ planes are obtained by expansion of the Fourier-transformed radiation equations about the vertical coordinate z. By use of these operators and functions in the context of the interaction principle, expressions are obtained for the mathematical synthesis of a vertically inhomogeneous, arbitrarily thick medium. A doubling theorem makes it possible to obtain the operators and functions for an arbitrarily thick, homogeneous layer from a similar layer of infinitesimal thickness. Because a thick, inhomogeneous layer can be conveniently simulated by a vertical sequence of homogeneous layers, each in sequence having slightly different properties, the radiation-transfer functions for the entire thick, inhomogeneous layer can be built up by the combination of adding and doubling techniques.

Following the derivation described above, the basic equations are restated, and all equations are rederived in matrix form. The scattering medium is vertically stratified into a number of different layers, each of which is internally homogeneous. As before, the adding and doubling relations are derived and used to model thick layers. Although the derivations and the resulting equations are complicated, the use of the Fourier-transform, matrix-operator approach to solve practical problems is expected to be simpler than direct solution of the complete three-dimensional, linear wave equations.

This work was done by John V Martonchik and David J. Diner of Caltech for **NASA's Jet Propulsion Laboratory.** *"Three Dimensional Radiative Transfer Using a Fourier Transform Matrix Operator Method," NPO-16563/TN*

FOR ADDITIONAL INFORMATION: *Contact: Director, Technology Transfer Division, P.O. Box 8757, BWI Airport, MD. 21240; (301) 621-0100 Ext. 241*
REFER TO THE NUMBER LISTED AT THE END OF THE ARTICLE

Software to Calculate Activities of Alpha Emitters

DOE/TIC/EG-86/042
OFFICE OF SCIENTIFIC AND TECHNICAL INFORMATION

This technical note was based on research conducted by Idaho National Engineering Laboratory for the U.S. Department of Energy.

INEL
Idaho National Engineering Laboratory

Technology Description. Two computer programs (AMPU and ALPHA) take raw data obtained from alpha spectrometry and calculate activities and uncertainties of the radionuclides present in the sample. One program (AMPU) determines Pu-239, Pu-238, and Am-241 using Pu-236 and Am-243 tracers. The other program (ALPHA) determines activities of any alpha emitter in a sample that has been directly precipitated with NdF_3. The results are then outputted in a tabular manner with their uncertainties.

Why Is This Better Than Existing Technology? These programs propagate all random and systematic uncertainties found anywhere in the experimental process to the final result. Other programs only propagate random uncertainties from counting statistics or not at all. The answer has been rounded and is in decimal agreement with the uncertainty. Other programs display all eight digits or more of the result and uncertainty.

Stage of Development. Computer programs used daily to calculate analytical data.

Potential Uses and Spinoffs. In conjunction with alpha spectrometers for reduction of data with rigorous error propagation.

FOR ADDITIONAL INFORMATION

For additional information, contact:
David S. Sill
EG & G Idaho, Inc.
P.O. Box 1625
Idaho Falls, ID 83415
Telephone No.: (208) 526-8031
FTS 583-8318

MANUFACTURING TECHNOLOGY NOTE

U.S. ARMY MATERIEL COMMAND

Deputy Chief of Staff for Manufacturing Technology, Alexandria, VA

Project Number: NONE

Filing Code : 73D077

Schlieren Photography of Combustion Processes

Individual burning granules can be examined in detail.

A schlieren photographic system, developed by the U.S. Army Armament Research and Development Center, can be used to study combustion processes in single granules of black powder. The system uses a streak camera and a high-power modulated stroboscopic argon laser as the light source to provide a dynamic sequence of time-resolved, high-spatial-resolution schlieren photographs of the combustion products. The combustion processes have never before been analyzed in detail because available photographic techniques could not record the hot gaseous flow field.

With the new system, the expansion rate of the gaseous products and the velocity history of the flying particulate matter were measured. The combustion products were found to consist of hot gases, reactive and nonreactive solid particles, and molten droplets. Large nonreactive particles appear to result from subsurface explosions of the black-powder granules. Reactive particles may play an important role in grain-to-grain flame propagation.

Particle velocity histories were obtained by tracking particles from frame to frame and determining the velocity at various intervals (see figure). Several particles were tracked from their origin at the parent granule until they left the field of view. Particles were located and followed for periods of 50 milliseconds or more, despite the difficulty created by smoke around the granule.

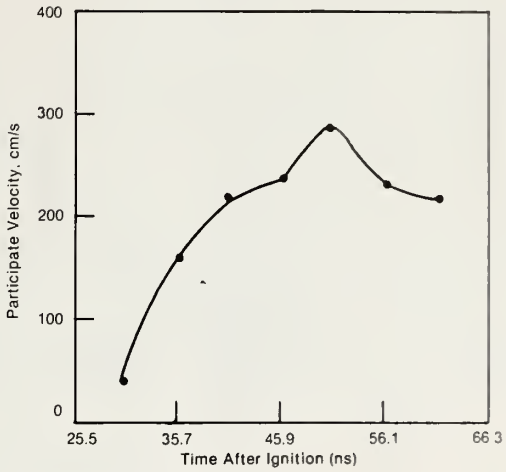

A representative **Particle Velocity History** shows the variation in velocity of a combustion-product particle with time. The sudden rises in velocity at the start of the curve and at 45.9 milliseconds indicate that variable forces are acting in the gas flow.

FOR ADDITIONAL INFORMATION

You can learn more details about this technology by ordering the NTIS reports:

Combustion Characteristics of Single Granules of Black Powder
Order number: AD-P004547/NAA
Price code: A02

Order from
National Technical Information Service
5285 Port Royal Road
Springfield, VA 22161

This document was prepared under the sponsorship of the U.S. Government. Neither the United States Government nor any person acting on behalf of the United States Government assumes any liability resulting from the use of the information contained in this document, or warrants that such use will be free from privately owned rights.

NASA Tech Brief
National Aeronautics and Space Administration
Marshall Space Flight Center, Alabama

Licensing Opportunity

Ball-and-Socket Mount for Instruments

Jaws engage an instrument precisely but release it readily.

A mounting mechanism holds a scientific instrument securely, allows the instrument to be oriented, and minimizes conduction of heat to and from the instrument. The mechanism also allows quick replacement of the instrument.

The mechanism includes a stationary base containing part of the spherical-socket surface, two jaws that contain the rest of the socket surface, and an adjusting screw. A ball on the instrument sits in the spherical socket formed by the opposing jaws and base (see figure). The adjusting screw is threaded into one of the jaws and rotates in a collar in the opposite jaw. Rotating the screw counterclockwise opens the mechanism by sliding the jaws outward on a dovetail track on the base. The instrument ball can then be removed from the opened socket. Turning the screw clockwise draws the jaws together until the socket captures the ball.

Each jaw contains three T-shaped parts that maintain the alignments of the jaw parts and serve as internal stops. These parts have cylindrical arms that seat in cylindrical holes in the base as the jaws draw together. When the tees are seated, the adjusting screw is further turned to a torque of 35 lb-ft (47 N-m) to preload the mechanism and prevent the tees from separating from the base. When thus assembled, the mechanism maintains a diametral clearance of 80 to 240 μin. (2 to 6 μm) between the socket and the ball.

This work was done by Everett Kaelber of Perkin-Elmer Corp. for **Marshall Space Flight Center.**

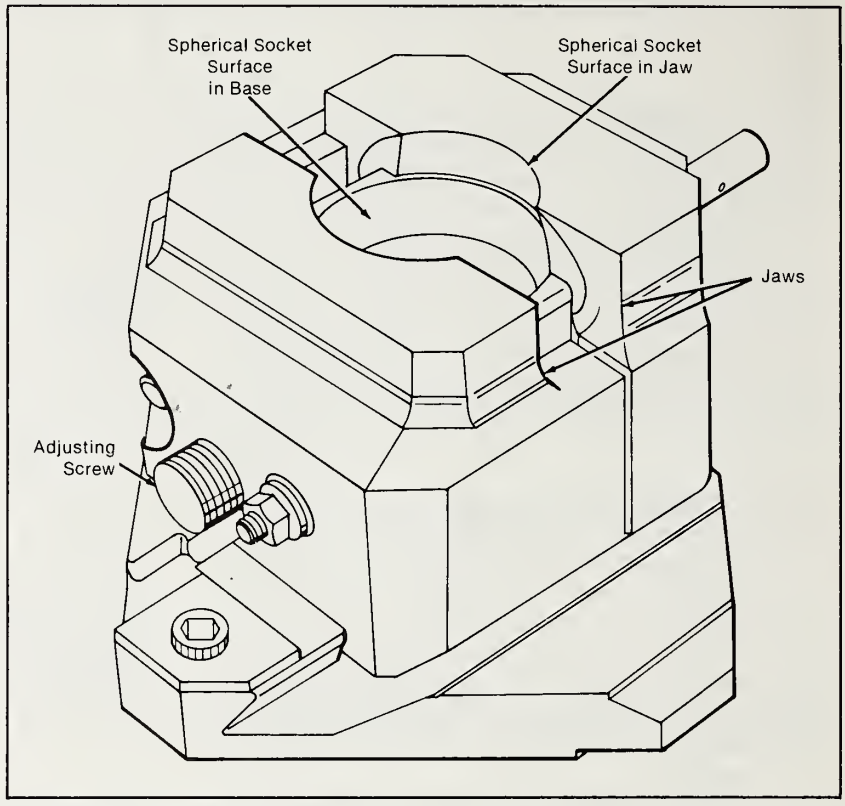

Opposing Jaws Sliding on a Base form a socket that holds the mounting ball of a scientific instrument.

Inquires concerning rights for the commercial use of this invention should be addressed to the Patent Counsel, Marshall Space Flight Center
Refer to MFS-28064/TN

Ismail Akbay
George C. Marshall Space Flight Center
Code AT01
Marshall Space Flight Center, AL 35812
(205) 453-2223

FOR ADDITIONAL INFORMATION: *Contact: Director, Technology Transfer Division, P.O. Box 8757, BWI Airport, MD. 21240; (301) 621-0100 Ext. 241*
REFER TO THE NUMBER LISTED AT THE END OF THE ARTICLE

NASA Tech Brief
National Aeronautics and Space Administration
Marshall Space Flight Center, Alabama

Licensing Opportunity

Recording Interferograms Holographically

Images of experiments are stored for later analysis.

A holographic system reconstructs interferometer images recorded during experiments for later, more detailed analysis. The system was developed for experiments on crystal growth during space flights. With it, images are recorded rapidly under the constraints of the experiments and are later examined on the ground.

The holographic images are reconstructed in a modified Mach-Zehnder interferometer, an instrument often used to measure the spatial variation of the index of refraction of a gas. In its classical form, the Mach-Zehnder interferometer consists of two beam splitters (semitransparent mirrors) and two wholly reflecting mirrors at alternate corners of a rectangle. Halves of an incoming light beam travel along opposite faces of the rectangle. The halves combine at a semitransparent mirror to form an interference pattern.

The classical interferometer was modified for holography by removing the entrance semireflecting mirror and inserting the holographic recording in one of the legs (see figure). A collimated laser beam is projected through the hologram and directed to the remaining semitransparent mirror. There it combines with a reference beam from the same laser to form a virtual image of the original experiment.

This work was done by Ellis R. Comeens and Robert L. Kurtz of TAI Corp. for **Marshall Space Flight Center.**

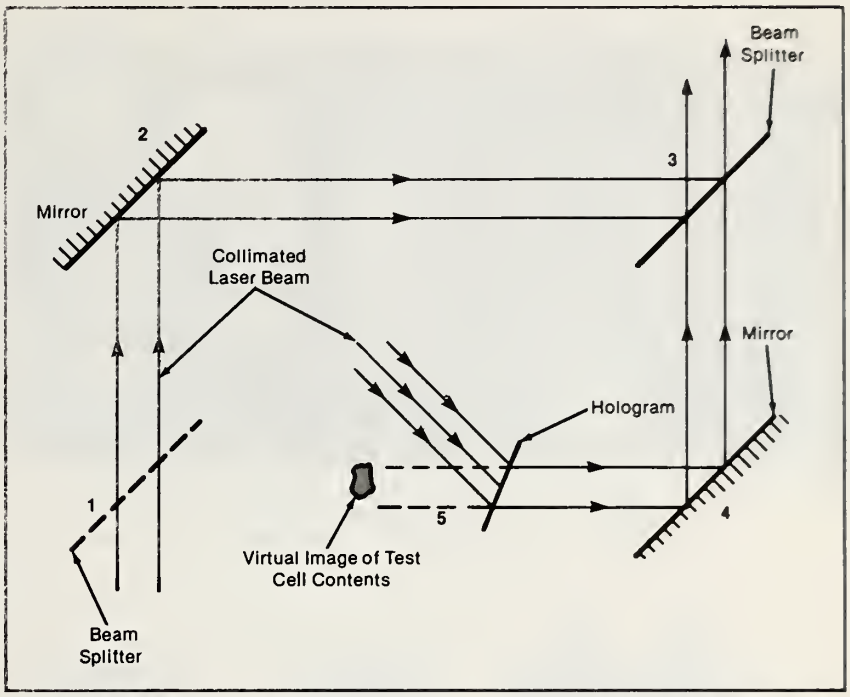

In a **Classical Mach-Zehnder Interferometer,** path 1-2-3 is the reference leg, and path 1-4-3 is the object leg. In the interferometer modified for holography, the beam splitter at 1 is removed, as indicated by the dotted line, and path 1-2-3 is still the reference leg, but path 5-4-3 is now the object leg.

Inquiries concerning rights for the commercial use of this invention should be addressed to the Patent Counsel, Marshall Space Flight Center Refer to MFS-26024 /TN

Leon D. Wofford, Jr.
George C. Marshall Space Flight Center
Mail Code: CC01
Marshall Space Flight Center, AL 35812
(205) 453-0020

FOR ADDITIONAL INFORMATION: *Contact: Director, Technology Transfer Division, P.O. Box 8757, BWI Airport, MD. 21240; (301) 621-0100 Ext. 241*
REFER TO THE NUMBER LISTED AT THE END OF THE ARTICLE

NASA Tech Brief
National Aeronautics and Space Administration
Lyndon B. Johnson Space Center, Houston, Texas

Licensing Opportunity

Solid-Sorbent Air Sampler

Portable unit takes eight 24-hour samples.

Volatile organic compounds in air are collected for analysis by a portable, self-contained sampling apparatus. The sampled air is drawn through the sorbent material, a commercial porous polymer of 2,3-diphenyl-p-phenylene oxide. High-boiling-point organic compounds are adsorbed onto the polymer, while low-boiling-point organics, O_2, N_2, Ar, CO_2, CO, and H_2O, pass through and are returned to the atmosphere.

The sampling apparatus (see figure) includes eight glass-lined stainless-steel sample tubes filled with the sorbent. The tubes are normally isolated from each other (to prevent cross-contamination) and from the atmosphere by a manually-operated 18-port switching valve.

As shown schematically at the bottom of the figure, the valve is turned to connect the desired sample tube to the atmosphere, and air is drawn through the tube by a pump. At the end of the sampling period (normally, 24 hours), the operator turns the valve handle to the next position, thereby exposing a new sample while isolating and protecting the previous sample(s).

Electrical power for the 1.5-V pump motor is controlled by a 3-V timing circuit, the output of which is adjustable from one pulse every 7 seconds to continuous: This enables the sampling airflow rate to be preset at a value between 0.1 and 0.5 cm^3/min. The motor and timer are both powered by alkaline C-cells, which operate continuously for up to 21 days.

For analysis, the sample tubes remain in place and are connected through the valve to a standard gas-chromatographic/mass-spectrometric system. Since the tubes do not have to be handled or exposed to the atmosphere during analysis, the risk of sample contamination is further reduced.

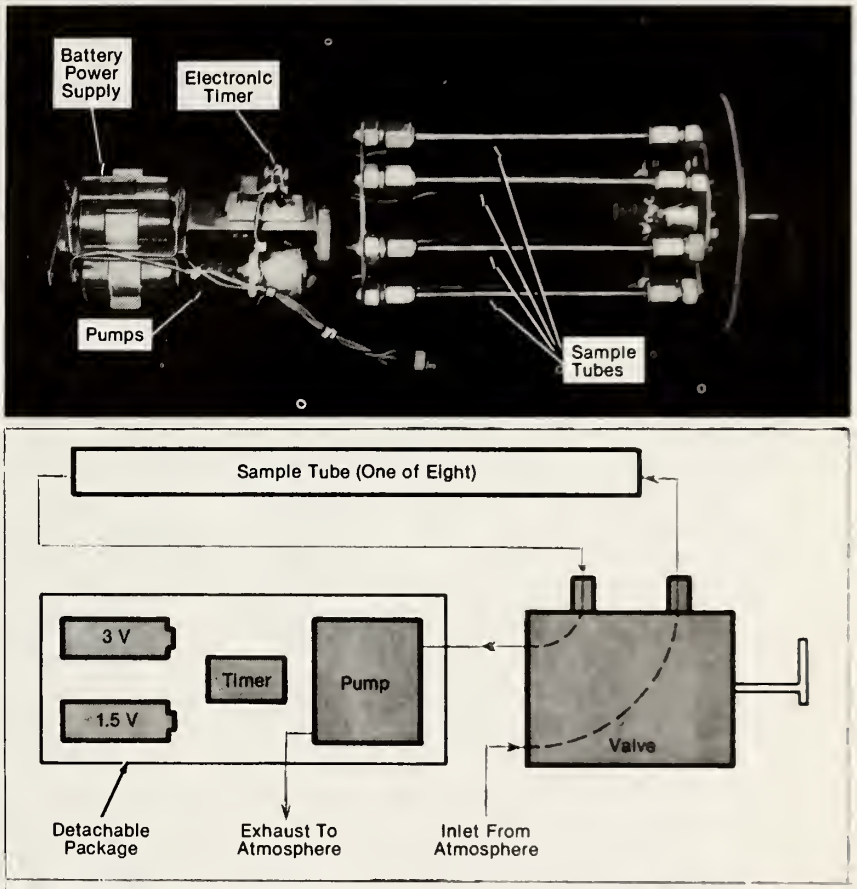

The **Solid-Sorbent Air Sampler** includes eight sample tubes filled with a polymeric sorbent. Organic compounds in the atmosphere are adsorbed when air is pumped through the sorbent.

Although designed for checking air in spacecraft, the sampler is readily adaptable to such other applications as leak detection, gas-mixture analysis, and ambient-air monitoring. The unit is lightweight and compact [3.3 lb (1.5 kg), 4.5 in. (11.4 cm) in outside diameter, and 8 in. (20.3 cm) long]. Operation is simple: Power must be turned on and off, and the valve handle must be turned manually; but no other operator intervention is required.

This work was done by Theodore J. Galen of Northrop Services, Inc., for **Johnson Space Center.**

This invention is owned by NASA, and a patent application has been filed. Inquiries concerning nonexclusive or ex-

clusive license for its commercial development should be addressed to the Patent Counsel, Johnson Space Center Refer to MSC-20653 / TN

Marvin F. Matthews
Lyndon B. Johnson Space Center
Mail Code: AL3
Houston, TX 77058
(713) 483-4871

FOR ADDITIONAL INFORMATION: *Contact: Director, Technology Transfer Division, P.O. Box 8757, BWI Airport, MD. 21240; (301) 621-0100 Ext. 241*
REFER TO THE NUMBER LISTED AT THE END OF THE ARTICLE

1142 Icing Effects on the YEH-60A (Quick Fix) Helicopter—Tests were performed to establish a moderate icing flight envelope.

1143 Amphibious Vehicle Designed

Testing & Instrumentation

1144 Sensing Horizontal Heading in Aircraft Maneuvers—A modified gyroscopic system indicates the geographic heading even in nearly vertical flight.

1145 Two-Axis, Self-Nulling Skin-Friction Balance—The two-dimensional aerodynamic skin-friction force is measured directly.

1146 Continuous, Multielement, Hot-Film Transition Gage—Measurements can be taken along a single line in the streamwise direction.

MANUFACTURING TECHNOLOGY NOTE

U.S. ARMY MATERIEL COMMAND

Deputy Chief of Staff for Manufacturing Technology, Alexandria, VA

Project Number: EJ4-103-AC-01-EJ-EC

Filing Code : 51A041

Icing Effects on the YEH-60A (Quick Fix) Helicopter

Tests were performed to establish a moderate icing flight envelope.

Artificial and natural icing flight tests were conducted by the U.S. Army Aviation Engineering Flight Activity to establish a moderate-icing flight envelope for the YEH-60A (Quick Fix) helicopter, a twin-turbine, single-main-rotor helicopter capable of day and night operations under visual and instrument meteorological conditions. An additional goal of the tests was to determine the effectiveness of electrically anti-icing direction-finding (DF) antennas (see figure).

After damage to an unprotected DF antenna during an icing encounter, the original DF antenna was removed, and a prototype thermoelectrically anti-iced DF dipole antenna was installed. The icing flight tests were conducted at an average density altitude from 830 to 7,630 ft (272 to 2502 m). Icing was accomplished at ambient temperatures of −22.5 to −4 °C. Test airspeeds ranged from 93 to 131 knots (47.8 to 67.3m/s) true airspeed, and the main-rotor speed was 258 rpm. Anti-ice and deice systems were operated continuously in the icing environment.

Shortcomings noted during the icing evaluation included damage to the unheated DF antenna element mounts and phenolic blocks caused by excessive element oscillation due to ice accumulation, poor reliability and high maintenance requirements of the main-rotor blades, and the accumulation of chaff in the tail-rotor slipring assembly, which caused electrical sparks in the tail rotor blade deice system. As originally configured (unheated DF antenna), the YEH-60A was not suitable for flight in moderate icing conditions; however, it has good potential for flight under these conditions when equipped with anti-icing DF antennas.

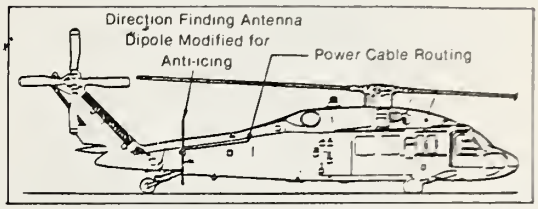

The **YEH-60A (Quick Fix) Helicopter** performs suitably in a moderate-icing environment when it is equipped with thermoelectrically anti-iced direction-finding antennas

FOR ADDITIONAL INFORMATION

You can learn more details about this technology by ordering the NTIS report(s):

Artificial and Natural Icing Tests YEH-60A Quick Fix Helicopter
Order number: AD-A155147/NAA
Price code: A05

Order from:
National Technical Information Service
5285 Port Royal Road
Springfield, VA 22161

This document was prepared under the sponsorship of the U.S. Government. Neither the United States Government nor any person acting on behalf of the United States Government assumes any liability resulting from the use of the information contained in this document, or warrants that such use will be free from privately owned rights.

Amphibious Vehicle Designed

A technology demonstrator of an amphibious vehicle, designed at the David Taylor Naval R&D Center (DTNSRDC) was recently tested on the Severn River in Annapolis, Maryland. The Automotive Test Rig (ATR) is the first step in the development of a tracked amphibious vehicle for the United States Marine Corps that will have a water speed above 20 knots.

These initial tests focused on the vehicle's operation and maneuverability in the water (especially turning and reversing operations), and static and dynamic trim.

The ATR has on board five new components and systems intended to improve performance over those on current vehicles, including a retractable Hydropneumatic Suspension System, a Hydrostatic Transmission that is computer controlled (drive-by-wire), Two-Speed Final Drive Units, and a Wire-Link Band Track System.

Initial feasibility testing of the ATR's automotive components began in 1985 and will continue through 1986. Then, the vehicle will be modified, and a higher-power water drive system will be installed to attain the water speed goal.

For Additional Information, Contact:
Navy Domestic Technology Fact Sheet Reader Reply Service
Code E211
Naval Surface Weapons Center
Dahlgren, VA 22448-5000
(703) 663-8921
Refer to 110301/TN

ATR Embarks on Amphibious Demonstration

NASA Tech Brief
National Aeronautics and Space Administration
Dryden Flight Research Center, Edwards, California

Licensing Opportunities

Sensing Horizontal Heading in Aircraft Maneuvers

A modified gyroscopic system indicates the geographic heading even in nearly vertical flight.

Modifications to an existing two-gyroscope attitude-sensing system supply azimuth (geographic heading) information, rather than the usual roll information when the aircraft climbs or dives within 15° of vertical. Previously, no azimuth heading was available during nearly vertical flight due to the nature of the gimbal-lock-avoidance subsystem. Now, the azimuth signal in the modified system indicates what the aircraft heading would be if it were to resume level flight from a climb or dive.

The relationship among the gimbals, gyroscopes, and aircraft axes during a nearly vertical dive is shown in the figure. In the unmodified system, the outer roll gimbal is held fixed in space when the pitch axis comes within ±15° of vertical. This causes the azimuthal gimbal to become fixed with respect to the outer roll gimbal, even when the small horizontal component of the aircraft heading changes: Thus, the horizontal (directional) gyro ceases to supply a correct azimuth-heading signal.

In the modified system, the outer roll gimbal is held fixed with respect to the aircraft frame when the pitch angle is within ±15° of vertical. A roll about the longitudinal axis then causes a movement of the pitch gimbal about the azimuthal gimbal, which gives rise to an azimuthal indication as in level flight. If the roll were to suddenly stop and the aircraft pitched back to level, the resulting aircraft azimuthal heading would be indicated correctly.

The outer roll gimbal, the pitch gimbal, and the inner gimbal of the vertical (pitch) gyro remain mutually orthogonal during nearly vertical maneuvers. Therefore, when the aircraft pitches from vertical toward horizontal flight, the outer roll gimbal is free to follow the aircraft platform without disturbing the spatial orientation of the pitch and inner roll gimbals of the vertical gyro. Similarly, departure from vertical flight induces no movement of the inner gimbals of the horizontal (directional) gyro. Thus, the probability of gyro tumble due to gimbal lock during such maneuvers is reduced.

Antitumble performance is improved over that of the original system except

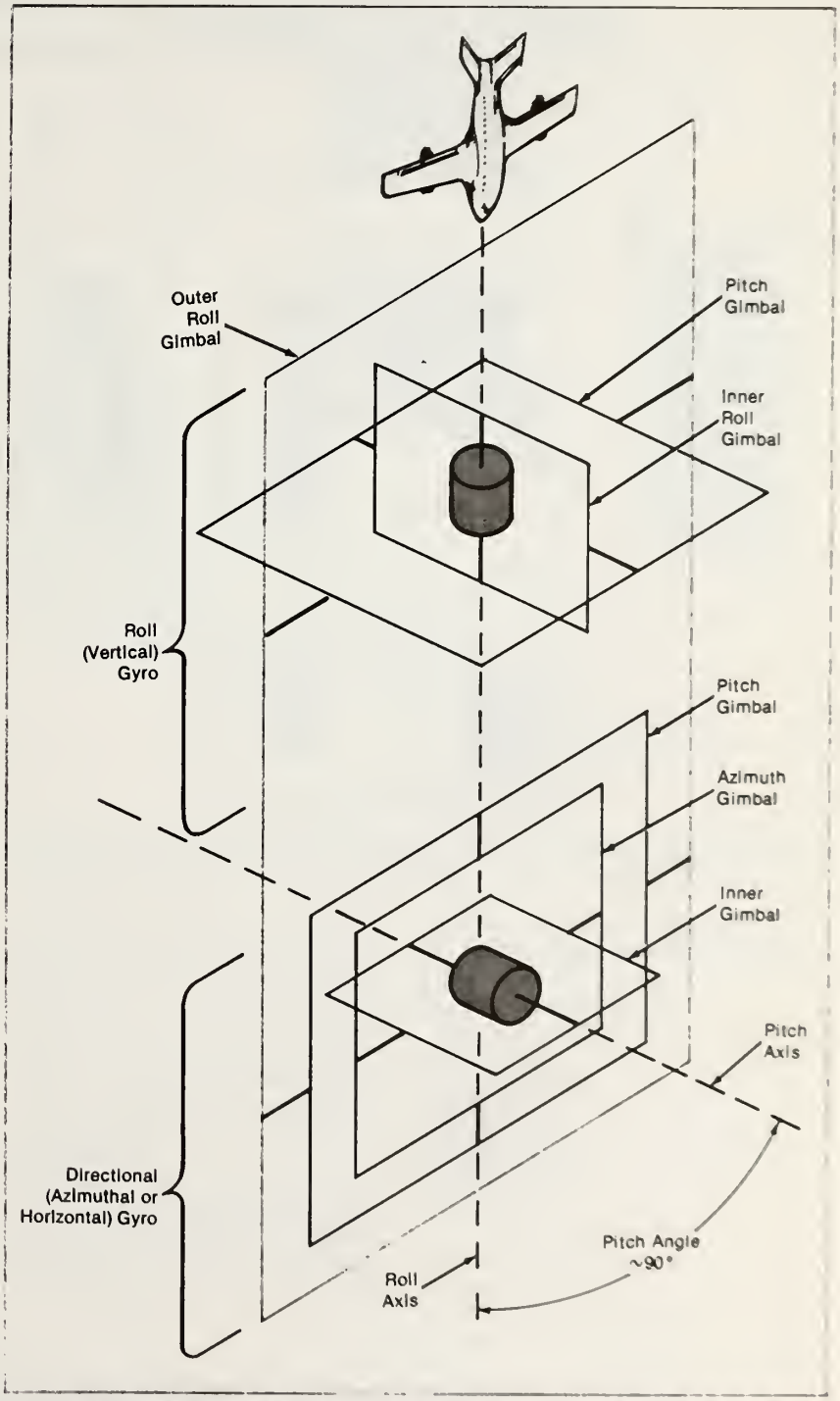

The **Gyroscopes and Gimbals** of the system assume this configuration when an aircraft has pitched into a vertical dive. The outer roll gimbal is fixed with respect to the aircraft frame in this orientation.

when the aircraft enters nearly vertical flight while at or near a 90° roll angle. In that case, antitumble capability matches that of the original system.

This work was done by Kenneth T. Cowdin of **Dryden Flight Research Center.**

This invention has been patented by NASA (U.S. Patent No. 4,387,513). Inquiries concerning nonexclusive or exclusive license for its commercial development should be addressed to the Patent Counsel, Ames Research Center Refer to FRC-11043./TN

Ames Research Center
Technology Utilization Officer:
Laurance A. Milov
Mail Code 204-10
Moffett Field, CA 94035
(415) 694-5761
Patent Counsel:
Darrell G. Brekke
Mail Code 200-11
Moffett Field, CA 94035
(415) 694-5104

FOR ADDITIONAL INFORMATION: *Contact: Director, Technology Transfer Division, P.O. Box 8757, BWI Airport, MD 21240; (301) 621-0100 Ext. 241*
REFER TO THE NUMBER LISTED AT THE END OF THIS ARTICLE

NASA Tech Brief
National Aeronautics and Space Administration
Langley Research Center, Hampton, Virginia

Licensing Opportunities

Two-Axis, Self-Nulling Skin-Friction Balance

The two-dimensional aerodynamic skin-friction force is measured directly.

A two-axis, self-nulling skin-friction balance, designed to measure accurately the x and y components of the skin-friction force in the plane of airflow, is illustrated in the figure. The disk-shaped prototype design has overall dimensions of 1.25 inches (3.18 centimeters) diameter and 0.5 inch (1.27 centimeters) height. It is composed of two connecting arms, three flexural pivots, one sensing element, two force motors, two linear variable-differential transformers (LVDT's), and a case. A unique mechanism consisting of two flexural pivoted arms connected in tandem but at a right angle with each other is designed to impart the plane motion needed to sense the two-axis flow over the sensing elemen of the balance. The sensing element, 0.370 inch (0.940 centimeter) in diameter, that is attached to the end of the second arm is to be servoed by two restoring-force motors orthogonally mounted in the plane of airflow.

Two LVDT's will be used to provide the x-and y-axis displacement measurement for nulling the instrument. Care has been taken in the design of motor and LVDT housings to allow relative movements in these components only along their intended axes of operation. The balance is designed with a full-scale force range of 1 g (0.0098 N) in both x and y axes. The electronic circuit that provides the feedback signal for self-nulling operation and the continuous output signals is to be externally packaged.

A one-arm configuration with one restoring-force motor and a single LVDT can be used for the design of a miniature single-axis skin-friction balance. Also, the two-axis configuration can be converted into a three-dimensional or three-axis device by attaching a third pivoted arm in series but normal to the plane formed by the other two arms. The two- or three-axis configurations can also be designed to measure the velocity vectors of waterflow.

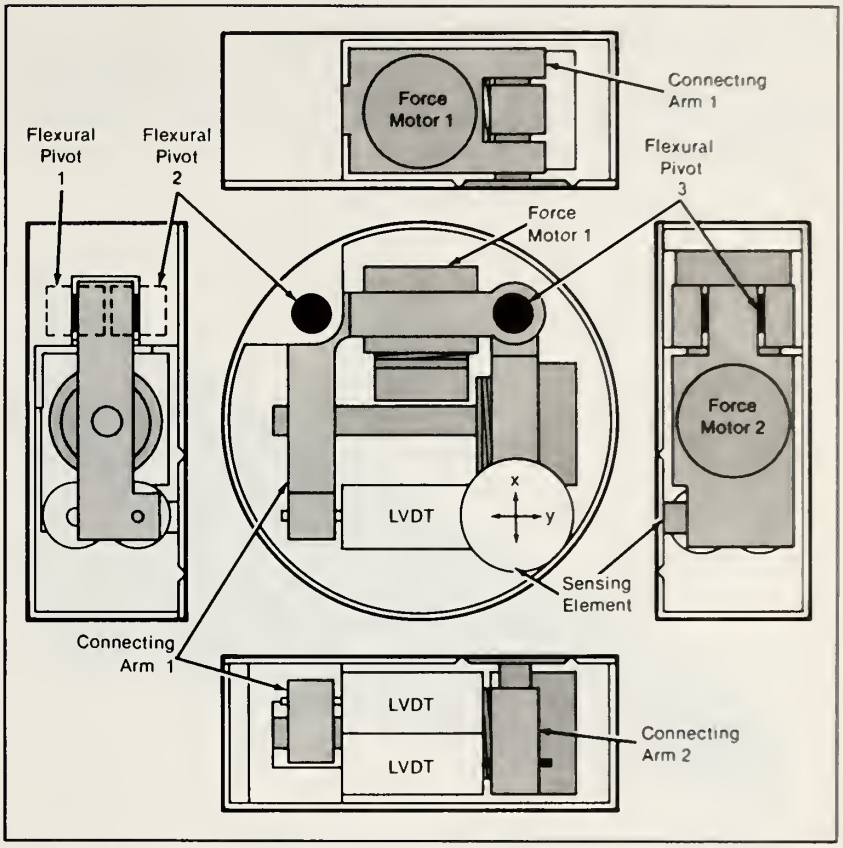

The **Skin-Friction Measuring Disk** connected to the sensing element measures the x and y components of skin friction in the plane of airflow.

The present design measures directly the skin-friction force over a single sensing element. The two-axis mechanism allows the free plane motion of the sensing element with no friction, and the balance is self-nulled to provide direct plane skin-friction force measurements continuously.

This work was done by Ping Tcheng and Frank H. Supplee, Jr., of **Langley Research Center.**

This invention is owned by NASA, and a patent application has been filed. Inquiries concerning nonexclusive or exclusive license for its commercial development should be addressed to the Patent Counsel, Langley Research Center. Refer to LAR-13294/TN

Langley Research Center
Technology Utilization Officer
John Samos
Mail Stop 139A
Hampton, VA 23665
(804) 865-3281
Patent Counsel
Howard J. Osborn
Mail Code 279
Hampton, VA 23665
(804) 865-3725

NASA Tech Brief
National Aeronautics and Space Administration
Langley Research Center, Hampton, Virginia

Continuous, Multielement, Hot-Film Transition Gage

Measurements can be taken along a single line in the streamwise direction.

The accurate measurement of the location where a laminar boundary layer undergoes the transition to a turbulent one serves many purposes in basic aerodynamic research and developmental testing. For example, a complete understanding of performance, stability, and control of a laminar-flow airplane requires knowledge of transition locations on the wing surfaces, empennage surfaces, fuselage, and nacelles. Visual, acoustic, and electronic methods are capable of providing this transition information.

One very useful device for large-scale wind tunnel and flight applications is the thin, surface-mounted, hot-film gage. Hot films indicate transition by responding to the differences in heat transfer between laminar and turbulent flows. These gages are approximately as small as postage stamps and are applied to the test surfaces by conventional strain-gage installation techniques.

However, the wiring attached to the downstream end of each gage is large enough to cause a transition wedge (emanating downstream at about a 7° half angle); thus, these individual gages must be staggered to avoid the formation of false turbulence at the downstream gages (see Figure 1). This need for staggering is the source of the most significant disadvantages of individual hot-film gages.

The continuous, multielement, hot-film transition gage overcomes the disadvantages of the individual, hot-film gages by integrating the required number and distribution of hot-film sensing elements into a long, continuous, thin sheet. The length of the sheet covers the area of interest for transition measurements, beginning at the leading edge and continuing downstream of the transition region (Figure 2). For example, on an airplane wing of 10 ft (3 m) chord length, the gage might be as much as 7 or 8 ft (2.1 or 2.4 m) long.

The leading edge of a gage mounted on the upper surface of a wing would wrap around, beneath, and downstream of the wing leading edge. A method for installing the gage eliminates the formation of transition wedges at the lateral edges of the gage. The spanwise-facing step along the sides of the gage may be faired with thin adhesive tape, or, if necessary, filling materials can be used to fair these edges smooth. The gage adheres to the surface with a very thin [0.001-in. (0.0254-mm)] double-backed adhesive tape.

In this fashion, no disturbance from the film leading edge will cause turbulent wedges to affect the hot-film sensors in

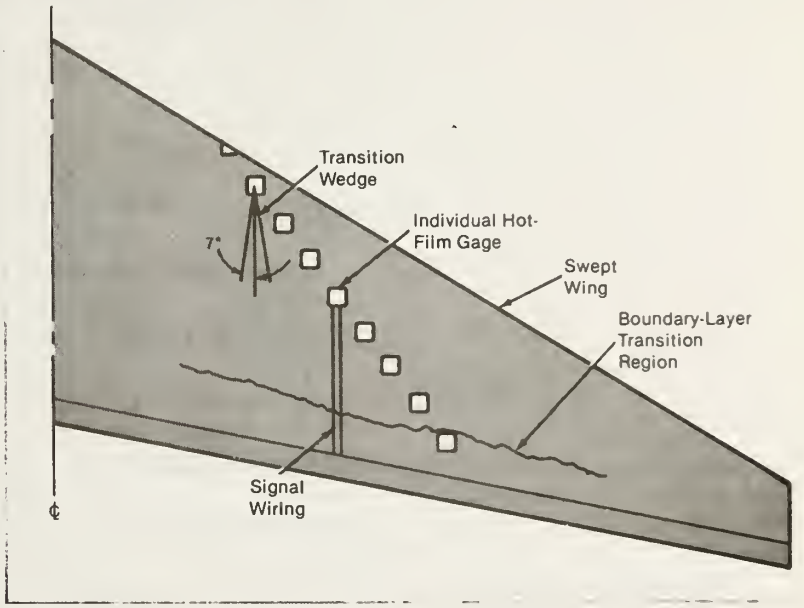

Figure 1. **Individual Gages Must Be Staggered** to prevent the formation of turbulence at the gages downstream. This arrangement precludes accurate measurements of laminar/turbulent transition regions along a streamline.

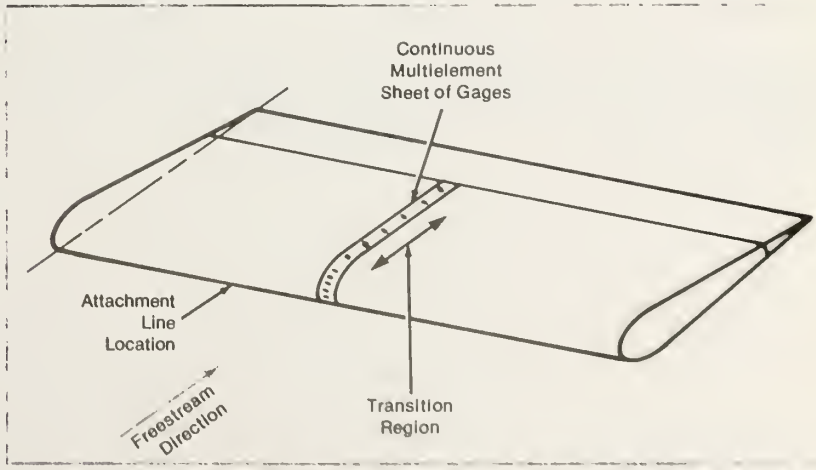

Figure 2. A **Continuous Sheet Containing Many Gage Elements** can be placed in line with the airstream without perturbing the flow and the flow measurements.

the transition region. The gage incorporates as many hot-film sensing elements as needed, distributed as needed along the length of the sheet. Because of the close spacing of the elements near the upstream end of the sheet, the stagnation-or attachment-line location can be documented. Further downstream, the elements are more widely spaced for transition-location measurement. The width of the sheet provides space for the signal leads to be carried laterally away from each hot-film element and longitudinally to the downstream end of the sheet where external wiring arrangements are made.

The multielement gage uses an improved circuit that serves as an electronic switch. The switch is a power MOSFET (metal oxide/semiconductor field-effect transistor). It can switch far greater currents (10 A) than the hot-film elements require. The MOSFET switch does not oxidize as do conventional contacts, is not affected by vibration or acceleration, and is not position-sensitive. Its very high switching speed allows sensor elements to be switched into the servo loop at very high rates without damage to the sensors.

This work was done by B. J. Holmes, J. P. McPherson, F. K. Harris, J. K. Diamond, and N. R. Johnson of **Langley Research Center** *and J. J. Chapman of Kentron International, Inc. LAR-13319 /TN*

FOR ADDITIONAL INFORMATION: *Contact: Director, Technology Transfer Division, P.O. Box 8757, BWI Airport, MD 21240; (301) 621-0100 Ext. 241*

REFER TO THE NUMBER LISTED AT THE END OF THIS ARTICLE

*U.S. GOVERNMENT PRINTING OFFICE: 1986-491-065:40012

NTIS Order Form

NTIS Telephone Numbers

To Order Reports
(703) 487-4650

For Subscription Questions
(703) 487-4630

Other Information
(703) 487-4600

Editorial Questions
(703) 487-4838

Postage:
NTIS uses First Class Delivery, or equivalent service, on all shipping. For information about one day RUSH ordering, call (703) 487-4600.

NTIS PRICE CODE SCHEDULE *

This schedule gives the current values to the price codes cited in those Tech Notes having a backup report available from NTIS.

Microfiche	
A01	$5.95
Paper copy	
A02 and A03	9.95
A04 and A05	11.95
A06 through A09	16.95
A10 through A13	22.95
A14 through A17	28.95
A18 through A21	34.95
A22 through A25	40.95
A99	Call for price

Customers in Canada, United States, and Mexico use this schedule. Other addresses should write for the price listing, number PR-360-4.

Prices effective January 1, 1986

Use this form ONLY to order reports designated as available from NTIS

MAIL ORDER TO: National Technical Information Service
U.S. DEPARTMENT OF COMMERCE
5265 Port Royal Road
Springfield, VA 22161
(703) 487-4650

Send me the reports I have selected on this form. I have placed order numbers in appropriate blanks and have indicated the quantity. IF ADDRESS LABEL IS NOT CORRECT, CALL OUR SUBSCRIPTIONS DEPARTMENT.

Last Name: .....

Title: .....

Company/Organization: .....

Address: .....

.....

City/State/Zip: .....

Telephone Number: .....

METHOD OF PAYMENT

☐ Check enclosed payable to NTIS for $ .....

☐ Charge to my NTIS Deposit Account, No: ....-.....

☐ Purchase order number: .....

Charge to: ☐ American Express ☐ VISA ☐ MasterCard

Card Number: .....

Expation date: .....

Signature: .....
(Required to validate order)

NTIS ORDER NUMBER (Use only for backup reports stated as available from NTIS)

NTIS Order Number	*Price**	*Quantity*	*Total Price*
.....	.....	.....	.....
.....	.....	.....	.....
.....	.....	.....	.....
.....	.....	.....	.....
.....	.....	.....	.....
		Shipping and handling fee	$3.00
		Total	.....

To Return Order Form Please Fold Here First

Please make second fold here and seal opening with tape

RETURN ENVELOPE

Please put stamp here

National Technical Information Service
U.S. DEPARTMENT OF COMMERCE
5285 Port Royal Road
Springfield, VA 22161

NTIS Order Form

NTIS Telephone Numbers

To Order Reports
(703) 487-4650

For Subscription Questions
(703) 487-4630

Other Information
(703) 487-4600

Editorial Questions
(703) 487-4838

Postage:
NTIS uses First Class Delivery, or equivalent service, on all shipping. For information about one day RUSH ordering, call (703) 487-4600.

NTIS PRICE CODE SCHEDULE *

This schedule gives the current values to the price codes cited in those Tech Notes having a backup report available from NTIS.

Microfiche	
A01	$5.95
Paper copy	
A02 and A03	9.95
A04 and A05	11.95
A06 through A09	16.95
A10 through A13	22.95
A14 through A17	28.95
A18 through A21	34.95
A22 through A25	40.95
A99	Call for price

Customers in Canada, United States, and Mexico use this schedule. Other addresses should write for the price listing, number PR-360-4.

Prices effective January 1, 1986

Use this form ONLY to order reports designated as available from NTIS

MAIL ORDER TO: National Technical Information Service
U.S. DEPARTMENT OF COMMERCE
5265 Port Royal Road
Springfield, VA 22161
(703) 487-4650

Send me the reports I have selected on this form. I have placed order numbers in appropriate blanks and have indicated the quantity. IF ADDRESS LABEL IS NOT CORRECT, CALL OUR SUBSCRIPTIONS DEPARTMENT.

Last Name:.....

Title:.....

Company/Organization:.....

Address:.....

.....

City/State/Zip:.....

Telephone Number:.....

METHOD OF PAYMENT

☐ Check enclosed payable to NTIS for $.....

☐ Charge to my NTIS Deposit Account, No: ....-.....

☐ Purchase order number:.....

Charge to: ☐ American Express ☐ VISA ☐ MasterCard

Card Number:.....

Expation date:.....

Signature:.....
(Required to validate order)

NTIS ORDER NUMBER (Use only for backup reports stated as available from NTIS)

NTIS Order Number	*Price**	*Quantity*	*Total Price*
.....	.....	.....	.....
.....	.....	.....	.....
.....	.....	.....	.....
.....	.....	.....	.....
.....	.....	.....	.....
		Shipping and handling fee	$3.00
		Total	.....

To Return Order Form Please Fold Here First ▼

Please make second fold here and seal opening with tape

RETURN ENVELOPE

Please put stamp here

National Technical Information Service
U.S. DEPARTMENT OF COMMERCE
5285 Port Royal Road
Springfield, VA 22161

PENN STATE UNIVERSITY LIBRARIES
A0000720098 19

)EPARTMENT OF COMMERCE
nal Technical Information Service
ield, Va. 22161

—

AL BUSINESS
/ for Private Use, $300

AN EQUAL OPPORTUNITY EMPLOYER

POSTAGE AND FEES PAID
U.S. DEPARTMENT OF COMMERCE
COM-211

U.S.MAIL

Special Fourth-Class Rate
Book

PRINTED MATTER

Route To: